LBL-11861
Preprint

Lawrence Berkeley Laboratory
UNIVERSITY OF CALIFORNIA

To be published as a chapter in ADVANCES IN
RADIATION BIOLOGY, Spring/Summer 1983,
J.T. Lett, ed., Academic Press, New York, NY

HEAVY-ION RADIOBIOLOGY: CELLULAR STUDIES

Eleanor A. Blakely, Frank Q.H. Ngo,
Stanley B. Curtis, and Cornelius A. Tobias

February 1983

Prepared for the U.S. Department of Energy under Contract DE-AC03-76SF00098

DISCLAIMER

LBL-11861

HEAVY-ION RADIOBIOLOGY: CELLULAR STUDIES

Eleanor A. Blakely, Frank Q.H. Ngo,*

Stanley B. Curtis, and Cornelius A. Tobias

Biology and Medicine Division
Lawrence Berkeley Laboratory
University of California
Berkeley, California

* Present Address: Radiobiology Laboratory
Cleveland Clinic Foundation
9500 Euclid Avenue
Cleveland, Ohio 44106

HEAVY-ION RADIOBIOLOGY: CELLULAR STUDIES

		Page
I.	Introduction	1
II.	Historical Background	3
	A. Depth-Dose Distribution	3
	B. Relative Biological Effectiveness	4
	C. Oxygen Enhancement Ratio	7
III.	Physical Characteristics of Heavy-Ion Beams	10
	A. Particle Interactions	10
	1. Electromagnetic Interactions	10
	2. Nuclear Interactions	16
	B. Depth Modulation: Range Filters	18
	C. LET Distributions and Average Values	20
	D. Beam Monitoring and Practical Dosimetry of Heavy-Ion Beams	27
IV.	Heavy-Ion Cellular Radiobiology of Bevalac Beams	31
	A. Cell Systems	31
	B. Monoenergetic Bragg Peak Dose-Effect Relationships	34
	1. Modeling of Survival Measurements	35
	2. RBE and OER Values for Monoenergetic Beams	38
	C. Extended Bragg Peak Studies	44
	1. RBE and OER Values for Modified Beams	45
	2. Isoeffective Cell Killing	57
	D. Studies on Repair and Expression of Damage	62
	1. The Early Work with Low-Energy Heavy Ions	62
	2. Repair of Sublethal Damage	65
	3. Potentiation Effects	67
	4. Combined High- and Low-LET Radiations	70
	5. Repair of Potentially Lethal Damage	76
	E. Cell Age Response and Progression Effects	84
	F. Radiosensitizers and Radioprotectors	99
	G. Spheroid Studies	108
V.	Applications to Cancer Research	112
VI.	Summary	118
VII.	Acknowledgements	122
VIII.	References	123

I. INTRODUCTION

Interest in the physical and biological characteristics of charged particle radiations has greatly increased over the past ten years because of their potential usefulness for the understanding and treatment of cancer. With the growing expertise in accelerator design, it has become practical to investigate the radiobiological actions of these ions. The construction of synchrotrons at Princeton and Berkeley (Grunder et al., 1971; White et al., 1971; Isaila et al., 1972) first permitted examination of the biological effects of heavy ions with atomic numbers (z) between 6 and 18 at higher energies than were previously available (i.e., several hundred MeV/u). Although the initial heavy-ion energies at these machines were limited as to the production of beams with clinically significant ranges in tissue, biological studies indicated a likelihood of an enhanced therapeutic potential as compared to ion beams of lower atomic number (Tobias and Todd, 1967; Tobias, 1973). Because the range of particle beams at a fixed energy per nucleon decreases with increasing z of the particle, tissue penetration of the heavy-ion beams is limited by the magnet radius and field used in the accelerator.

Today we have variable energy beams that have more than sufficient range to penetrate the human body. This was accomplished at the Lawrence Berkeley Laboratory (LBL) by using a high energy linear accelerator (the HILAC) as an ion source for the high energy Bevatron (Ghiorso et al., 1973). The permanent installation of the HILAC source into the Bevatron created the Bevalac accelerator complex, which was completed in 1974. The major goals of the radiobiological program at the Bevalac have been: (1) to obtain a fundamental understanding of the nature of high-energy, heavy-ion effects on living cells and tissues; (2) to test the biological rationale for the therapeutic use of

heavy ions; (3) to test the dose-effect-time relationships of heavy ions on mammalian cells and tissues in order to enable the therapist to deliver effective therapy sequences safely; and finally, (4) to study molecular, cellular, and tissue aspects of heavy ion effects which relate to carcinogenesis, mutagenesis, and the effects of high-energy, heavy particles in space.

This article parallels the recent review of heavy-ion tissue radiobiology (Leith et al., 1982). Cell transformation effects due to heavy ions (Yang and Tobias, 1980) have been separately reviewed. There are also several recent books (Raju, 1980; Fowler, 1981; Skarsgard, 1983), and the published proceedings of a recent symposium (Hall, 1982), which provide rather complete overviews of physical and biological high LET particle data of interest for radiotherapy. This chapter reviews studies of: (1) the dose-response of various in vitro mammalian cell lines to high-energy carbon, neon, silicon, and argon beams under aerobic and hypoxic exposure conditions; (2) repair and expression of damage; and (3) the effects of cell age and of chemical modifiers on heavy-ion effects. The results of these studies generally justify and support earlier proposals made with respect to the potential clinical usefulness of high-energy, heavy-ion beams (Castro and Quivey, 1977), and Phase I and II clinical trials using these beams are in progress (Castro and Lawrence, 1978; Castro et al., 1980, 1982; Castro, 1981).

II. HISTORICAL BACKGROUND

Early accelerated proton, deuteron, and helium beams were successfully used for the cyclotron production of radioisotopes for the therapy of leukemia and polycthemia vera (Hamilton and Stone, 1937a; 1973b; Lawrence et al., 1939; Hahn et al., 1939), for the diagnosis of thyroid diseases (Hamilton and Soley, 1939), and for the treatment of cancer with radiocolloids (Jones et al., 1939). In 1946 Wilson suggested the use of protons for direct radiotherapeutic applications. The improved depth-dose distribution of proton and helium beam therapy has provided a feasible alternative to conventional radiotherapy, and these modalities are considered the treatment of choice for specific treatment sites surrounded by critical normal tissues. For reviews see: Lawrence and Tobias, 1967; Archambeau et al., 1974; Graffman and Larsson, 1975; Lawrence et al., 1976; Linfoot, 1979; Raju, 1980; Larsson, 1980; Verhey and Munzenrider, 1982.

Based on physical considerations of improved multiple scattering and straggling, and on biological factors such as enhanced cell killing effectiveness, Wilson (1946) also suggested the clinical usefulness of heavier particles (e.g., carbon). The additional advantage of enhanced biological killing of hypoxic cells by high linear energy transfer (LET) particle beams was suggested by Tobias and Todd (1967). The rationale for the use of high LET radiation for cancer therapy is thus based on three considerations: depth-dose distribution, relative biological effectiveness, and oxygen enhancement ratio.

A. Depth-Dose Distribution

The fundamental physical research which preceded the therapeutic application of particle beams revealed that charged ions deposit maximal dose at the Bragg peak, near the end of their range of penetration (Holloway and

Livingston, 1938). The clinical implications of using particle beams to improve dose distributions to tumors with the concomitant sparing of surrounding normal tissues have been compared to the current strategies for improving dose distributions with state-of-the-art techniques for super voltage radiation modalities (Suit and Goitein, 1980). Based purely on dose localization, particle beams can maximize dose at depth; however, the degree of localization of dose with heavy ions is reduced with increasing charge on the ion, but is in all cases superior to that achievable with fast neutrons (Raju et al., 1978a; Lyman, 1982). Current advances in computerized tomography are used to exploit this fact in treatment planning for particle therapy (Chen et al., 1981; Chen and Pitluck, 1982).

B. Relative Biological Effectiveness

A variety of observations have shown that heavily ionizing particulate radiations (such as charged particles of atomic number greater than one) are several times more effective per unit dose in producing biological effects than are X rays. The concept of high biological effectiveness originated in the work of Zirkle (1935; 1936) who studied the lethal effects of alpha particles on cells. The early cellular studies of Zirkle and Tobias (1953) with helium and deuteron beams demonstrated that in addition to depositing dose at depth, these particles had increased effectiveness in the Bragg peak region, which led to the development of the terms relative biological effectiveness (RBE) and linear energy transfer (LET).

The International Commission on Radiological Units and Measurements defines the RBE as the ratio of absorbed doses of two radiations required to produce the same biological effect (ICRU, 1963, 1979). In most determinations of RBE,

^{60}Co gamma rays are preferred as the standard radiation, although in the past it has been customary to use orthovoltage X rays. The definition of LET is described in detail later in this chapter.

Tobias and Todd (1974) have summarized the most relevant early radiobiology which led to an understanding of the actions of ionizing particulate radiation on microorganisms, mammalian cells, and molecules of biological interest. The early accelerated particle radiobiology largely was accomplished at sister linear accelerators which were constructed in the 1950s at Yale University and at the University of California, Berkeley. Basic dose responses of macromolecules and viruses to charged particles were initiated by Pollard et al. (1952), who demonstrated single hit inactivation and introduced a cross-section concept to evaluate such data. The molecular weight of particles, irradiated dry, could be estimated fairly accurately from heavy-ion experiments.

The group in Berkeley began the first cellular experiments with accelerated carbon ions (5.6 MeV/u) using S. cerevisiae. Sayeg et al. (1959) demonstrated the high relative biological effectiveness of these ions. The effects of accelerated low energy heavy ions were explored with a variety of biological samples: yeast (Manney et al., 1963), B. megaterium spores (Powers, 1965), bacteriophage DNA (Schambra and Hutchinson, 1964), and human lymphocytes (Madhvanath et al., 1976). The spores of B. megaterium are very useful for radiation research because a number of environmental factors, such as the water content, can be accurately controlled. These spores can also survive exposure to high vacuum and can be stored and exposed to radiation at a wide range of temperatures. The survival curves are exponential functions of dose. Powers et al. (1968) exposed dry spores of B. megaterium to a variety of accelerated nuclei, from helium to argon, which were produced at the HILAC. Whereas most of the damage in dry spores from low LET radiation could be annealed by high

temperature or hydrogen sulfide gas, the heavier particles produced irreversible lesions. The oxygen effect was essentially eliminated by the heaviest particles and the cross section for inactivation was approximately the same as the projected area of the spore nucleus.

Techniques for radiation studies of cloned human cells were developed by Puck and Marcus (1955). Several years later, Barendsen and his colleagues were the first to study the killing of cultured human T-1 cells with polonium alpha-particles (Barendsen et al., 1960). Later they used cyclotron-produced helium ions and deuterons at the Hammersmith Hospital in London (Barendsen et al., 1963, 1966; Barendsen and Walter, 1964; Barendsen, 1968a). Survival was measured over an LET range from 5.6 to 165 keV/μm by changing the velocity of the helium ions. The human cells exhibited a maximum sensitivity to alpha particles at 110 keV/μm. Exposure to greater LET values resulted in higher survival, which suggested wasted energy deposition or overkill. All survival curves obtained at LET values greater than 60 keV/μm were exponential.

Todd (1964) examined survival effects on the same human cell line used by Barendsen, and also on the Chinese hamster M3-1 cells cultured in vitro, using the Berkeley HILAC. He studied the LET range of 4.5 to 1940 keV/μm at a fixed velocity for charged particles from helium to argon. Todd measured a maximum RBE value for both cell lines at an LET of 220 keV/μm with carbon ions. Survival curves obtained at LET_{∞} values less than 200 keV/μm appeared sigmoidal, whereas at higher LET they appeared exponential. In a single set of experiments Todd (1964) also showed that lithium ions of various velocities appeared to have similar effectiveness for the inhibition of colony-forming ability as did heavier ions having similar LETs (up to 200 keV/μm). This suggested biological effects were a unique function of LET. The difference in LET values for maximum effectiveness between the Barendsen and Todd results for

the same cell line, however, indicated that LET_{∞} might not be an appropriate universal parameter (Barendsen, 1968b). Additional biological features of reduced repair of radiation damage (Todd, 1964) and suppression of the age-response function (Bird and Burki, 1971) with high LET particle beams have been demonstrated and are being further explored for their clinical potential (see Section IV below).

C. Oxygen Enhancement Ratio

The fact that cells are most sensitive to ionizing radiation in the presence of oxygen than in its absence has been known since Holthusen's bacterial experiment (1921), and was further substantiated by Henshaw's experiments with yeast cells (1940). The first mammalian work on the oxygen effect was carried out by Lacassagne (1942). The term oxygen enhancement ratio (OER) has been defined as the ratio of absorbed doses required to produce the same effect for irradiations in the absence and presence of oxygen. A quantitative relationship describing the oxygen concentration dependence of the oxygen effect was first established by Alper (1956) and Alper and Howard-Flanders (1956) using bacteria. A summary of the effects of oxygen has been presented by Kiefer (1975).

The relationship of the oxygen effect to the radiation sensitivity of tumors was demonstrated by L.H. Gray and his group (Gray et al., 1953). Gray suggested that necrotic, hypoxic tumor cells are relatively more resistant to low LET X rays and gamma-rays than normal oxygenated cells, and he provided evidence that fast neutrons significantly reduced the magnitude of the oxygen effect. This led ultimately to neutron therapy trials at Hammersmith hospital and elsewhere (for recent review see: Cohen and Awschalom, 1982).

The fact that the radioresistance of hypoxic cells to low LET radiations can be diminished for radiations with high ionization densities suggested an

additional rational for the clinical use of charged particle beams (Tobias and Todd, 1967). Tobias et al. (1971a) pointed out that accelerated heavy ions combine the good depth penetration properties of protons and pions with high RBE and low OER. Attention then turned to existing accelerators as possible sources of heavy ions, and in August 1971 two independent groups, one at Princeton (White et al., 1971) and the other at Berkeley (Grunder et al., 1971) accelerated nitrogen ions to several hundred MeV/u kinetic energies by introducing heavier gases into the injector designed for protons. Initial biological and physical results were reported by Tobias (1971), Todd et al. (1971), and Schimmerling et al. (1973, 1976, 1977). The additional potential of using heavy ions for medical research became evident when radioactive beams were produced for the first time (Tobias et al., 1971b), and when heavy ions produced the first radiographic images (Benton et al., 1973).

In the next four years the HILAC was adapted as an injector to the Berkeley Bevatron, and since 1974 a national heavy-ion physics, nuclear science, and biomedical research program has been underway at this hybrid accelerator--the Bevalac (Tobias et al., 1979; LBL, 1977). Particle beams of carbon, neon, silicon, argon, and iron are available with variable kinetic energies; the highest biomedical energy used to date is 670 MeV/u (silicon and neon), but the machine is capable of delivering particles with energies up to 2.1 GeV/u (Pirruccello and Tobias, 1980). In 1981 the Bevalac was upgraded with a new vacuum liner to permit acceleration of high energy beams of most of the nuclei in the periodic table, and in 1982 the first accelerated uranium ions (150 MeV/u) became available. At the time of this writing, groups in several countries (Canada, West Germany, Japan, the Soviet Union, and the United

States) are making preliminary design studies for future biomedical research accelerators. The rapidly developing field of heavy-ion cellular radiobiology has been reviewed several times (Tobias et al., 1971; Raju and Phillips, 1977; Raju, 1980; Hall, 1981; Fowler, 1981; Skarsgard, 1983; Tobias, 1982).

III. PHYSICAL CHARACTERISTICS OF HEAVY-ION BEAMS

A. Particle Interactions

1. Electromagnetic Interactions

The most important energy loss process occurring in a beam of charged particles is caused by electromagnetic interaction with the target molecules (for review: Bichsel, 1968). This energy loss phenomenon can be quantitatively described by the well known Bethe (1930) stopping power formula:

$$-\frac{dE}{dx} = \frac{4\pi z^2 e^4}{mc^2\beta^2} NZ \left[\ln \frac{2mc^2\beta^2}{I(1-\beta^2)} - \beta^2 + \text{correction terms} \right] \qquad (1)$$

where -dE/dx is the rate of energy loss by the heavy charged particle of atomic number z and velocity is equal to βc (c is the velocity of light). NZ is the number of electrons in the medium molecules per unit volume, I is the mean excitation potential of the molecules of the medium, and mc^2 is the rest energy of an electron. Approximations of the Bethe-Bloch formula have been described by Steward (1968), and other compilations of range-energy relationships for particles are also available (Richard-Serre, 1972; Northcliffe and Schilling, 1970; Janni, 1966). When the velocity of the heavy particle is below the critical velocity for Cerenkov radiation, the stopping power (i.e., -dE/dx) is equal to LET_∞ (the subscript ∞ refers to the inclusion of all electrons of all energies allowed by energy conservation).

To understand the biological effects of heavy ions, one must consider the geometrical pattern of energy deposition around a heavy particle trajectory. This geometrical pattern of energy deposition is sometimes called the track structure. The structure of a stopping heavy-ion track is schematically depicted in Figure 1. The core is primarily a result of excitation processes,

Figure 1 Heavy-ion charged particle track and fragmentation effects.

Left panel: A joint reproduction is shown of the latent and the emulsion tracks of a single stopping heavy ion. The unfolding of the emulsion track in terms of its latent structure can be described in terms of core and penumbra. A cross-sectional view of the concentration of the penumbra is shown at three points just below the emulsion track. The dots represent ionization events; excitation events are not shown. The dense inner region of ionizations is the core, and the more diffuse peripheral region in each cross-section is the penumbra. The conical shape of the track is due to the decreasing maximum delta-ray energy, rather than a decrease in ionization. As the stopping particle slows, its halo of delta rays becomes denser because the ionization is increasing. At the same time the maximum delta-ray energy shrinks and the range of the delta-rays become shorter. At intermediate velocities delta-rays become so profuse the track resembles a bottle brush. Single stopping heavy-ion tracks of 10 MeV/u ^{40}A, ^{20}Ne, ^{16}O, ^{14}N, and ^{12}C are shown in the lower half of the panel in photomicrographs from Ilford K.5 nuclear track emulsions. The nucleons traverse the emulsion from left to right. The terminal 20 μm of all tracks are indistinguishable from each other. For a given residual range, the track width is seen to increase with the charge of the particle. (From: Benton and Tochilin, 1966).

Middle panel: Photomicrographs of four types of heavy ion fragmentation events. (1) Pure projectile fragmentation. Two heavy fragments and two protons were produced; both large fragments appear to have $Z \geqslant 8$; one ionizes slightly less than the other. Two large fragments like this are very rare. (2) Pure projectile fragmentation. This is a more common example of a projectile fragmentation, demonstrating production of multiple small fragments. (3) Projectile fragmentation with target breakup. A 2 GeV/u argon particle strikes a small nucleus and both break up. This event is an excellent example of transverse momentum transfer in a collision. The projectile fragments undergo a drastic collective deflection. The bar = 50 μM. (4) Catastrophic destruction of projectile and target nuclei. This is most probably a central collision between a silver or iodine and an incident high energy argon particle. There are 63 fragmentation tracks, making this one of the most prolific collisions yet encountered. Bar = 100 μM. (Private communication from "The Atlas" of H. Crawford and D. Tuttle.)

Right panel: Range dependence of the relative ionization dose ratio from primary and secondary particles and the associated fluence and stopping particle distribution for an example heavy-ion beam. (XBB 819-8965).

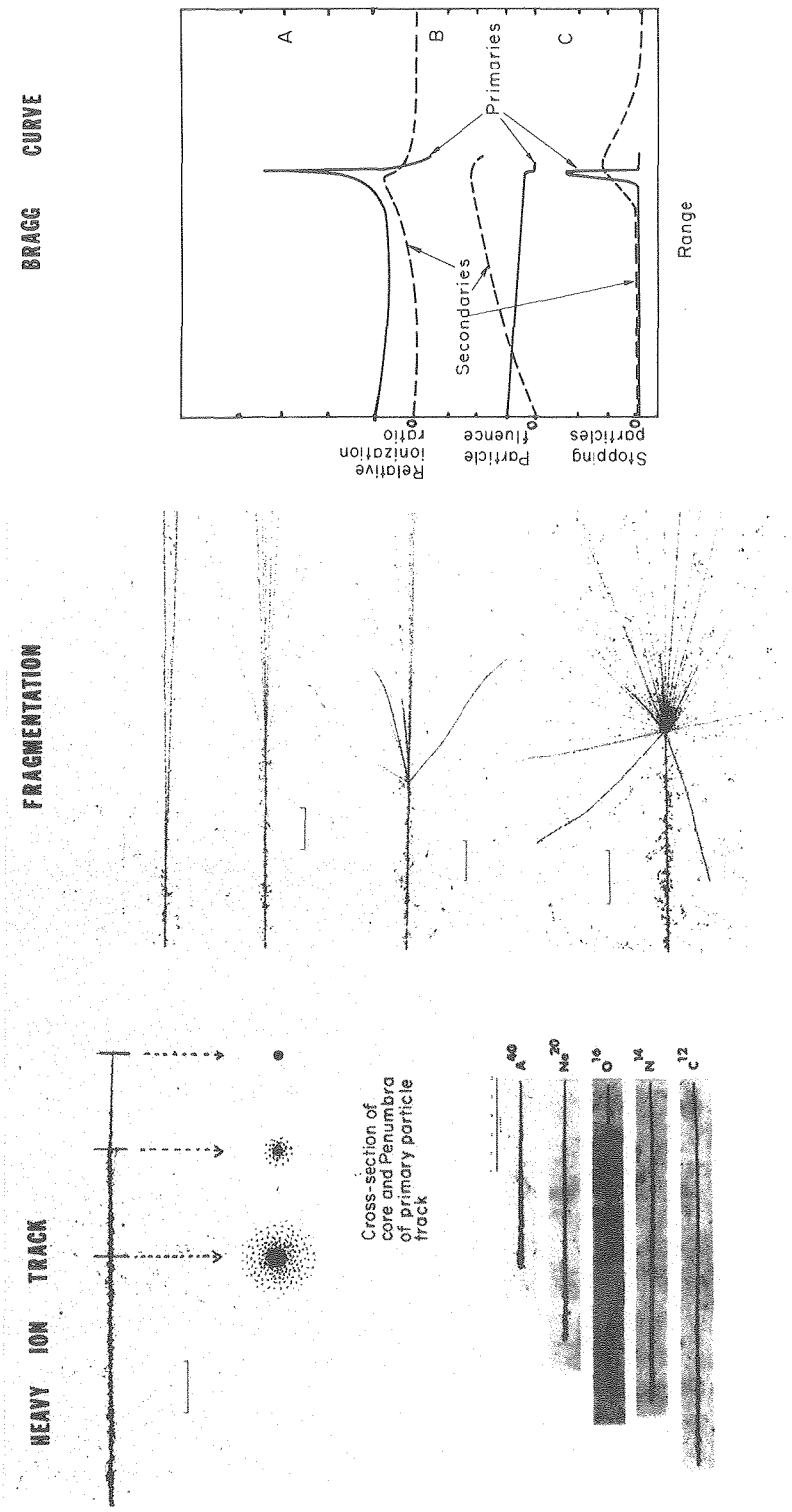

XBB 819-8965

Figure 1

and of ionization events produced in glancing collisions. The penumbra is due to secondary electrons (delta rays) arising from ionization processes. Fano (1952) and others called attention to the fact that the frequency of delta rays with energy E originating in the center of the track falls off as $1/E^2$. Many quantitative calculations (Paretzke and Burger, 1970; Baum, 1970; Katz, 1970; Chatterjee et al., 1973) and some experimental measurements (Wingate and Baum, 1969; Varma and Baum, 1980) are now available for quantitative characterization of the dependence of the average energy density of a charged particle track as a function of radial distance. In many instances, this quantitative evaluation has come about through the calculation of the restricted deposition of energy around a heavy charged particle track. It is generally agreed that the radial density of energy deposition falls off as the square of the reciprocal radial distance from the particle trajectory.

There is still controversy as to the exact quantitative details of the track structure. For example, Paretzke (1980) has stated that one must determine the detailed cross-section of physical processes, and then evaluate the energy loss events in various channels before any correlation with chemistry or biology can be made. He has recently completed extensive and detailed calculations using Monte Carlo methods and cross-section data in the gas phase. There are quantitative differences in track structure between tracks produced in a gas phase and those in a condensed phase, and studies of these differences are in progress (Turner et al., 1981). A controversy also exists between those who believe that microdosimetric measurements give important data on radiation quality (Keller and Rossi, 1978), and those who believe that the information obtained from microdosimetry cannot be used quantitatively in predicting biological results (Goodhead, 1977; Goodhead et al., 1980).

It is convenient to divide particle collisions into two distinct categories: glancing and knock-on (Rossi, 1952; Uehling, 1954; Magee, 1961). Using such a subcharacterization, Mozumder et al. (1968) have described the geometrical pattern of energy deposition in terms of two physically distinct regions called "core" and "penumbra." The concept of core is more suitable for applications in condensed states of matter in radiation chemistry and radiation biology, and the exact size of the core will depend on the chemical composition of the absorbing material. The core is created by the glancing collisions of the particle with excitations in the range from 6.5 eV to 100 eV for water (Platzman, 1952). Bohr's adiabatic criterion sets a limit on the radial distance from the trajectory of the incident particle within which molecules can be excited by this mechanism. Similar limits have also been obtained by Brandt and Ritchie (1974), based on plasma oscillations, and can be given by:

$$r_c = \frac{\beta_c}{\omega_p} \tag{2}$$

where r_c is the radius of the core and ω_p is the plasma oscillation frequency of the medium, given by $4\pi ne^2/m$, where n is the density of valence electrons, e the electronic charge, and m the mass of an electron.

The penumbra is composed of the tracks of the knock-on electrons, called δ-rays. Based on the detailed calculations of Chatterjee et al. (1973), the r_p, the radius of the penumbra in water at 20°C can be approximated by:

$$r_p = 396(v)^{2.7} \tag{3}$$

where v is in units of 10^9 cm/sec.

Chatterjee and Schaefer (1976) have also shown empirically that the energy density, ρ_{core}, in the core is given by:

$$\rho_{core} = \frac{LET_\infty}{\pi r_c^2} \frac{(1+\ln r_p/r_c)}{(1+2 \ln r_p/r_c)} \tag{4}$$

and the energy density in the penumbra, ρ_{pen}, is given by:

$$\rho_{pen}^{(r)} = \frac{LET_\infty/2}{\pi r^2(1+2 \ln r_p/r_c)} \tag{5}$$

Chatterjee and Magee (1980a) and Magee and Chatterjee (1980) have applied this track model to make explicit calculations for the radiation chemistry of water and the Fricke solution system, but this model has not been tested to describe radiobiological effects even though Chatterjee and Tobias (1975) have made some limited attempts.

Characterization of biological effects by the physical parameter LET_∞ has various shortcomings: (1) in many situtations, the extent of space over which a heavy particle loses its energy (as described by the LET_∞ parameter), is much larger than even the nuclear dimensions of mammalian cells (Chatterjee and Magee, 1980a); and (2) different charged particles having the same LET_∞ values have been shown to exhibit quantitatively different biological effects as noted by Bewley (1968) and Curtis (1970), and shown experimentally with the stopping heavy ion beams at the Bevalac (Blakely et al., 1979), so that the LET_∞ parameter is not always adequate to uniquely describe biological effects (see Section IV).

Thus, it is clear that many problems still exist in correlating biological and chemical effects with the details of track structure. At present there is

no single physical parameter to describe the biological effects uniquely. Suggestions have been made to correlate the physical parameter z^{*2}/β^2 with quantitative observations in radiobiology (Turner and Hollister, 1965; Curtis, 1970), but they have also not been very satisfactory (Blakely et al., 1979). In the absence of any definitive physical parameter, we have decided to continue using LET_∞ as a parameter with the full knowledge of the shortcomings presented earlier.

2. Nuclear Interactions

As heavy charged particles traverse absorbing targets, nuclear interactions of heavy ions with target nuclei may occur (for a review see Bichsel, 1968). Nuclear interactions cause fragmentation of the primary ion into particles of predominantly lower charge and mass, and also may result in the disintegration of the target nuclei producing a star of very short ionizing tracks.

Immediately after a glancing nuclear collision with a target atom, the resulting fragments from the primary ion have similar velocity and direction as the primary particles; fragments produced in central collisions may have lower velocity and may veer off the direction of the main beam as depicted in the fragmentation events shown in the middle panel of Figure 1. The lower atomic number fragments that travel parallel to the beam have longer ranges than the primary particles and so produce an exit dose beyond the stopping region of the primary beam. A primary ion that loses only neutrons has a shorter range than the main beam. The nuclear interaction is a rare occurrence relative to the electromagnetic interaction, but it is more catastrophic because the primary particle is transformed into fragments of lower charge and mass. The total probability for nuclear interaction is related to the square of the sum of the radii of the target and projectile nuclei (Bradt and Peters,

1950; Chatterjee et al., 1976). Thus, fragmentation is more prominent in heavier charged particle beams.

The combined influence of the electromagnetic and nuclear collision processes causes a characteristic pattern of energy or dose distribution within matter, as shown schematically in a representative Bragg curve in Figure 1 (panel A). The plot of relative ionization (absorbed dose) versus depth rises to a sharp peak region at a well-defined range, then drops precipitously to a lower value. The peak region of dose is caused by the increase in the rate of energy loss (-dE/dx) from electromagnetic interactions as the primary beam slows down. The dose distribution beyond the peak is caused by fragments from the nuclear interactions of both the primaries and the nuclear secondaries produced upstream.

The dose contribution of each fragment is generally smaller than the dose from the primary particle because the atomic number of the fragment is smaller than that of the primary. However, as depth in the absorber increases, the sum total of the fragment doses can become a significant fraction of the total dose. The diagram in Figure 1 is intended to approximate the physical dose distributions from primaries and secondaries for a neon beam of 425 MeV/u initial energy. The relative contribution of primary to secondary effects is specific to each particle species. In a monoenergetic beam of heavy particles near the entrance point into tissue (plateau) the dose contribution from fragments is generally negligible or very small (a few percent at most). The maximum fragmentation dose occurs very near the Bragg peak and the relative ratio of the total fragmentation dose to the dose from pristine primaries increases with increasing depth in the absorber and is greater for heavier particles. The usefulness of heavy ions for therapy is thought to be limited

to particle beams where the fragmentation dose is less than half of the total dose. As we show below, fragmentation is a factor in the selection of beams suitable for therapy. The study of fragmentation products at relativistic energies has been reviewed separately (Heckman et al., 1960, 1978; Schroeder, 1981). At energies of biomedical interest, fragmentation work is in progress by Schimmerling (1980) and Llacer et al. (1980).

B. Depth Modulation: Range Filters

Monoenergetic Bragg peaks of protons, helium, and high energy heavy ion beams occur at the end of their range within a narrow depth dimension of only several millimeters in tissue. In order to irradiate tumor regions of larger dimensions with Bragg peak radiation, the peak region can be extended by spreading the energies of the incoming particles. Usually this is done by modulating the amount of material in the beam line in order to vary the range of the beam. We use the generic name "range filters" to describe these devices. There are several types of range filters currently in use, for example a moving double wedge, or the most frequently used spiral ridge filter (Karlsson, 1964; Lyman and Howard, 1977; Lyman et al., 1980). Ridge filters are constructed either as a series of exactly shaped parallel ridges or as one continuous spiral ridge. The result of using one of these range filters is that you effectively have superimposition of Bragg curves with different residual ranges. The addition of many peaks side by side created at various depths by the range filter extends the effective region over distances of several centimeters, depending on the design of the filter. Dose versus depth curves for both the unmodified and the extended peaks used in the experiments reported here are shown in Figure 2. The slopes of these curves in the peak regions are determined by the filter design. The doses were chosen to decrease

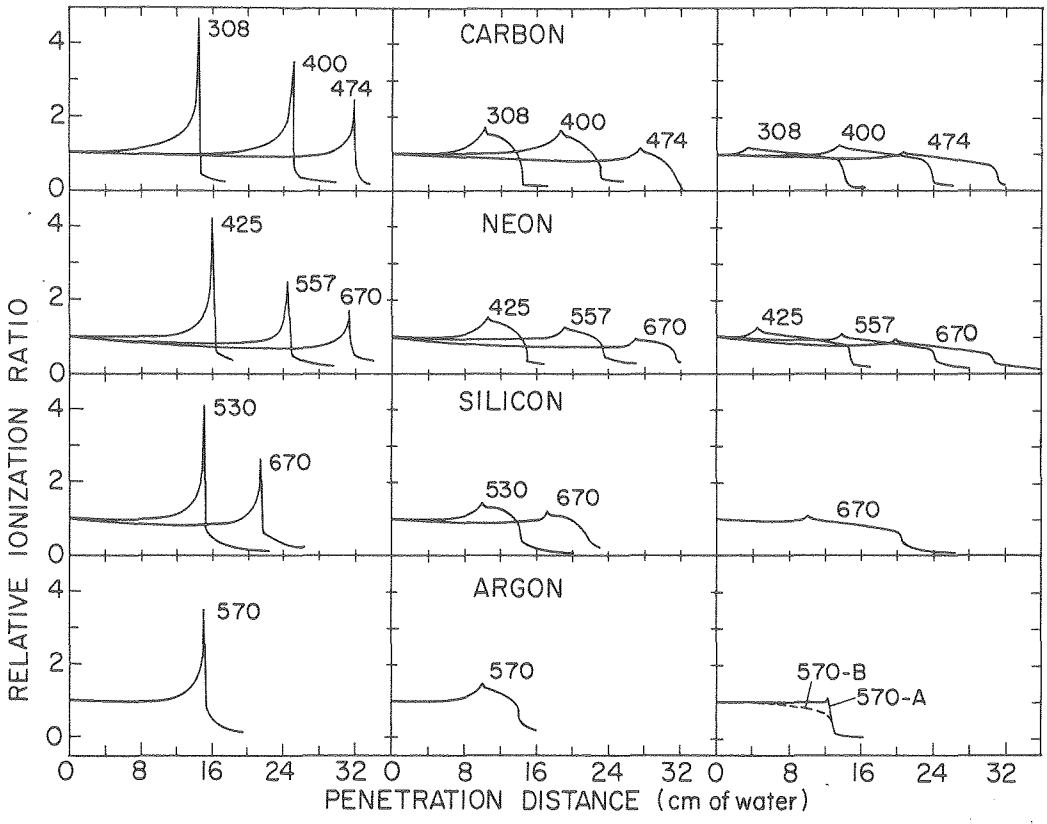

Figure 2 Composite figure of Bragg curves of available Bevalac beams of carbon, neon, silicon and argon. Initial energies of each beam are indicated.

Left panels: Unmodified monoenergetic Bragg peaks.

Middle panels: 4-cm extended Bragg peaks.

Right panels: 10-cm extended Bragg peaks, including two spiral ridged filter designs for argon. Thicknesses of between 0 to 1.8 g-cm^{-2} of lead scattering foils were used for these beams. (XBL 819-1849).

slightly with increasing depth from the proximal to the distal end of the peak in order to compensate for the expected increasing radiobiological effect as the number of stopping particles increases, and thus to approximate uniform cell killing across the peak region (Lyman, 1982).

Figure 3 illustrates the relative residual range positions that have been studied with a variety of biological systems at the Bevalac (see Section IV). In those experiments in which monolayers of cells were irradiated, the track segment covered is narrow; however, a broader range was covered if the biological system had an extension along the beam direction (i.e., cells in suspension chambers). The former situation results in a higher effective LET than the latter. This aspect of the physical situation in the beams varies considerably for the particular biological systems used and complicates precise comparisons of results. An approximation of the dose-average LET_∞ values for various residual range positions in Bevalac beams has been made based on the calculations of Curtis (see Section IIIC). These LET values are described below. Such calculations are of necessity approximate; accurate predictions of mean LET await detailed calculations utilizing cross sections based on experimental measurements of the detailed distribution of fragments.

C. LET Distributions and Average Values

Linear energy transfer is a physical parameter that is a measure of the mean rate of energy deposited locally along the track of a charged particle by electromagnetic interactions. The parameter is called LET_∞ if one includes all energy transfers up to the highest energy delta rays or knock-on electrons that are kinematically possible.

LET values increase as charged particles slow down. Since at any depth of particle range there is a mixture of primary and secondary particles with

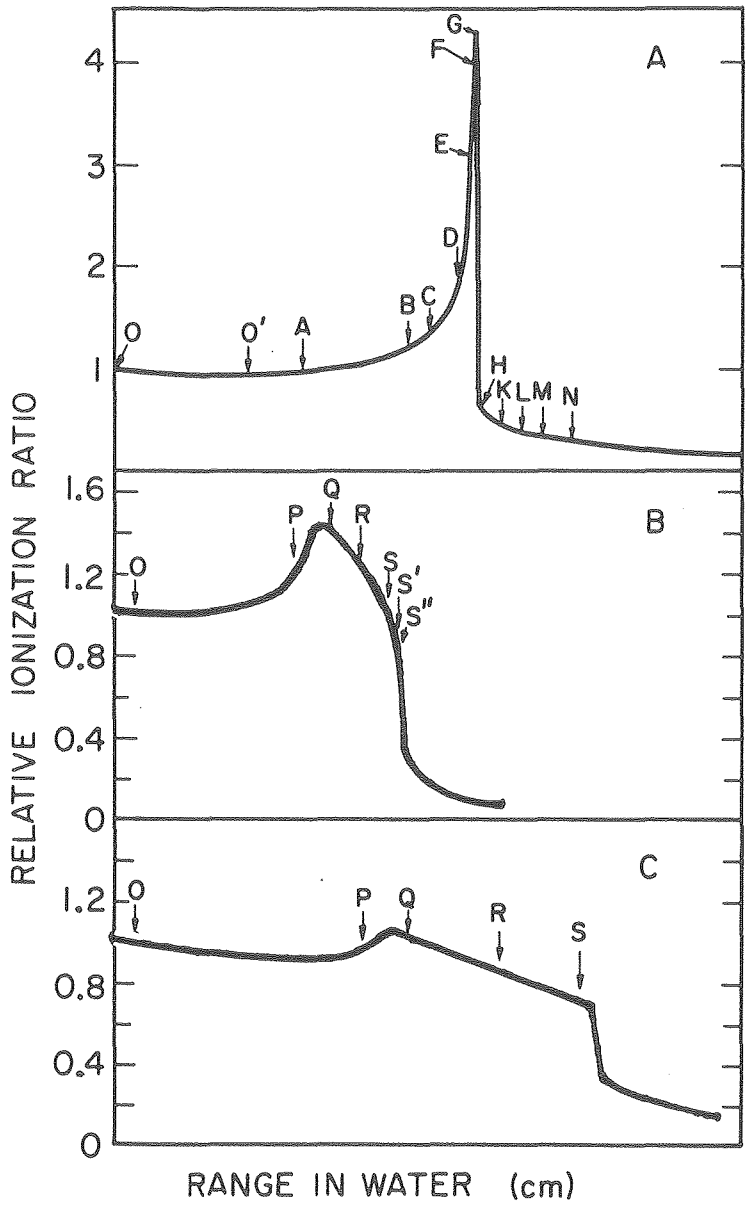

Figure 3 Designation of relative beam ranges studied with respect to the monoenergetic Bragg peak (upper panel), and the 4-cm (middle panel) and 10-cm (lower panel) extended Bragg peaks. (XBL 815-3841)

different energies, the spectrum of LET can be quite broad and does not necessarily follow a Gaussian distribution. This is most significant at the Bragg peak. An example of a calculated LET distribution at 16.03 cm of water, near the peak of a 425-MeV/u neon ion beam, is shown as the insert in Figure 4. A function D(L) where L is the LET can be defined such that the absorbed dose D is given by:

$$D = \int_0^\infty D(L)\, dL = 2.3 \int L\, D(L)\, d(\log_{10} L) \qquad (6)$$

with rad for the units of D. D(L) has the units of rad-g/MeV-cm^2 with L in units of MeV-cm^2/g. Thus, a plot of 2.3L$\cdot$D(L) against $\log_{10}$L allows the area under any portion of the curve to be proportional to the absorbed dose. The large peak is due to the primary neon-ion beam. The tail at high L is caused by those neon ions at lower energy that are about to stop. The small contribution at lower L is due to the nuclear fragments of lower charge and mass.

The dose-averaged LET is defined as:

$$L_D = \int L\, D(L) \Big/ \int D(L) dL \qquad (7)$$

and the track-averaged LET as:

$$L_T = \frac{\int L\phi(L) dL}{\int \phi(L) dL} = \frac{\int L\phi(L) dL}{\Phi} \qquad (8)$$

where ϕ is the differential fluence in units of number of particles per unit LET per unit area, and Φ, the total fluence (number of particles per unit area) is given by:

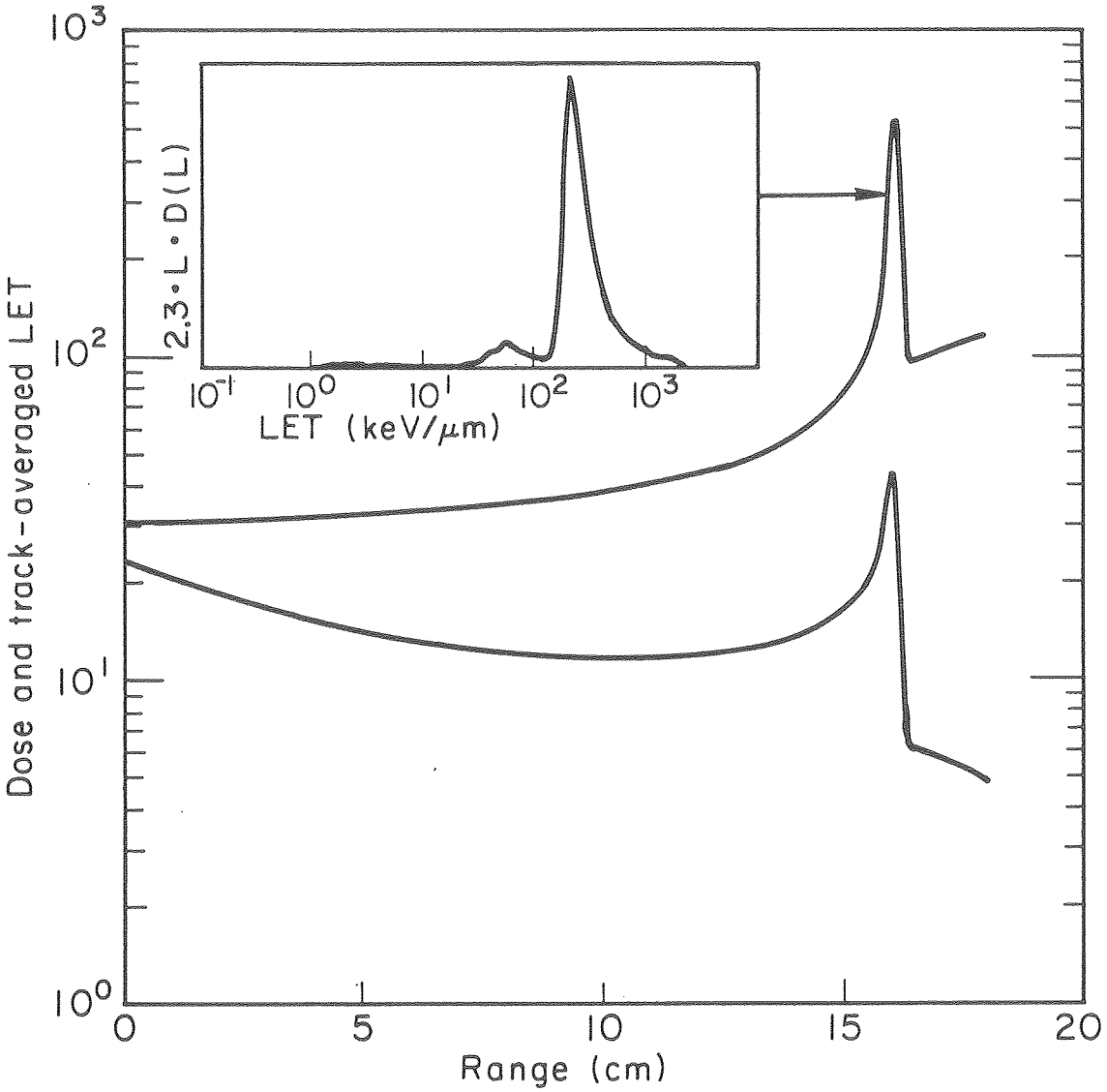

Figure 4 Calculated range dependence of dose and track-averaged LET for a monoenergetic 425 MeV/u neon ion beam. The upper curve is the dose-averaged LET and the lower curve, the track-averaged LET. Both LET calculations are shown as a function of depth in a water phantom. (XBL 815-3842)

$$\Phi = \int \phi(L)dL \tag{9}$$

The total absorbed dose D can be defined as:

$$D = \int L\phi(L)dL \tag{10}$$

and combining equations (8) and (10), we obtain the following for L_T:

$$L_T = \frac{\text{total absorbed dose}}{\text{total fluence}} = \frac{D}{\Phi} \tag{11}$$

Therefore, the track-averaged LET is simply the total absorbed dose per particle fluence.

Under the assumption that the probability of a biological effect per track traversal is proportional to L^2, the linear coefficient of dose in the exponent of the survival expression is proportional to L_D. Under the assumption that the probability is independent of L (e.g., at high LET), the coefficient is proportional to $1/L_T$. Therefore, neither average LET can be assumed to be adequate to characterize biological responses in a broad spectrum of LET values. Dose and track averaged LET values vary with depth as shown in Figure 4 for a 425 MeV/u neon-ion beam.

Measurements of LET are limited by the sensitivity of existing radiation dose monitoring devices. For example, plastic particle track detectors usually have a higher threshold of sensitivity to low LET particles than do electronic monitors. Measurements of y, the microdosimetric analog of LET, using gas proportional counters are dependent on the physical dimensions of the counter, whether it is walled or wall-less, and the composition of the gas in the chamber and its equivalent thickness, which is related to the gas pressure

inside the counter. Fricke dosimeters (Schuler and Allen, 1957) and thermoluminescent and film dosimeters (Tochilin et al., 1968; Patrick et al., 1976) lose sensitivity at high LET.

Early measurements of the fraction of dose from delta ray events of low-atomic-number charged particles from van de Graaff accelerators using gas proportional counters (Kliauga and Rossi, 1975) yielded satisfactory agreement with theoretical calculations of track structure with respect to the relative importance of energy transport by delta rays (Paretzke et al., 1973). Similar experiments have now been performed at the Bevalac using particle beams of high atomic number ($z \geq 6$) and high velocity ($E \geq 400$ MeV/u) in which the delta-ray spectrum is more energetic (Kliauga et al., 1978). Measurements of lineal energy transfer were made with wall-less chambers at several values of particle residual range along the monoenergetic 400 MeV/u carbon and 450 MeV/u argon beams. The wall effects were greatest in the plateau where the primary beam and its concomitant delta rays have the greatest energy. Wall effects became negligible at the peak. Dose mean lineal energy density measurements were also variable depending on the counter size and site diameter used. The trend of the data agree with calculations of LET values published in Blakely et al. (1979), but large quantitative differences are noted. Additional microdosimetric spectra have been obtained with the 557 MeV/u neon beam by Zaider et al. (1981).

Lineal energy measurements of Luxton et al. (1979) in the 400 MeV/u carbon and neon beams are compared to calculations by Curtis (1977; 1979) and Curtis et al. (1982) in Figure 5. The calculations indicate the dose-averaged LET varies from 6 to 180 keV/μm in the 4-cm extended peak of the 400 MeV/u carbon beam, a distribution of 100 to 350 keV/μm in the 4-cm extended peak of the

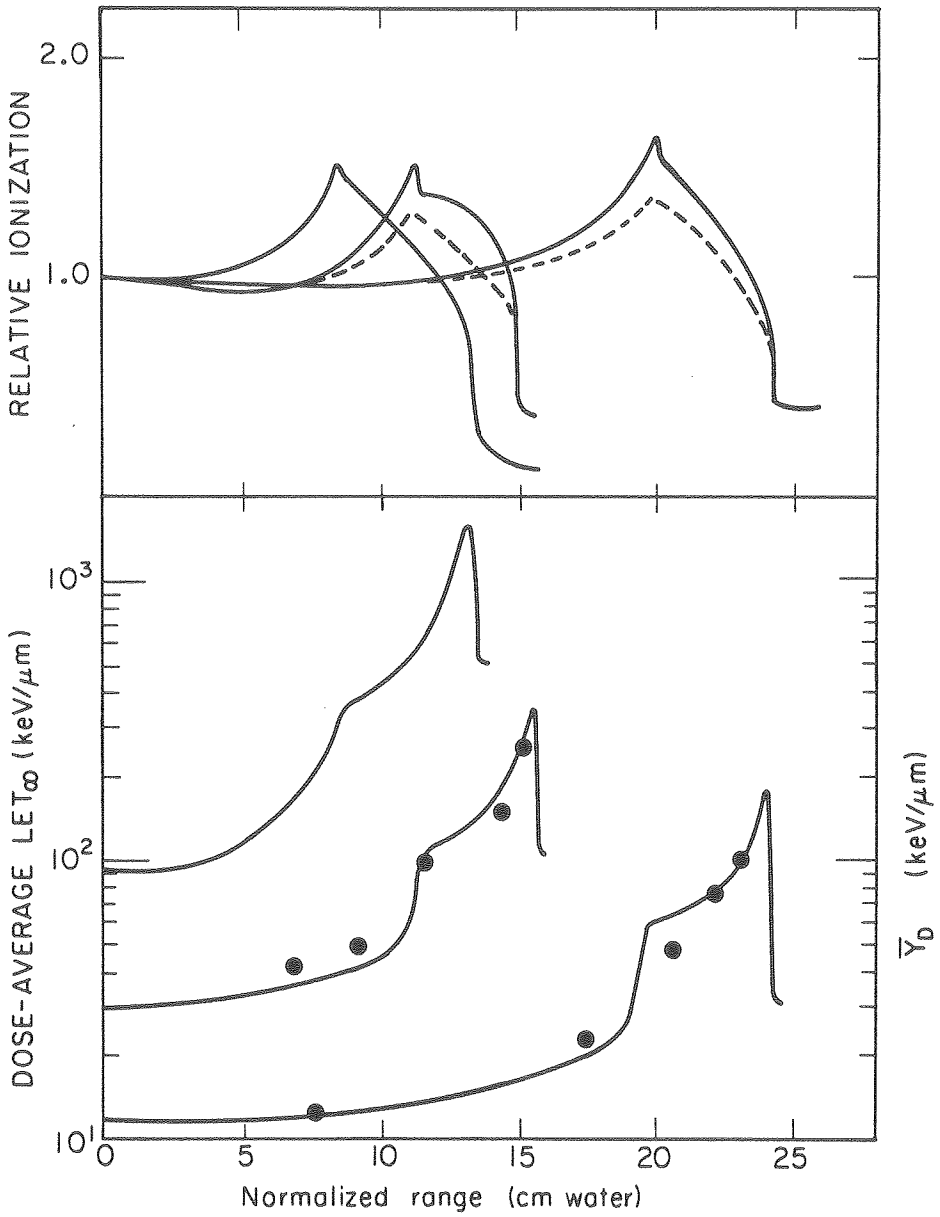

Figure 5 Calculated range dependence of the dose-averaged LET_∞ of (left to right) 570 MeV/u argon, 425 MeV/u neon, and 400 MeV/u carbon beams (Curtis, 1977, 1979; Curtis et al., 1982). Curtis used the Bragg curves (solid lines) obtained from a rotating brass spiral ridge filter (also designed to produce 4-cm extended Bragg peaks) for his calculations of dose-averaged LET for each beam. To compare the calculated dose-averaged LET_∞ values with measured dose averaged lineal energy values, the L_D values were multiplied by 1.13 before plotting. Data points are y_D measurements of Luxton et al. (1979). Bragg curves from Luxton's linear reciprocating action lead ridge filter are shown in broken lines for the neon and carbon beams. (XBL 815-3844)

425 MeV/u neon beam, and 350 to 1400 keV/μm in the 4-cm extended peak of the 570 MeV/u argon beam. To compare the calculated dose-averaged LET values directly with the measured dose averaged lineal energy, certain assumptions with respect to the spherical geometry of the chamber have to be made; with these assumptions, the dose-averaged lineal energy values are 9/8 of the dose-averaged LET values, and the L_D values must be multiplied by 1.13. Despite differences in the Bragg ionization curves from the use of different ridge filters, the comparison of the calculations and the measured values show fairly good agreement. Figure 6 summarizes calculated dose-averaged LET values of unmodified and extended Bragg peaks of carbon, neon, silicon, and argon ion beams.

D. Beam Monitoring and Practical Dosimetry of Heavy-Ion Beams

Beam monitoring of data for biological and medical heavy-ion irradiations are based on thin-foiled parallel-plate ion chambers filled with pure nitrogen gas. Bragg curve ionization measurements are made with a pair of ion chambers using an interposed variable absorber (Lyman and Howard, 1977; Alonso et al., 1980). The following methods have been used to verify ion chamber dosimetry; (1) comparisons of absorbed dose measurements with calculations of absorbed dose based on the geometric properties of the irrradiated volumes within the ion chambers and using for each beam the same values of W, the average energy required to make one ion pair in nitrogen gas (Thomas et al., 1980; Thomas, 1982; Schimmerling et al., 1983); (2) cross-calibrations of dose measurements with calorimetry methods (McDonald et al., 1976; J. T. Lyman, private communication); (3) thermoluminescent dosimetry cross-calibrations for low LET particle beams where calculations of dosimetry efficiencies at the appropriate LET values are known (Patrick et al., 1976); (4) cross-calibrations of

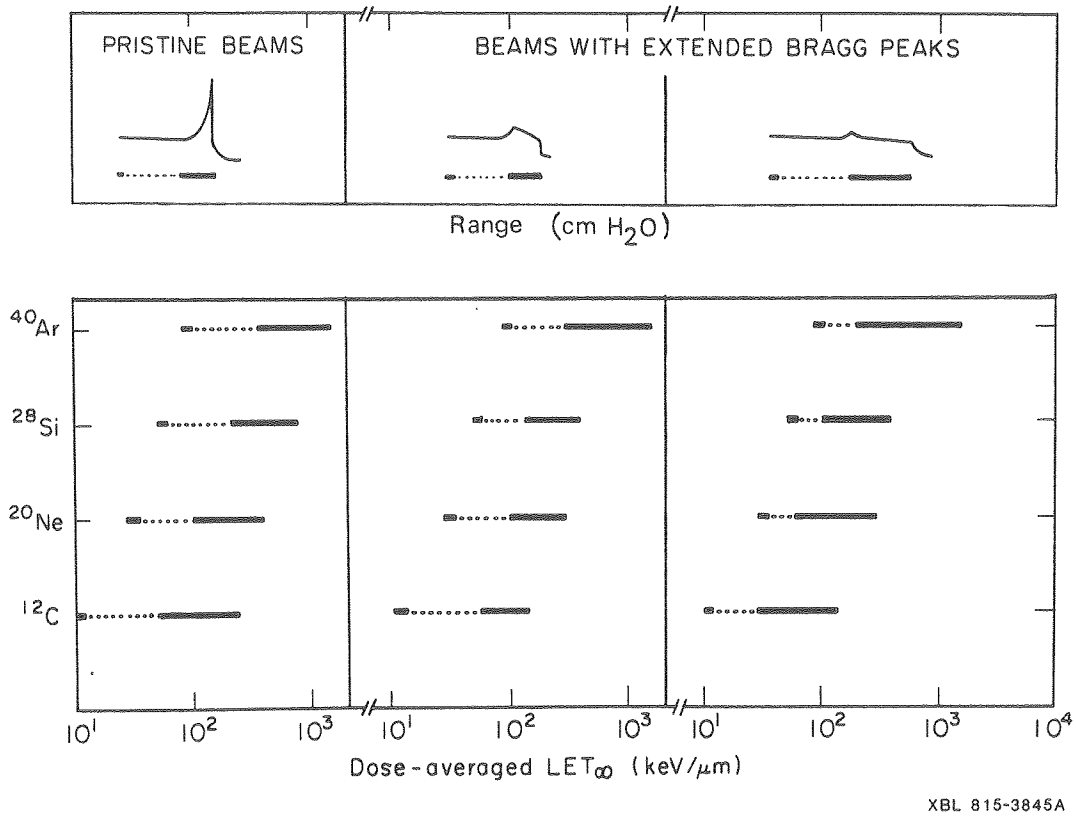

Figure 6 Calculated dose-averaged LET_∞ values for pristine and extended Bragg peaks of 570 MeV/u argon, 530 MeV/u silicon, 425 MeV/u neon, and 400 MeV/u carbon. (XBL 815-3845A)

ionization ratios between the parallel-plate chambers and the spherical tissue-equivalent ion chambers (i.e., EGG chambers, Far West Technologies, Golleta, CA) with the EGG as a standard for each individual experiment (Blakely et al., 1979); and (5) absolute dose intercomparisons of charged particle beams (Smith, 1982), including Bevalac dosimetry, are being conducted by a multilaboratory dosimetry group.

Many of the dosimetric methods used at the Bevalac were patterned after the procedures used with helium, protons, or deuteron beams (Tobias et al., 1952; Birge et al., 1956; Raju et al., 1969). W values for the higher energy, high atomic number Bevalac beams have been characterized by several methods including time-of-flight measurements that correlate physical factors such as fragmentation and LET distributions (Schimmerling et al., 1976, 1983; Stephens et al., 1976; Schimmerling, 1980; Thomas et al., 1980; Thomas, 1982). Results to date show that in nitrogen the same W applies to a wide range of particles and energies (e.g., carbon to argon from 100 to 700 MeV/u).

Chemical dosimetry is useful as a separate method to verify ionization chamber dosimetry by measuring free radical yields and alteration of these yields at high LET. Appleby and Christman (1974) and Christman et al. (1981) have made basic measurements of G values, the number of molecules damaged or formed per 100 eV of energy absorbed, for heavy ions at the Princeton and Berkeley Bevalac accelerators. Chatterjee and Magee (1980a) have recently calculated the response of the Fricke dosimeter from basic considerations and compared the available experimental data to it, including the work of Schuler (1967) and Schuler and Allen (1957).

There is reasonable agreement between Fricke dosimetry, parallel-plate ion chambers, EGG ion chambers, and TLD dosimetry where it is available for dose

measurements in the "plateau." We believe that the "plateau" measurements of dose are within 5 percent and the "peak" within 15 percent of absolute dose measurements. A comparison of argon beam depth-dose measurements in our laboratory with those done independently later by Goodman and Colvett (1977) showed excellent agreement.

IV. HEAVY ION RADIOBIOLOGY OF CELLS AT THE BEVALAC

A. Cell Systems

In order to characterize the biological response to the LET spectrum currently available with high energy carbon, neon, silicon, and argon beams at the Bevalac, a series of cellular experiments using unmodified and modified beams has been conducted since the fall of 1974 (see Table 1). Data are included from both *in vitro* and *in vivo* cell studies by investigators from laboratories in the United States, Canada, Europe, and Japan.

Ten different cell lines (human T-1, human Na11 melanoma, Chinese hamster lung V-79, Chinese hamster ovary, rat rhabdomyosarcoma R-1, rat gliosarcoma 9-L, mouse mammary EMT-6, mouse embryo BALB/C 3T3, mouse C3H10T1/2, and mouse epithelioma) have been used to assay radiation-induced effects including loss of reproductive integrity, the oxygen effect, the effects of radiation modifiers, effects on synchronized cells, effects on cellular repair, enhancement of viral transformation, and the relationship of DNA strand breakage to cell lethality.

Several assay techniques have been used in the cellular investigations:

1. Exposure of cells in monolayers contained in controlled-atmosphere chambers (Blakely et al., 1979).
2. The use of cells suspended in nutrient medium of low calcium content and controlled atmosphere (Chapman et al., 1977; Curtis et al., 1982).
3. Suspended cells in sealed vials in a state of hypoxia due to metabolic depletion (Hall et al., 1977).
4. The submarine, a tissue phantom consisting of an array of glass or plastic coverslips onto which cellular monolayers have been grown; the coverslips are immersed in liquid medium and the cells are therefore exposed simultaneously all along the range of the Bragg ionization curve (Tobias, 1973; Roisman et al., 1974).

Table I. Summary of Cell Experiments Completed at the Bevalac (1974-1982)

Cell System	Technique	Assay	OER Data	Ion(s)	Ridged Filter	Reference
T-1 in vitro:	Monolayer	Reprod. Integrity	Yes	C, Ne, Si, Ar	4 and 10 cm brass	Blakely et al., 1978, 1979, 1980a, 1980b, 1980c, 1982
	"Submarine"	Reprod. Integrity	No	C, Ne, Ar	4 cm Pb and 4 and 10 cm brass	Raju et al., 1978b, 1980c. Tobias, 1973, Roisman et al., 1974.
	Monolayer	DNA SSB	No	C, Ne, Ar	No	Roots et al., 1979
	Monolayer (Sensitizer)	Reprod. Integrity	No	C	No	Schroy et al., 1980
CH-V79 in vitro	Suspension (15 mm wide) (sensitizers and protectors)	Reprod. Integrity	Yes	C, Ne, Ar	4 cm Pb and 10 cm brass	Chapman et al., 1977, 1978, 1979.
	Sealed capsules (2-4 mm wide)	Reprod. Integrity	Yes	Ar	No	Hall et al., 1977
	Monolayer	Reprod. Integrity	No	C, Ne, Ar	No	Ngo et al., 1981
	Monolayer (Synch.)	Reprod. Integrity	No	Ar	No	Hall et al., 1977
	Sealed capsules 2.5 mm wide	Reprod. Integrity	Yes	C, Ne, Ar	10 cm brass	Raju and Phillips, 1977 Raju et al., 1978c
	Suspension (1.5 mm wide)	DNA SSB	No	C, Ne	10 cm brass	Roots et al., 1980a
	Spheroids	Reprod. Integrity	No	C, Ne, Ar	4 cm Pb	Lucke-Huhle et al., 1980
	Monolayer	G_2 block	No	C, Ne, Ar	No	Lucke-Huhle, et al., 1979
CHO in vitro	Monolayer (hyperthermia)	Reprod. Integrity	No	C	No	Gerner and Leith, 1977
	Monolayer vessels (Protectors)	Reprod. Integrity	Yes	C, Ne, Ar	No	Roots et al., 1980b
9L-21 Rat brain gliosarcoma	In vivo (in situ) (suspension-15 mm)	Reprod. Integrity	Yes	C, Ne	No	Leith et al., 1975 Wheeler et al., 1979, 1980
	In vitro (suspension-13 mm)	Reprod. Integrity	No	C, Ne, Ar	4 cm brass	Rodriguez and Alpen, 1980, 1981
	Spheroids	Reprod. Integrity	No	C, Ne, Ar	4 cm brass	Rodriguez and Alpen, 1980, 1981
R-1 Rat rhabdo-myosarcoma	In vivo (sensitizer)	Tumor regression Reprod. Integrity	No Yes	C, Ne, Si, Ar	4 cm brass	Curtis et al., 1978 Tenforde et al., 1980 1981a, 1981b, 1982a, 1982b
	In vitro (suspension-15 mm)	Reprod. Integrity	Yes	C, Ne, Ar	4 and 10 cm brass	Curtis et al., 1982
Mouse embryo BALB/C 3T3	Monolayer (confluent)	Enhancement of viral transformation	No	Ne	No	T. C. Yang (personal communication)
Mouse C3H 10T1/2	Monolayer (confluent)	Enhancement of viral transformation	No	Ne	No	Yang et al., 1980 T. C. Yang (personal communication)
Mouse mammary EMT-6 tumor	In vivo and in vitro (sealed capsules, 2 ml size)	Reprod. Integrity	Yes	C, Ne, Ar	4 cm and 10 cm brass	Fu and Phillips, 1976 Phillips et al., 1977 Goldstein et al., 1981a
	Monolayer	Division time	No	Ne	No	Collyn-d'Hooghe et al., 1981
Mouse epithelioma	In vivo	Reprod. Integrity	No	Ne	4 cm brass	Sakamoto et al., 1983
Human melanoma	In vivo	Reprod. Integrity	No	Ne	10 cm brass	Guichard et al., 1982

5. The jello submarine in which cells are suspended in a gelatin matrix (Raju et al., 1976; 1978c, 1980c).
6. Multicellular spheroids in which the survival of cell populations in close three-dimensional contact are evaluated (Lücke-Hühle et al., 1980; Rodriguez and Alpen, 1980, 1981).
7. Measurement of DNA strand breaks by sucrose-gradient centrifugation (Ritter et al., 1977).
8. Measurement of single- and double-strand DNA breaks by mild alkaline uncoiling combined with ion-exchange chromatography (Roots et al., 1979, 1980a).
9. Measurement of division delay using flow microfluorimetry (Lücke-Hühle et al., 1979) or microcinematography (Collyn-d'Houghe et al., 1981).
10. Combined application of drugs, hyperthermia, anisotonic solutions, time delay, and radiations including sequential treatments of heavy ions and X rays (Chapman et al., 1977, 1978, 1979; Gerner and Leith, 1977; Guichard et al., 1982; Ngo et al., 1981; Roots et al., 1982; Schroy et al., 1980b; Tenforde et al., 1981b, 1982b).
11. In vivo tissue and tumor exposures for cell killing and single strand break studies (Curtis et al., 1978; Fu and Phillips, 1976; Phillips et al., 1977; Keng and Lett, 1981; Leith et al., 1975, 1977; Tenforde et al., 1980, 1981a, 1981b, 1982a, 1982b; Wheeler et al., 1979, 1980; Sakamoto et al., 1983; Ainsworth et al., 1983).

Radiobiologists are limited in the use of cell lines for experimental work of this kind because of the requirement for stability of the radioresponse with a high plating efficiency over the period of years needed for comparisons with various radiation modalities. It is for this reason that fibroblastic cultured

cell lines like those listed in Table 1 have been used. The established human and rodent cell lines have provided an estimation of appropriate dose levels for initial clinical studies with high energy heavy-ion beams. At the same time, investigators in the field are mindful of the need to examine distinctions between the radiation response of normal versus tumor cells, human cells versus other mammalian cells, and established cultured lines versus radiosensitive and radioresistant tissues in vivo. Epithelial cells obtained de novo from human normal and tumor tissues appear to be considerably more varied in their radiation response than was previously appreciated (Rofstad and Brustad, 1981; Smith et al., 1980; Fertil et al., 1980). It is also not known if those cells that selectively grow from primary tissue explants are representative of the total cell populations from which they come (Fertil and Malaise, 1981; Cox and Masson, 1980; Weichselbaum et al., 1980).

B. Monoenergetic Bragg Peak Dose-Effect Relationships

Survival-dose response relationships have been measured in track segment experiments, with residual range of the ions functioning as the independent variable. As discussed in Section III above, particle track structure, nuclear fragmentation products, and other characteristics of energy transfer specific to each particle species are unique to each residual range studied in a monoenergetic Bragg ionization curve. The most extensive set of survival data using unmodified Bevalac beams has been acquired with the human T-1 cell line. This cell line was selected for our studies because of the abundance of data already in existence on its responses to X rays, γ rays, neutrons, and low-energy accelerated heavy ions (Todd, 1967; Barendsen, 1968a). Aerobic and hypoxic human T-1 cell survival measurements of 400 MeV/u carbon, 425 MeV/u neon, 570 MeV/u argon beams have been published (Blakely et al., 1979, 1980a).

A preliminary report on the first biological response to monoenergetic silicon beams (530 and 670 MeV/u) is also available (Blakely et al., 1980b). The predominant feature of the survival data measured at the various residual range positions of the Bevalac beams is the change in the shape of the survival curves from linear (single-hit) multitarget (LMT) at low LET, to exponential in the Bragg peak of the neon, silicon, and argon beams.

1. Modeling of Survival Measurements

Several analytical equations have been used to evaluate cell survival data, including the classical linear multitarget expression (Lea, 1955; Elkind and Sutton, 1960; Wideroe, 1966), the linear-quadratic (LQ) model (Jacobson, 1957; Neary, 1965; Sinclair, 1966; Chadwick and Leenhouts, 1975, 1978), including the dual theory of radiation action (Kellerer and Rossi, 1972, 1978), the ion-kill gamma-kill model (Katz et al., 1971; Roth and Katz, 1980), the repair-saturation model (Haynes, 1966; Green and Burki, 1972), and the repair-misrepair (RMR) model (Tobias et al., 1980). The accuracy and the predictive capabilities of these models are still being evaluated.

Precise analysis of data obtained with the same cell system over several years is hampered by the day-to-day variations in the biological response. Even in experiments designed to minimize this limitation, (e.g., self-contained experiments using the same stock of cells), the available theoretical models of cell inactivation do not fit adequately the particle dose-survival data that have been obtained at all dose levels covering three or four logs of survival.

In order to reduce some of the variation in analyzing the dependence of biological effects on particle velocity, an analysis was completed which was restricted to an evaluation of the linear coefficient of the data fitted to the LQ model. Subtraction of the biological response to primary particles from

the response to secondary fragments, uncovered the atomic number and particle velocity dependence of the inactivation parameter (Blakely et al., 1979). As shown in Figure 7 a separate curve is obtained for each particle beam studied when a theoretical expression for the cross-section σ is plotted as a function of the particle velocity parameter $(1/\beta^2)$. The cross section σ is given by:

$$\sigma = \sigma_{min} + \sigma_{max} \left[1 - \exp(-a\, z^h/\beta^k)\right] \qquad (12)$$

where σ_{max} represents the saturation value of the cross section, a is a constant that depends on the gas milieu; σ_{min} represents a limiting cross section for values of β near unity at high kinetic energies where the track structure is lost, and the radiation effects resemble those from low-LET radiation. The exponent k relates to the effect of velocity on the radial structure of energy transfer, and should be independent of the atomic number (z). The exponent h, which relates to the charge dependence of energy transfer and should be independent of the velocity, is assumed to be about 4. As expected, the curves are spaced by the approximate factor of the ratio of Z^4 values. For hypoxic cells the data agree with a slope of $Z^4/\beta^{4.6}$, and for aerated cells the slope is Z^4/β^4.

This analysis and the evaluation of RBE and OER measurements summarized in the next section led to the suggestion that a particle beam intermediate between neon and argon in atomic weight would have an OER advantage, and would generally produce less fragmentation and less overkill effect than an argon beam.

The data in general indicate that neither dose-averaged or track-averaged LET adequately described the effects as a uniquely single valued function of LET, and that three independent physical variables are needed to model survival

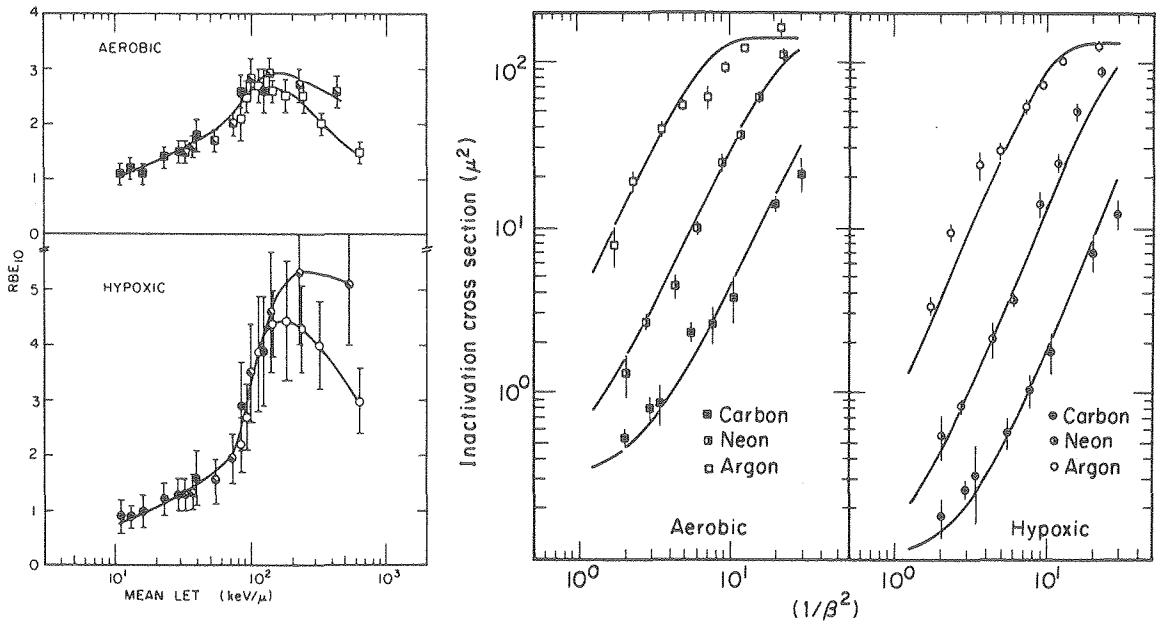

Figure 7 Left panel: Aerobic and hypoxic RBE at 10 percent human cell survival in vitro as a function of track-average mean LET: carbon data (●,■), neon data (◐,◧), and argon data (○,□). Error bars are for 95 percent confidence limits.

Right panel: Human cell inactivation cross section in vitro versus $1/\beta^2$. (From Blakely et al., 1979).
(XBL 781-12333B)

(Blakely et al., 1979). Convenient variables may be fluence, particle velocity, and charge, or alternatively dose, mean LET_{∞} and charge.

2. RBE and OER Values for Monoenergetic Beams

Figure 8 is a composite plot of OER and hypoxic RBE values at 10 percent survival over the last seven centimeters of residual range of 400 MeV/u carbon, 425 MeV/u neon, 530 MeV/u silicon, and 570 MeV/u argon beams. The comparison indicates increasing effectiveness and decreasing oxygen effect with increasing atomic number of the particle, especially in the last few centimeters of range near the Bragg peak. The order of the relationship of the effects for the beams continues even at residual ranges beyond the peak, where fragments of the primary beam are solely responsible for cell killing.

The carbon and neon beams both show sharp and rather narrow RBE peaks and OER valleys with respect to these values as a function of range; the silicon and argon RBE peaks and OER valleys are somewhat broader. The neon, silicon, and argon hypoxic RBE values are greatest (at values of between 4 and 5) just upstream of the Bragg peak; carbon hypoxic RBE values peak at just less than 4 at the closest residual range measured near the Bragg peak. The width of the RBE peak increases dramatically as a function of residual range with increasing atomic number from neon to argon. The OER is low (<1.5) for both silicon and argon beams over the last few centimeters of residual range.

The data accumulated with unmodified Bevalac beams permit a comparison of the LET dependence of aerobic RBE measurements from beams of high atomic number and high initial energy, with that of RBE measurements from deuterons to argon ions of low initial energy. Figure 9 summarizes the results obtained with four human and three hamster cell lines. With the exception of the human lymphocytes (Madhvanath et al., 1976), all of the RBE-LET plots peak between

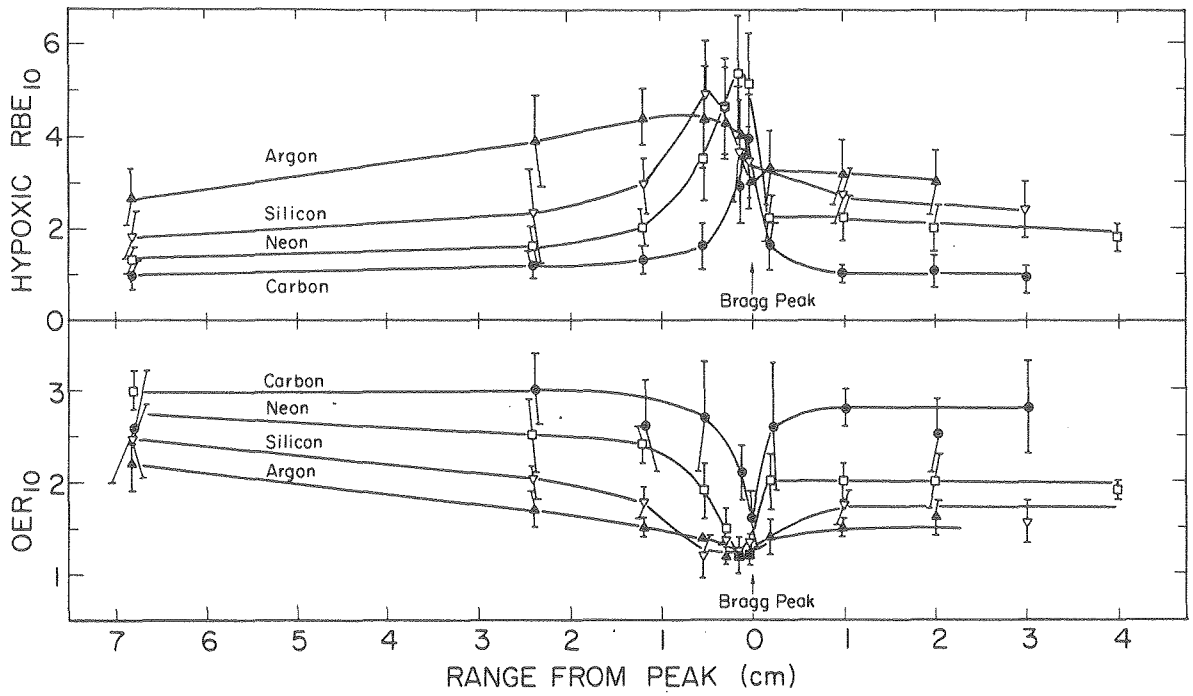

Figure 8 Range dependence of hypoxic RBE and OER at 10 percent human cell survival in vitro for 570 MeV/u argon, 530 MeV/u silicon, 425 MeV/u neon, and 400 MeV/u carbon beams. (XBL 819-4168)

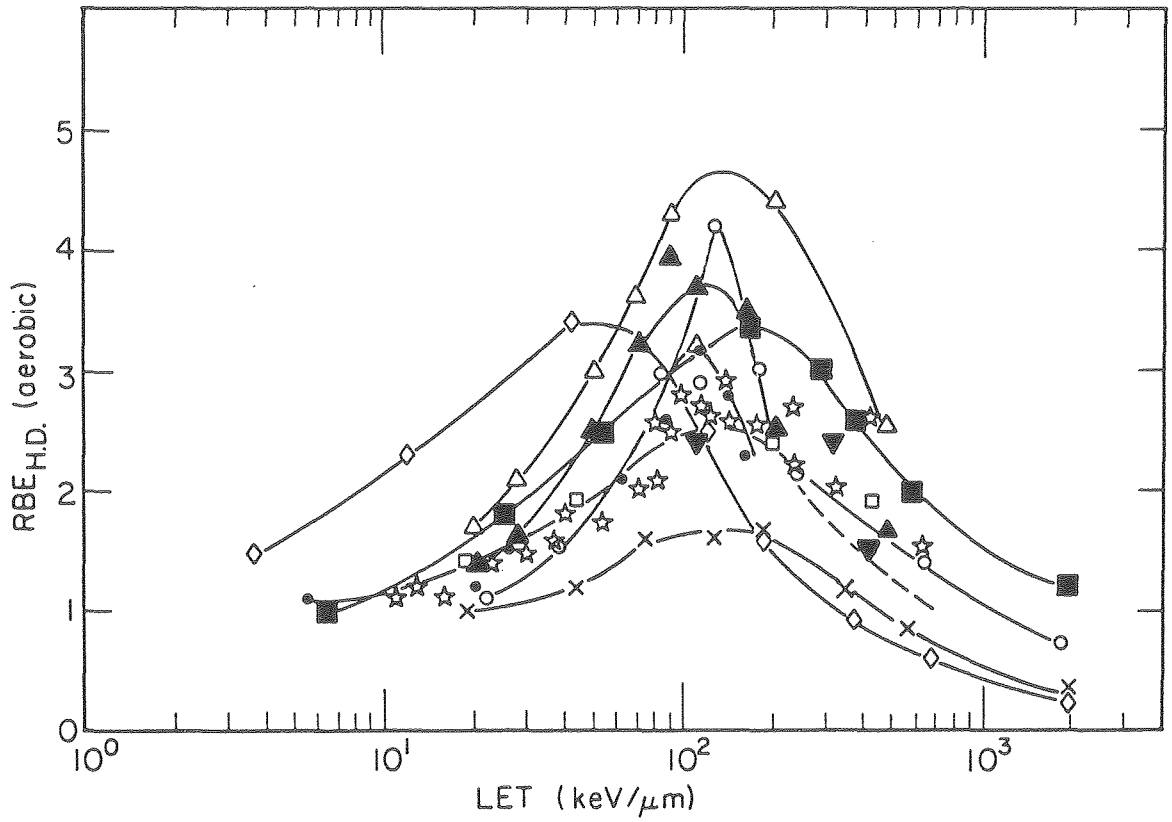

Figure 9 LET dependence of aerobic high dose mammalian cell RBEs for monoenergetic heavy ion beams. Comparison is made between data from heavy-ion beams of low initial energy:

- ● Barendsen, 1968 (human T-1 cell),
- ■ Todd, 1967 (human T-1 cell),
- ▲ Cox et al., 1977 (human fetal lung),
- △ Cox et al., 1977 (Chinese hamster V-79),
- □ Deering and Rice, 1962 (HeLa)
- X Skarsgard et al., 1967 ($CH2B_2$)
- ◇ Madhvanath et al., 1976 (human lymphocytes)

and data from heavy-ion Beavalac beams of high initial energy ($\geq$400 MeV/u):

- * Blakely et al., 1979 (human T-1 cell)
- ▼ Hall et al., 1977 (Chinese hamster V-79)
- ○ Ngo et al., 1981 (Chinese hamster V-79). (XBL 819-4167A)

100-200 keV/μm. The lymphocytic survival end point may not be comparable to the reproductive integrity end point of the other cell lines, which may account for the suggestion of a maximum RBE at a lower LET. Although the other cell lines show a common LET range for maximum cell killing, the value of the maximum RBE varies fourfold. The significance of this apparent RBE difference between cell lines is unknown, but may be due to differences in the cross section of sensitive targets or to differences in repair capacity. The variations in cell specific RBE can be even more significant at low-dose when cell lines with quite different low-dose and low-LET responses are compared.

As demonstrated in the left panel of Figure 7, mean LET is not an adequate predictor of biological effects because above 100 keV/μm mean LET_∞ does not uniquely characterize RBE. At each LET_∞ above 100 keV/μm, the RBE values for argon are lower than for neon. The separation of the RBE curves above 100 keV/μm may be caused by the velocity dependence of these effects, or by the presence of different degrees of fragmentation, or both.

Analysis of the monoenergetic Bevalac cellular data shows that despite considerable scatter, the velocity dependence of primary beam killing effects can delineate particle charge differences. As shown in the right panel of Figure 7, the analysis also demonstrates that the slope dependence of the velocity parameter is different for aerobic and hypoxic irradiation conditions.

Physical processes that fragment the primary beam are currently under study (see Section III), and biological experiments are being conducted under identical beam conditions to evaluate the fragmentation effects on living systems. In general, argon beams have considerably more fragmentation than neon beams of similar range, and silicon beams have intermediate levels. Both cellular (Blakely et al., 1979; Chapman et al., 1977; Curtis et al., 1982;

Raju et al., 1978c) and tissue studies (Alpen and Power-Risius, 1981; Alpen et al., 1980; Goldstein et al., 1981a, 1981b; Raju and Carpenter, 1978) have demonstrated diminished effectiveness for stopping argon ions where fragmentation is prominent. What is not yet understood is to what extent primary beam effects will be altered by simultaneous exposure of biological material to fragmentation products of lower LET.

A comparison of published measurements of the dependence of OER on mean LET is shown in Figure 10. The results from three separate investigators were all obtained with human T-1 cells, but each investigation involved charged particles of different energy ranges. Barendsen et al. (1966) used a variable low energy helium-ion and deuteron cyclotron and a ^{210}Po source for the lowest α-particle energies. Todd (1967) used various high energy heavy ion species of up to 10 MeV/u produced in a linear accelerator, and Blakely et al. (1979) used heavy ions of 400 to 570 MeV/u produced at the Bevalac. In each case the OER is high (2.7-2.9) at low LET, and decreases to 1.2 or less at greater than about 250 keV/μm. However, the OER dependence of the three sets of data is quite different between 10 and 70 keV/μm. The higher OER values measured using Bevalac beams may be due in part to the presence of low-LET fragments or differences in the delta-ray contributions in the beams that were studied. It has also been suggested that the difference between the results of Barendsen and Todd may be due to differences in delta ray distribution (Curtis, 1970).

Two mechanisms may be responsible for the reduction in the OER with increasing LET. Alper (1956) and Alper and Howard-Flanders first suggested the "interacting-radical" hypothesis, which proposed a greater probability of a fixation reaction occurring between radicals in dense ionization tracks, diminishing the importance of interactions with oxygen (1956). The second

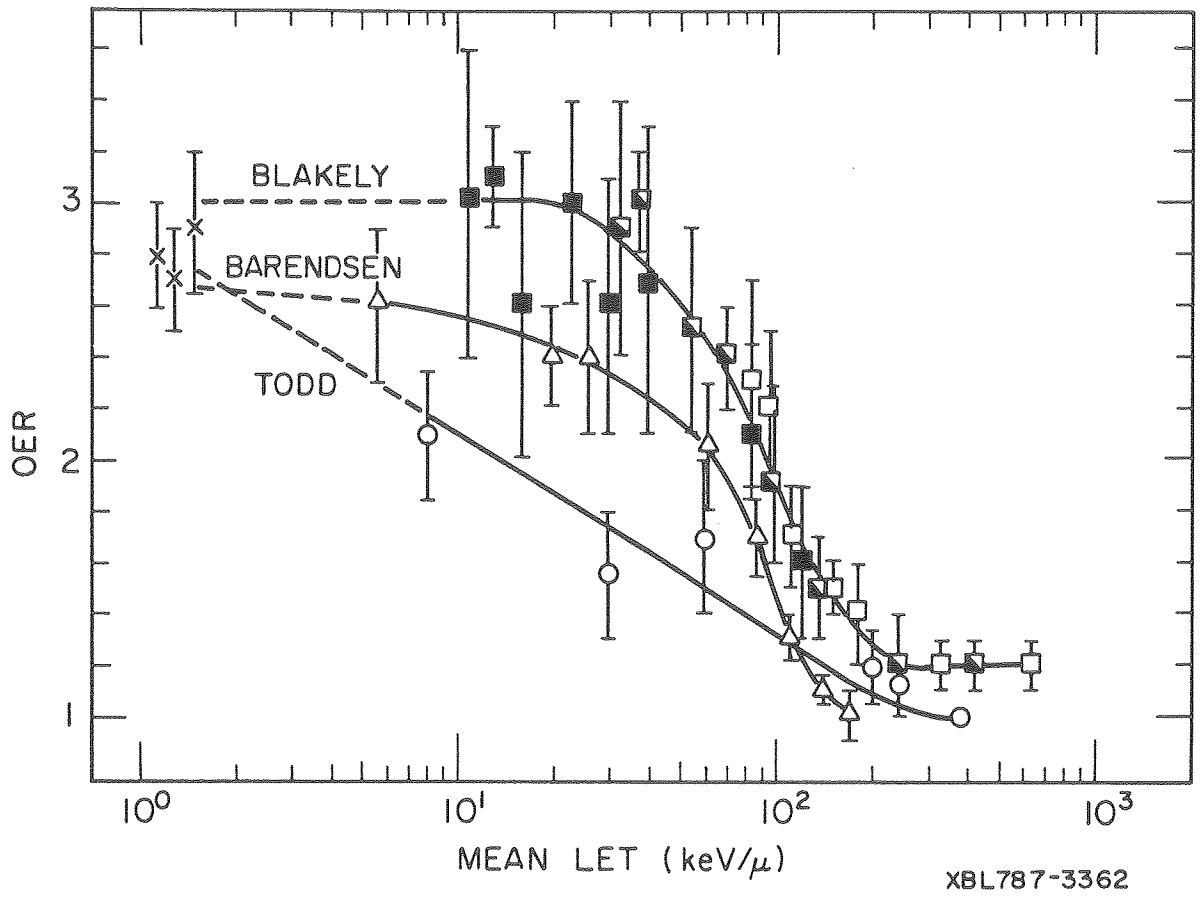

Figure 10 OER (95 percent confidence limits) versus track-average mean LET: carbon (■), neon (◪), and argon (□) beams from the Bevalac (Blakely et al. 1979); Barendsen et al. (1966) low-energy helium ion data (△); Todd (1967) heavy-ion data up to 10 MeV/u (○); and x-ray data (X). (XBL 787-3362)

mechanism is the "oxygen-in-the-track" hypothesis (Shekhtman, 1960; Neary, 1965) which assumes that molecular oxygen is produced by the radiolysis of water in the particle track and thereby renders the cell oxyenated at the time of irradiation. This hypothesis has been supported by calculations of oxygen production in particle tracks traversing an alga and also in a bacterium (Alper and Bryant, 1974; Bryant and Alper, 1976), but not convincingly by small G value measurements of molecular oxygen production in tracks of 20 MeV deuterons and 40 MeV alpha-particles, or even heavier ions (Baverstock and Burns, 1976, 1981; Sauer et al., 1978; Burns et al., 1981).

Preliminary work has been done with heavy ions to measure OER with different concentrations of oxygen to explore by what mechanism(s) oxygen sensitizes cells to ionizing radiation, and to inquire if that mechanism is different at high LET (Tobias et al., 1977). At about 90 keV/μm (OER of about 2) for both neon and argon beams, the oxygen concentration at which half of the maximum oxygen effect occurs (the K value) is significantly greater than the K value for X rays. Alper et al. (1967) reported similar results with bacteria for fast neutrons. We have tentatively concluded that the core of the heavy-ion tracks, in which free radicals reach a very high density, are chiefly responsible for the reduction of the OER from a value of 3 (X rays) to 2 (neon and argon at 90 keV/μm). The effects we see with oxygen concentrations less than 100 percent are probably due to modification of the effects in track areas having low free-radical density, or to oxygen reactions with relatively long-lived macromolecular free radicals (~10 sec). These questions are being studied in experiments with radical scavengers.

C. Extended Bragg Peak Studies

Table I is a summary of the experimental cellular systems that have been used to characterize extended Bragg peak heavy-ion beams. Experiments with

these systems were almost exclusively designed to measure RBE and OER values of heavy-ion beams modified with variable absorbers to widen the effective Bragg peak for clinical applications. The Bragg ionization curves depicted in Figure 2 indicate some of the ion beams and energies that are available at the Bevalac. Bragg peak widths ranging from 2 cm to 14 cm can be obtained, but for comparative purposes most investigators have concentrated on studies with a narrow, 4-cm peak or a broader, 10-cm peak. Rather than compare beams of different atomic number at the same energy, a more relevant question became how did the biological responses for different ions compare at the same beam range. As demonstrated in Figure 2, this comparison requires higher initial beam energies for the heavier ion beams in order to compare all the ions at similar range. Experiments conducted at identical beam atomic number and initial energy and with the same spiral filter may still have some differences in beam character or composition depending on the specific configurations (e.g., collimation or scattering) used by different investigators with the various cell systems. Dosimetric methods for delivering heavy-ion doses have been standardized and constitute a major contribution to the heavy-ion project from J. Howard, T. L. Criswell, J. T. Lyman, and the Bevalac operations staff.

1. RBE and OER Values for Modified Beams

a. Human T-1 Cell Monolayers

For purposes of comparison with the monoenergetic Bragg peak RBE and OER data, the human T-1 cell line was also used to measure RBE and OER values in extended peaks (Blakely et al., 1978; Blakely, 1983). Figure 11 is a composite of the OER and aerobic and hypoxic RBE values at 10 percent survival for pristine and extended Bragg peaks of carbon, neon, silicon, and argon beams of the various initial energies. The high LET effects of increased RBE

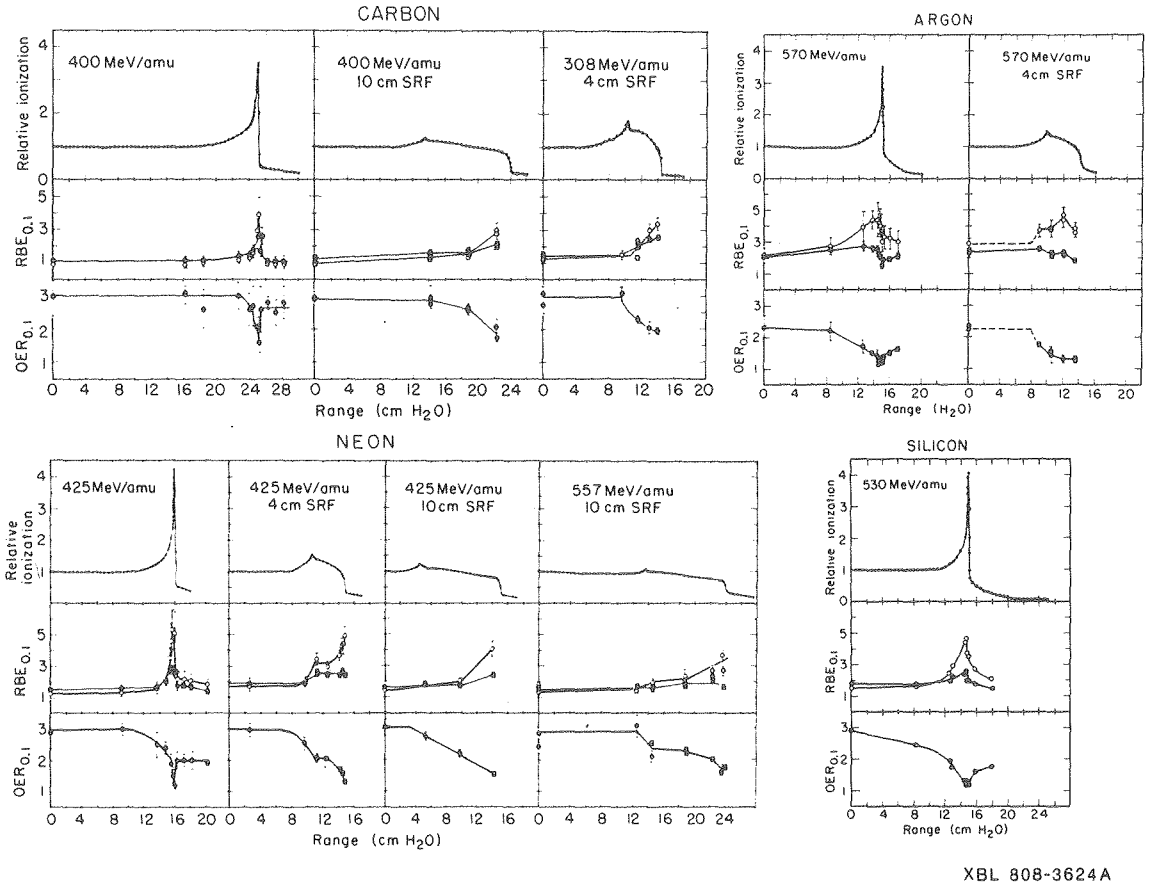

Figure 11 Composite figure of physical Bragg ionization curves and aerobic (solid symbols) and hypoxic (open symbols) RBE-10 and OER-10 measurements as a function of range for monoenergetic and 4-cm and 10-cm extended Bragg peaks of Bevalac beams. Biological data are based on human T-1 cell survival in vitro. Error bars are 95 percent confidence limits for monoenergetic beams and 50 percent confidence limits for extended Bragg peaks. (XBL 808-3624A)

and reduced OER occur predominantely in the Bragg peak region. The argon beam data are different than data from the other beams in that the aerobic RBE value for the human T-1 cell drops significantly upstream of the pristine Bragg peak, shows a high, flat RBE in the plateau, and then drops from the proximal to distal end of the sloped 4-cm peak ionization region design. The original spiral ridge filter design was not optimal for the argon ion beam; therefore, another filter was designed. Preliminary silicon data with both the 4-cm and 10-cm spiral ridge filter (not shown) indicate that the RBE value does not drop off across the peak. In general, the lower the initial beam energy, the higher the RBE and lower the OER over the full width of the extended peak. The RBE values at the distal end of beams of the same ion but with different Bragg peak widths were quite similar if the beams were of the same energy; however, in most cases the RBE was lower and OER higher for the proximal end of the wider extended Bragg peaks.

When beams of similar range were compared, the carbon beams consistently had the greatest peak-to-plateau physical dose ratio, as indicated by the height of the Bragg ionization peak. Increasing the initial beam energy decreased the peak-to-plateau dose ratio in all cases. The peak-to-plateau RBE ratio was greatest for neon, with carbon's peak-to-plateau RBE ratio being very similar at short range and less so at longer range. The argon beam had peak-to-plateau dose ratios that were similar to neon, but had peak-to-plateau RBE ratios that were significantly less than any of the other beams. However, argon was remarkable for its significantly low OER of 1.4 over broad ranges of both the pristine and extended Bragg peaks.

b. Cell Suspensions of the R-1 Rhabdomyosarcoma Cell Line

An extensive amount of cell survival information on the range-filtered Bevalac beams has been obtained using the R2D2 subline of the rat R-1 rhabdomyosarcoma tumor (Curtis et al., 1982). The cells in stirred suspension were

sequentially sampled before and after delivery of small dose increments. This technique was adapted from one used by Chapman et al. (1977). Figure 12 depicts a sample of the radiobiological RBE and OER data at four depths of the 14-cm range carbon, neon, and argon beams modified with the 10-cm spiral ridge filter. The cross-hatched area indicates the range dimensions the cell populations occupied during the exposure.

The rhabdomyosarcoma system is particularly valuable because it can be studied both in vitro (Curtis et al., 1982) and in vivo (Tenforde et al., 1980). Tumor regression studied with both acute and fractionated dose regimes have beem examined (Tenforde et al., 1981a), but only the in vitro work will be described here.

We compared the RBE and OER measurements made using the R-1 suspensions with the measurements made using the human T-1 monolayers. The upper panel of Figure 13 is a plot of the aerobic RBE values at 10 percent survival from both the T-1 and R2D2 systems for extended Bragg peaks of all beams studied versus the dose-averaged LET values estimated by Curtis et al. (1982). The RBE values for both sets of data were referenced to 225 kVp X rays. In the mixed LET fields of extended Bragg peaks (see Section IIIC), it appears that both these cell lines show an RBE maximum at an LET between 100 and 200 keV/μm. If there are differences in the LET at which the maximum RBE occurs for these cells, these differences are small and not resolvable in the highly mixed LET fields. Cell line comparison studies of this kind are more appropriately conducted using cell monolayers in monoenergetic beams.

The oxygen gain factor (OGF) is used to compare OER values in two systems that have different low-LET OERs. The OGF is the ratio of the OER obtained with the reference low-LET radiation source, to the OER obtained with the

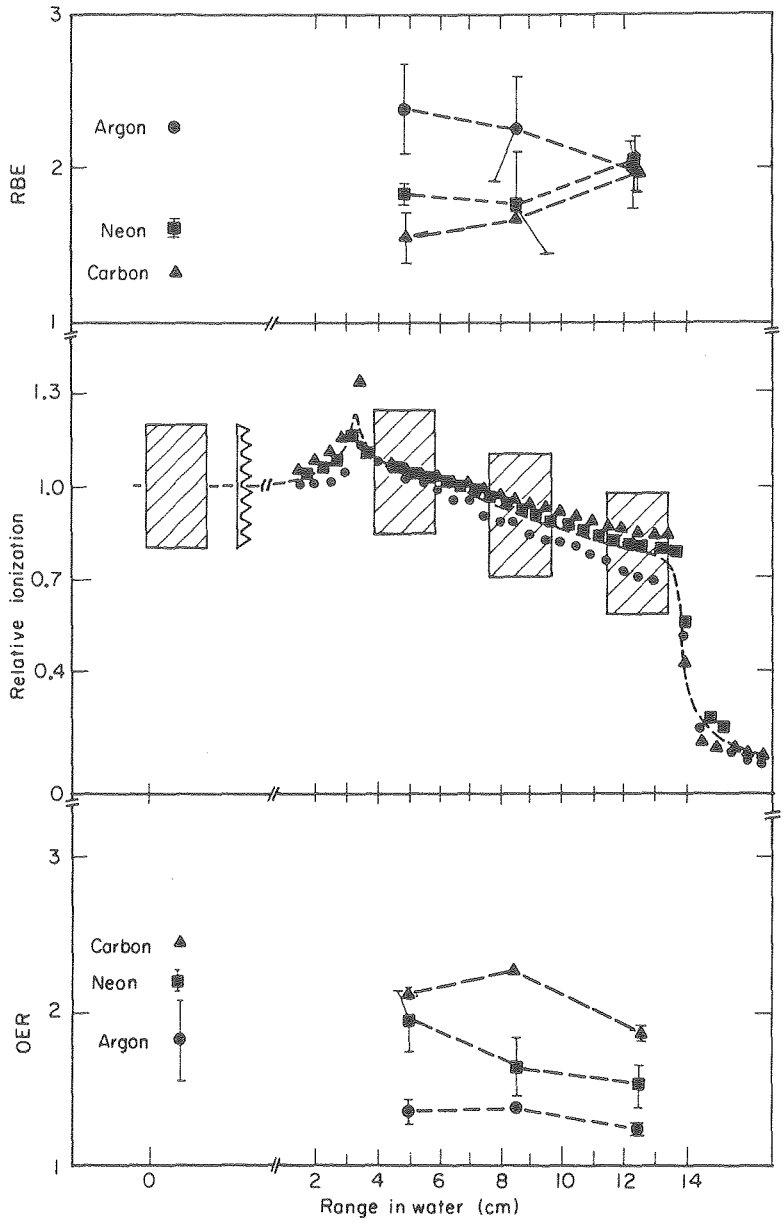

Figure 12 Physical depth-dose distributions, RBE values for oxic cell suspensions at the 10 percent survival level, and OER values of the 10 percent survival level are shown for carbon, neon, and argon beams with 10-cm extended peak regions and a range of approximately 14 cm in water. The error bars represent one standard deviation for RBE and OER values measured in two or four separate experiments. Biological data are based on measurements with rat rhabdomyosarcoma in vitro. (From: Curtis et al., 1982.) (XBL 808-3617)

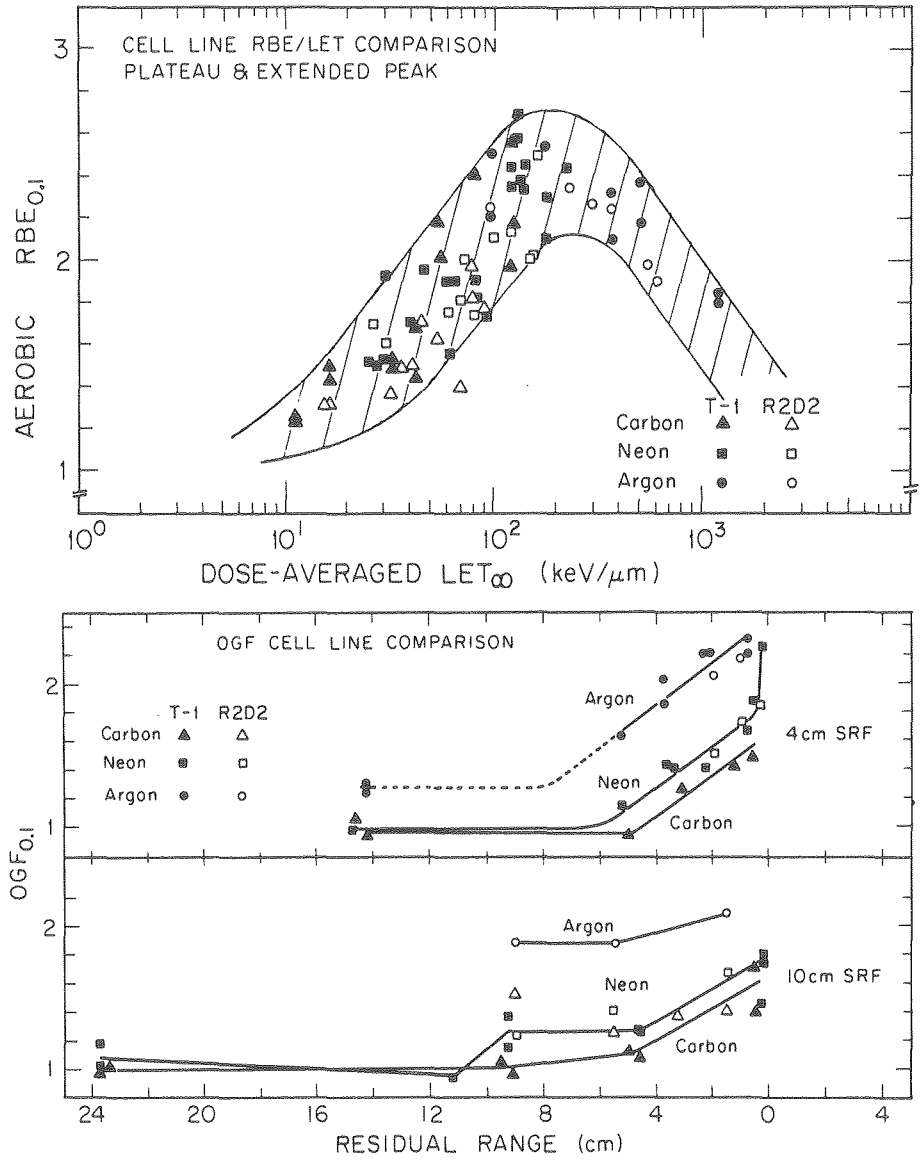

Figure 13 Upper panel: Aerobic RBE-10 values versus dose-averged LET (keV/μm) from plateau and extended heavy-ion Bragg peak data using human T-1 cell monolayers (Blakely et al., 1978) and rat rhabdomyosarcoma cell suspensions (Curtis et al., 1981).

Lower panel: OGF as a function of residual range for: 308 MeV/u carbon, 425 MeV/u neon, and 570 MeV/u argon beams with a 4-cm extended Bragg peak; 400 MeV/u carbon, 557 MeV/u neon, and 570 MeV/u argon beams with a 10-cm extended Bragg peak. Data are from human T-1 cell monolayer survival measurements (Blakely et al., 1978) and rat rhabdomyosarcoma cell suspension survival measurements (Curtis et al., 1981). (XBL 809-3678A)

high-LET test beam. Comparisons of OGF values eliminate differences in the efficiency of oxygen removal between experimental techniques. The lower panel of Figure 13 shows that for both cell lines, the OGF is greatest for argon, with neon and carbon showing successively less gain at the ranges studied.

c. Other Cell Systems

RBE data from the various beams for six cell lines in addition to the two described above are collected in Figure 14, including both high energy mono-energetic and ridge-filtered heavy-ion beams. There is a region that shows aerobic RBE increasing from 1.0 at low-LET levels (of less than 10 keV/μm), to a maximum of 3.0 at about 140 to 160 keV/μm. The RBE then decreases rapidly at higher LET. The mean LET values for most of the Bevalac data lie in the ascending region of the RBE plot. Although not demonstrated here, the RBE is a rapidly changing function of the survival level, increasing with decreasing dose.

Figure 15 is a summary plot of RBE and OGF trends for each beam for cellular systems using the Bevalac beams of two ranges and with two spiral ridge filters. The data are also tabulated in Tables IIA-IIC. The summary is consistent with the data sets of the human T-1 and rat R-1 cell systems, but it shows more scatter than each individual system. The results show the similarity of RBE and OGF values of both carbon and neon, the major distinction being the somewhat higher neon OGF and RBE obtained across the peaks of most of the beam configurations. On the other hand, the argon beam in the entrance plateau has a high RBE that drops precipitously across the peak region. These data led to the development of a special argon spiral ridge filter with a flat dose distribution (see Figure 2 and Raju et al., 1980c). The argon results show an OGF advantage at each range studied even in the distal peak where the

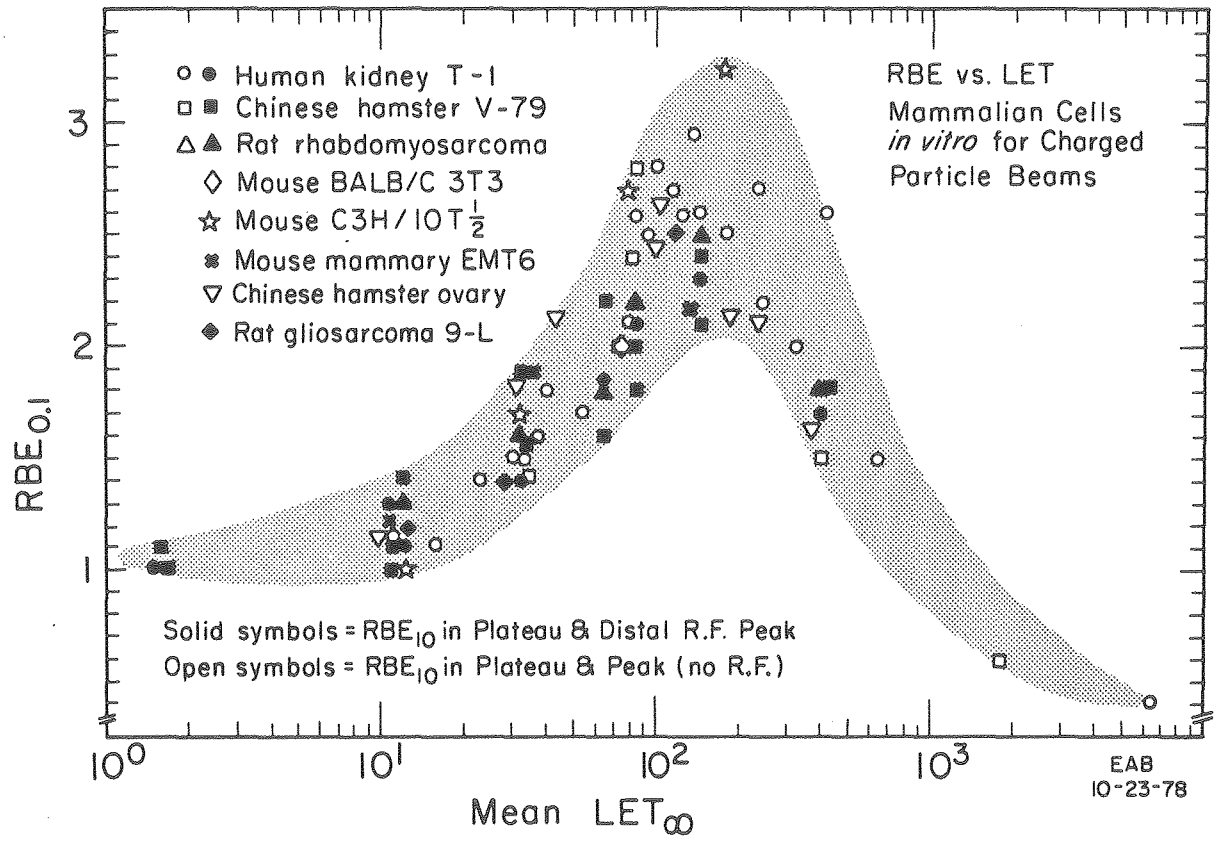

Figure 14 Aerobic RBE-10 vs. mean LET_∞ for monoenergetic and extended Bragg peak data using mammalian cell survival data measured in vitro. The results are compiled from eight different cell systems (Blakely et al., 1978, 1979, 1980a; Lücke-Hühle et al., 1979; Ngo et al., 1981; Roots et al., 1980; Chapman et al., 1977; Curtis et al., 1981; Leith et al., 1975; Yang et al., 1979, 1980; Goldstein et al., 1981a). (XBL 7810-3663A)

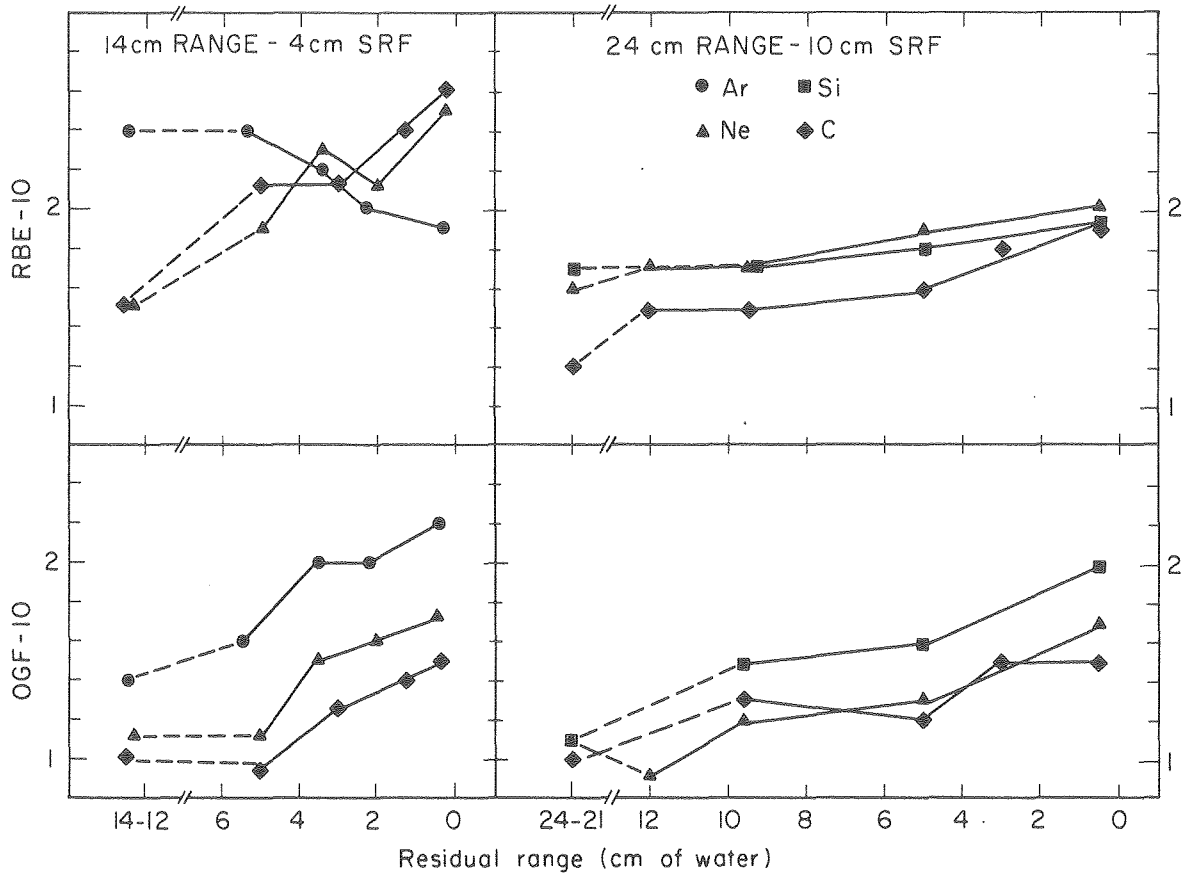

Figure 15 Summary of range dependence of aerobic RBE and OGF at 10 percent cell survival in vitro for Bevalac beams of approximately 14 cm range (with 4-cm extended Bragg peak) and of approximately 24 cm range (with 10-cm extended Bragg peak). Data are from: Blakely et al., 1978, 1980a, 1980b; Chapman et al., 1977, 1978; Curtis et al., 1981; Raju et al., 1978c; Rodriguez and Alpen, 1980, 1981; Lücke-Hühle et al., 1980. (XBL 832-3567)

Table IIA. Cellular Survival RBE* and OGF Values Measured In Vitro at Various Ranges of Extended Bragg Peak Ionization Regions

C A R B O N

	Initial Energy (MeV/u)	Plateau		Preproximal		Proximal		Mid		Mid Distal		Distal		Reference
		RBE_{10}	OGF_{10}	RBE_{10}	OGF_{10}	RBE_{10}	OGF_{10}	RBE_{10}	OGF_{10}	RBE_{10}	OGF_{10}	RBE_{10}	OGF_{10}	
4-cm Extended Peak	308	1.48(0.09)	1.00	2.06(0.12)	0.94	2.09(0.14)	1.26	2.42(0.12)	1.41	--	--	2.59(0.12)	1.48	Blakely et al., 1978, 1980a
	400	1.32(0.10)	1.07	--	--	1.39(0.04)	1.58	--	--	--	--	1.78(0.22)	1.51	Curtis et al., 1981
	400	1.40	1.08	--	--	--	--	2.48	1.65	--	--	--	--	Chapman et al., 1977
	400	1.55	--	--	--	--	--	3.53	--	--	--	--	--	Chapman et al., 1977
	400	1.41	--	--	--	--	--	2.16	--	--	--	--	--	Chapman et al., 1977
	400	1.0	--	--	--	--	--	--	--	--	--	--	--	Rodriguez and Alpen, 1980, 1981
	400	1.0	--	--	--	--	--	1.8	--	--	--	--	--	Lücke-Hühle et al., 1980
	$\bar{X}$ =	1.3	1.1	--	--	1.4	1.6	2.5	1.6	--	--	1.8	1.5	
10-cm Extended Bragg Peak	308	1.32	1.07	--	--	1.53(0.16)	1.23	1.66(0.02)	1.15	--	--	1.96(0.03)	1.38	Curtis et al., 1981
	400	1.22(0.08)	1.00	--	--	1.52(0.09)	1.02	1.56(0.10)	1.11	--	--	2.07(0.15)	1.56	Blakely et al., 1978, 1980a
	400	1.42	1.08	1.50	--	1.63	--	1.84	1.22	2.06	--	2.22	1.70	Chapman et al., 1978
	400	--	--	--	--	1.39(0.13)	1.53	1.48(0.05)	1.26	1.62(0.20)	1.49	1.82(0.22)	1.40	Curtis et al., 1981
	400	1.0	0.9	--	--	--	--	1.3	1.1	--	--	1.6	1.3	Raju et al., 1978c
	$\bar{X}$ =	1.2	1.0	1.5	--	1.5	1.3	1.6	1.2	1.8	1.5	1.9	1.5	

* Reference Radiation: 200-250 kVp X rays

Table IIB.

NEON

	Initial Energy (MeV/u)	Plateau RBE_{10}	Plateau OGF_{10}	Preproximal RBE_{10}	Preproximal OGF_{10}	Proximal RBE_{10}	Proximal OGF_{10}	Mid RBE_{10}	Mid OGF_{10}	Mid Distal RBE_{10}	Mid Distal OGF_{10}	Distal RBE_{10}	Distal OGF_{10}	Reference
4-cm Extended Bragg Peak	425	1.79(0.11)	0.96	1.94(0.12)	1.14	2.50(0.16)	1.42	2.34(0.12)	1.40	--	--	2.53(0.11)	1.79	Blakely et al., 1978, 1980a
	425	1.60(0.06)	--	--	--	2.16(0.0)	1.51	--	--	--	--	2.51(0.09)	1.68	Curtis et al., 1981
	400	1.57	1.17	--	--	--	--	2.08	1.75	--	--	--	--	Chapman et al., 1977
	400	1.35	--	--	--	--	--	1.90	--	--	--	--	--	Chapman et al., 1977
	400	1.46	--	--	--	--	--	2.00	--	--	--	--	--	Chapman et al., 1977
	425	1.1	--	--	--	--	--	--	--	--	--	--	--	Rodriguez and Alpen, 1980, 1981
	425	1.4	--	--	--	--	--	2.4	--	--	--	--	--	Lücke-Hühle et al., 1980
	$\bar{X}$ =	1.5	1.1	1.9	1.1	2.3	1.5	2.1	1.6	--	--	2.5	1.7	
10-cm Extended Bragg Peak	400	--	--	--	--	1.81(0.07)	1.34	1.75(0.33)	1.59	2.10(0.23)	1.44	1.98(0.19)	1.71	Curtis et al., 1981
	425	1.65(0.08)	0.94	--	--	1.92(0.10)	1.06	1.76(0.09)	1.31	--	--	2.44(0.14)	1.88	Blakely et al., 1978, 1980a
	400	1.9	1.2	--	--	--	--	2.2	1.4	--	--	2.4	1.5	Raju et al., 1978c
	$\bar{X}$ =	1.8	1.1	--	--	1.9	1.2	1.9	1.4	2.1	1.4	2.3	1.7	
	557	1.47(0.08)	1.11	1.68(0.10)	0.94	1.73(0.10)	1.26	1.83(0.08)	1.26	--	--	2.05(0.09)	1.66	Blakely et al., 1978, 1980a
	557	1.70	1.02	--	--	1.75(0.16)	1.24	2.01(0.09)	1.41	--	--	2.02(0.07)	1.66	Curtis et al., 1981
	$\bar{X}$ =	1.6	1.1	1.7	0.9	1.7	1.2	1.9	1.3	--	--	2.0	1.7	

* Reference Radiation: 200-250 kVp X rays

Table IIC.

A R G O N

	Initial Energy (MeV/u)	Plateau RBE_{10}	Plateau OGF_{10}	Preproximal RBE_{10}	Preproximal OGF_{10}	Proximal RBE_{10}	Proximal OGF_{10}	Mid RBE_{10}	Mid OGF_{10}	Mid Distal RBE_{10}	Mid Distal OGF_{10}	Distal RBE_{10}	Distal OGF_{10}	Reference
	570	2.30(0.14)	1.27	2.54(0.11)	1.64	2.15(0.17)	1.93	2.29(0.12)	2.20	—	—	1.83(0.16)	2.24	Blakely et al. 1978, 1980a
	570	2.24(0.04)	1.43	—	—	2.25(0.12)	2.06	—	—	—	—	1.92(0.22)	2.17	Curtis et al., 1981
4-cm Extended Bragg Peak	570	2.46	1.56	2.15	1.65	—	—	2.04	2.00	—	—	—	—	Chapman et al., 1977
	570	2.26	—	—	—	—	—	1.80	—	—	—	—	—	Chapman et al., 1977
	570	2.60	—	—	—	—	—	2.14	—	—	—	—	—	Chapman et al., 1977
	570	2.6	—	—	—	—	—	2.1	—	—	—	—	—	Rodriguez and Alpen, 1980, 1981
	570	—	—	—	—	—	—	2.1	—	—	—	—	—	Lücke-Hühle et al., 1980
	$\bar{X}$ =	2.4	1.4	2.4	1.6	2.2	2.0	2.0	2.0			1.9	2.2	
10-cm Extended Bragg Peak	570	—	—	—	—	2.36(0.29)	1.91	2.26(0.34)	1.86	—	—	1.97(0.36)	2.10	Curtis et al., 1981
	500	2.0	1.6	—	—	—	—	2.1	1.6	—	—	1.8	1.9	Raju et al., 1978c
	$\bar{X}$ =	2.0	1.6	—	—	2.4	1.9	2.2	1.7	—	—	1.9	2.0	

* Reference Radiation: 200-250 kVp X rays

RBE is dropping. Argon is clearly superior to all the beams in reducing the OER; however, no argon data are yet available at the 24-cm range.

Silicon has an intermediate atomic number between neon and argon. Preliminary results with a 670 MeV/u beam using the 10-cm spiral ridge filter indicate that it has an LET spectrum that (like argon) is superior in reducing the oxygeneffect (high OGF), but that also has RBE characteristics more like neon (Blakely et al., 1980b; Tenforde et al., 1982a). Further silicon experiments are underway.

2. Isoeffective Cell Killing

The objective of range filter design is to extend the effective Bragg peak region by accumulating stopping particles over the broader dimensions required in radiotherapy, i.e., to give a region of isoeffective cell killing several-fold wider than the stopping width of a pristine Bragg peak. There are several parameters to consider in this task, including the beam characteristics of energy deposition and fragmentation, the model for cell inactivation that is used to predict the low-dose response in the mixed LET radiation fields, the specific available cell line sensitivities selected for the modeling and their RBE-LET dependence, and the dose level desired for the isoeffective region.

Range filters in use at the Bevalac were designed by Lyman (1982), and were based on physical beam parameters and available biological data. As cellular information has accumulated with the initial filter designs, the information has been used to design better filters. A representative biological dose-response profile was developed, and several filters of a newer spiral design were tooled to extend Bragg peaks to a width of 4 or 10 cm. In some cases different particles require different filters in order to achieve isoeffective killing across the extended peak. As will be described below, in certain

other cases the physical and biological properties of beams appear to be similar enough to use the same filter for isoeffectiveness.

In order to demonstrate the isoeffectiveness of the available filters using a single cell line (T-1), the RMR model for cellular inactivation (Tobias et al., 1980) was used to fit heavy-ion survival data by least-squares regression, and to calculate aerobic RBE values at the 50 percent survival level. The RMR model was selected because it yields a fit to cell survival data that is representative of fits made with other available models. This model also has other characteristics useful for analytical interpretation.

The RBE-50 values for the ranges studied were multiplied by the measured physical dose at each range studied. The resultant normalized biologically effective dose (BED) has been plotted over each of five Bragg curves of physical dose in Figure 16. The same 4-cm and 10-cm spiral ridge filters were used for each beam studied. The data for the 4-cm carbon and neon beams show fairly good success in attaining uniformity of aerobic cell killing across the peak. However, the corresponding OER values plotted below each Bragg curve, and the corresponding hypoxic biologically effective dose values (not shown), demonstrated that it is not possible to design filters to simultaneously achieve isoeffectiveness for both aerobic and hypoxic cells. The Bragg peak carbon OER values are around 2.0 and the neon midpeak OER values are similar, but the OER decreases to about 1.6 in the distal neon peak. The 308 MeV/u carbon and 425 MeV/u neon beams with 4-cm extended peaks are, in general, very much alike in terms of the measured parameters at this range for this cell line.

The biologically effective dose and physical dose plots for the longer-ranged 400 MeV/u carbon beam with the 10-cm spiral ridge filter are depicted

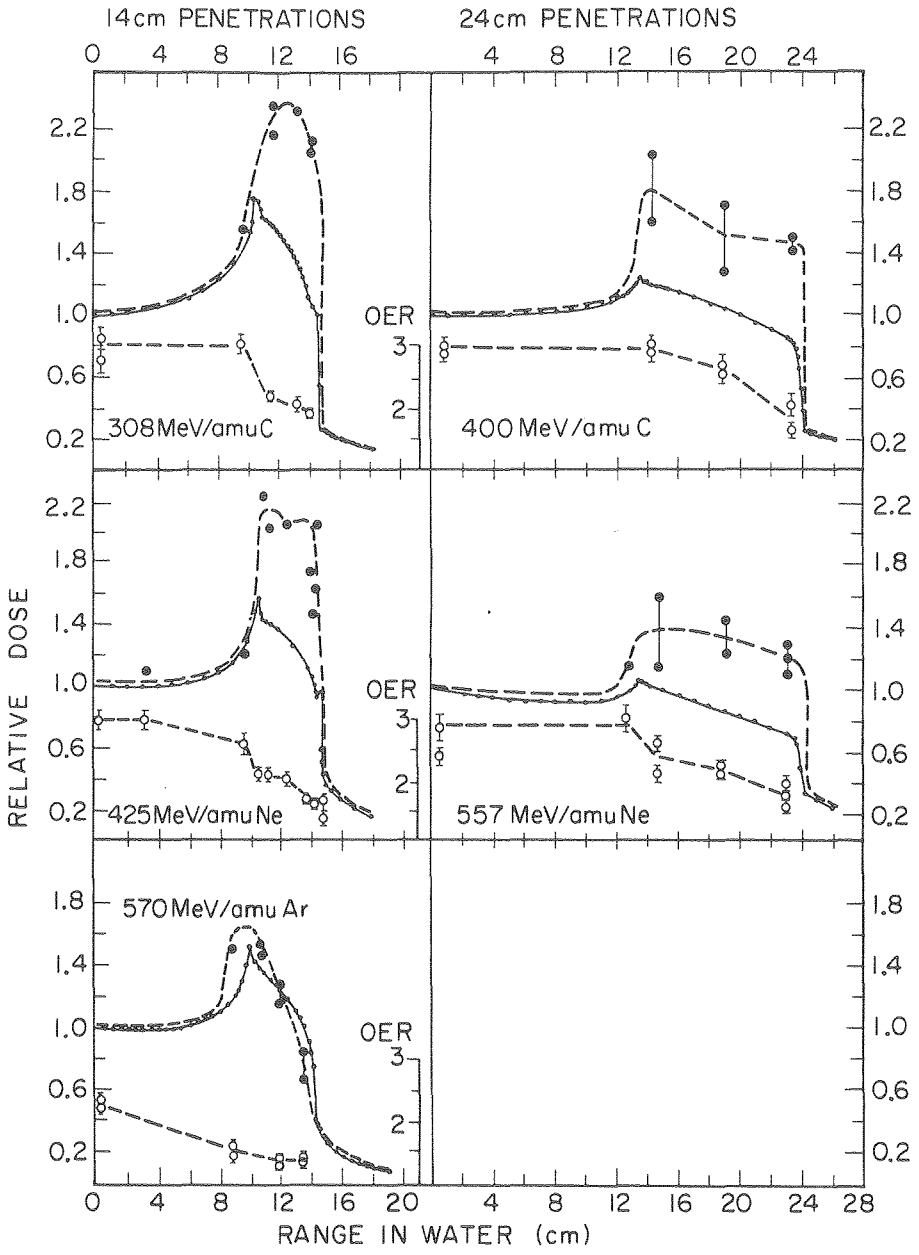

Figure 16 Physical Bragg ionization curves (—), and biologically effective dose (●) and OER (○) at 50 percent survival as a function of range for heavy-ion beams with 4-cm extended Bragg peaks at 14-cm range penetration, and with 10-cm extended Bragg peaks at 24-cm range penetration. (XBL 809-3681)

in the upper right hand panel of Figure 16. There is quite a bit of scatter in the replicate estimates of RBE-50 in the proximal and midpeak regions, and less scatter in the distal position; however, the filter design of physical dose appears to slightly overcompensate for effective dose in the distal peak. More physical dose in the distal end of the extended peak is needed for isoeffectiveness across the full range of the peak. The OER value for this long range carbon beam is rather high, averaging about 2.5 to 2.6 over the 10-cm width, but ranging from 2.8 ± 0.2 in the proximal peak to 1.9 ± 0.2 in the distal peak.

The biologically effective dose and physical doses for the 557 MeV/u neon beam with the 10-cm spiral ridge filter are plotted in the lower right hand panel of Figure 16. Notice that data from two replicate monolayer experiments show proximal and midpeak scatter for neon too; however, the isoeffect is somewhat flatter across the 10 cm of the extended peak. The OER values across the peak of this beam average about 2.1 to 2.3, and ranged from 2.3 ± 0.2 in the proximal peak to 1.6 ± 0.1 in the distal peak.

The final panel in the lower left of Figure 16 presents the 570 MeV/u argon OER values and physical and biologically effective doses as a function of range. This beam is different from the others because it shows that for the 4-cm filter design the biologically effective dose is quite similar to the physical dose, except that it is slightly less effective in the distal end of the peak. However, the normalized peak-to-plateau dose ratio is still quite advantageous (>1.5) in a narrower region straddling the physical proximal peak. This beam is also unique because of its extremely low OER, which averages about 1.4 across the entire width of the extended peak, including the preproximal and distal regions.

The 4-cm filter design appears to be adequate for the carbon and neon beams, but not for the argon beam. The biologically effective dose distribution can be optimized for the argon beam by using a spiral ridge filter design with a much less sloped physical dose. The 10-cm filter design appears to slightly overcompensate for biological killing in the distal peak of the 400 MeV/u carbon and 557 MeV/u neon beam.

a. Simultaneous Axial Exposures

A second method that has been used to evaluate isoeffectiveness and depth-dose characteristics is to measure cell survival as a function of range for a single entrance dose. This can be done with a single dose delivered to cells arranged along the axis of the beam--either plated in monolayers on glass or plastic discs (Tobias, 1973), or in gelatin suspensions that have been solidified (Raju et al., 1976). Preliminary results of this kind with Bevalac beams have been reported (Roisman et al., 1974) but the most extensive series of Bevalac experiments with carbon, neon, and argon ions and other high LET modalities has been completed by Raju et al. (1978b). Survival results for various incident doses confirm that the slope of the filter design for isoeffectiveness depends on the dose level selected. The carbon and neon results measured by Raju et al. (1978b) indicate a flat survival response at low doses (equivalent to 30 percent to 60 percent survival), but less uniform killing across the spread peaks of these beams at higher doses. Argon survival results were measured for two filter designs, the same 10-cm filter used for carbon and neon, and a new filter designed specifically for argon (Raju et al., 1980c). The argon results with the early filter design indicate reasonable isoeffectiveness across the 10-cm filter at low dose; even greater uniformity for a wider dose range is achieved with the new filter design.

b. Dual Parallel-Opposed Fields

Isoeffectiveness can also be evaluated with a technique that eliminates the variations in filter design and permits a reduced entrance and exit dose for an equivalent tumor dose from a single-port exposure. Dual parallel-opposed ports have been simulated for exposures in which the Bragg peaks overlap. The experimental description of the method is detailed in the left panel of Figure 17 for a specific beam condition. The human T-1 cell survival data obtained from this technique using carbon, neon, silicon, and argon beams of 14-cm range are presented in the middle panel of Figure 17.

Measurements of cross-fired survival using the gelatin technique have been made with the 570 MeV/u argon beam with a new argon 10-cm spiral ridge filter (Raju et al., 1980c). Although the absolute sensitivity of the T-1 cells in the gelatin appears to be different than the sensitivity measured in monolayers, the peak-to-plateau advantage of argon, and the uniform cell killing across the Bragg peak are confirmed as seen in the right panel of Figure 17.

D. Studies on Repair and Expression of Damage

1. The Early Work with Lower-Energy Heavy Ions

After Elkind and Sutton (1960) demonstrated sublethal X-ray damage repair in mammalian cells, the question arose as to whether repair of sublethal damage also occurs after exposure to high-LET radiations. In particular, a correlation was sought between the shape of single-dose survival curves and the repair of sublethal damage. Barendsen and co-workers (1960) investigated the effects due to alpha particles emitted from ^{210}Po, and Todd (1968) examined the split-dose repair dependence on LET using X rays, ^{4}He, ^{7}Li, ^{11}B, ^{12}C, ^{16}O, and ^{20}Ne particles generated at the Berkeley HILAC with LET values up to 580 keV/μm in experiments using asynchronously growing human T-1 cells.

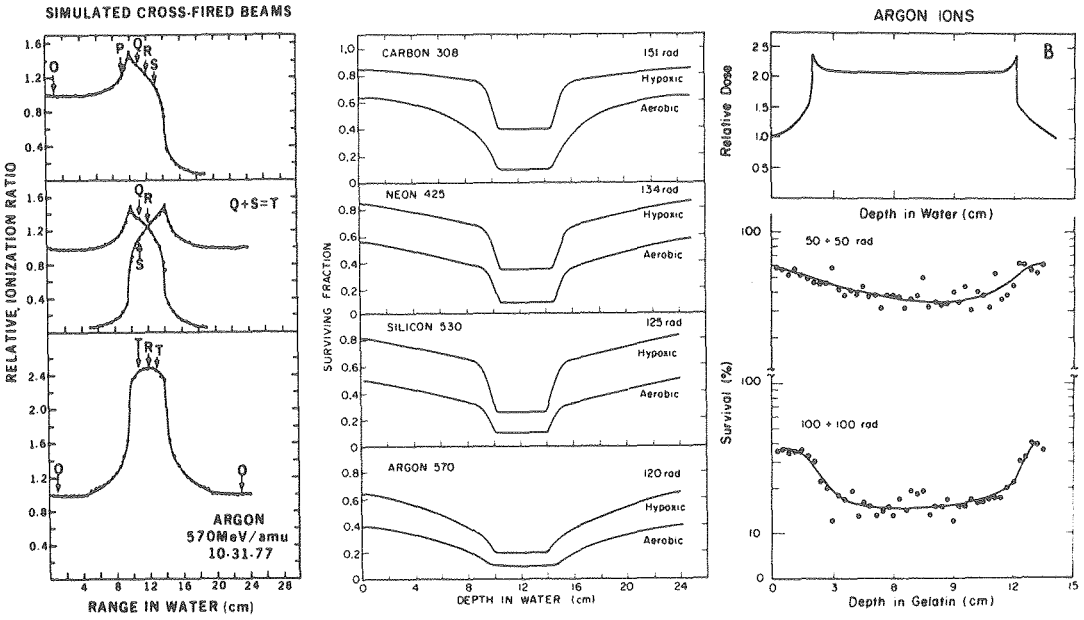

Figure 17 Isoeffectiveness of extended Bragg peaks.
Left panel: Physical Bragg ionization curves for single-port and simulated cross-fired dual parallel-opposed port 570 MeV/u argon beams for cell monolayer exposures in vitro.

Middle panel: Human T-1 cell depth survival curves following simulated cross-fire of carbon, neon, silicon and argon beams for hypoxic and aerated cells with a 4-cm extended Bragg peak. The oxygen effect in the "tumor" is smallest for silicon and argon.

Right panel: Relative dose and human T-1 cell survival with depth of penetratin for agon ions for two opposed and overlapping fields measured with a gelatin "submarine" of suspended cells. (From: Raju et al., 1980c). (XBL 809-3680A)

Todd found that whenever the single-dose survival curve had a shoulder, repair of sublethal damage was evident from experiments using fractionated exposures. On the other hand, he noticed that for particles which yielded a shoulderless or purely exponential survival curve, there was no evidence of two-dose repair. The latter results were consistent with the earlier observation by Barendsen with alpha particles. Todd reached the conclusion that the exponential survival curve is indicative of solely single-hit inactivation kinetics. These results have been interpreted to mean that there is no accumulation of sublethal radiation damage. The evidence described above has contributed to the single-track-to-kill concept in radiation biology (Lea, 1955; Barendsen, 1962).

Skarsgard et al. (1967), using charged particles of various atomic number produced at the Yale linear accelerator, studied repair of sublethal damage in synchronized Chinese hamster cells ($CH2B_2$). Their techniques for cell synchronization involved treatment with hydroxyurea (HU) or excess thymidine. The survival curves for synchronized populations always exhibited a shoulder, although the size of the shoulder decreased with increasing LET. While repair was observed between fractions of irradiation by helium and lithium ions, for which the shoulders of the survival curves were comparatively large, no repair was seen after irradiation by boron and carbon ions for which the shoulders were small. The latter results suggested that two-dose repair is not always correlated with the presence of a shoulder on the survival curve. This was in contrast to the conclusion reached by Todd (1968) based on his results with the human T-1 cells. Recent studies by Ngo et al. (1981) with hamster V79 cells, which will be discussed later, substantiated Skarsgard's observation.

2. Repair of Sublethal Damage

Beginning in 1977, studies on the effects of split or fractionated exposures were initiated using high-energy heavy-ion beams (of a few hundred MeV/u) produced at the Bevalac. The radiological properties of these high-energy beams are substantially different from those associated with lower-energy particles such as those used by the earlier investigators.

Apart from acquiring a basic understanding of cell killing effects of high energy heavy-ion beams, this study of split dose effects was also intended to test a hypothesis that more repair occurs when cells are irradiated at the plateau region than occurs after Bragg peak irradiation. This increase in repair enhances the effective therapeutic dose ratio to a tumor at depth while allowing recovery in overlying normal tissue (Ngo et al., 1983). This hypothesis was expected to hold for the carbon and neon ions because the LET is higher at the peak of these ions than it is at the plateau. It was not clear whether the same argument would be applicable to the argon ion beam because the LET at the argon peak, although higher than that at the plateau, falls into the "overkill" region of biologically effective LET.

Ngo et al. (1981) have completed the most extensive series of split dose cellular studies with Bevalac beams using unmodified Bragg peaks of carbon, neon, and argon ions. The effects of single and split-dose exposures of exponentially growing Chinese hamster cells were compared for cells irradiated in both the plateau and in the Bragg peak. Results were, however, not obtained in the plateau of the argon beam.

Figure 18 shows the survival data. The results from carbon (400 MeV/u) and neon ions (425 MeV/u) are in partial support of the hypothesis of the therapeutic advantage at depth because repair of sublethal damage was

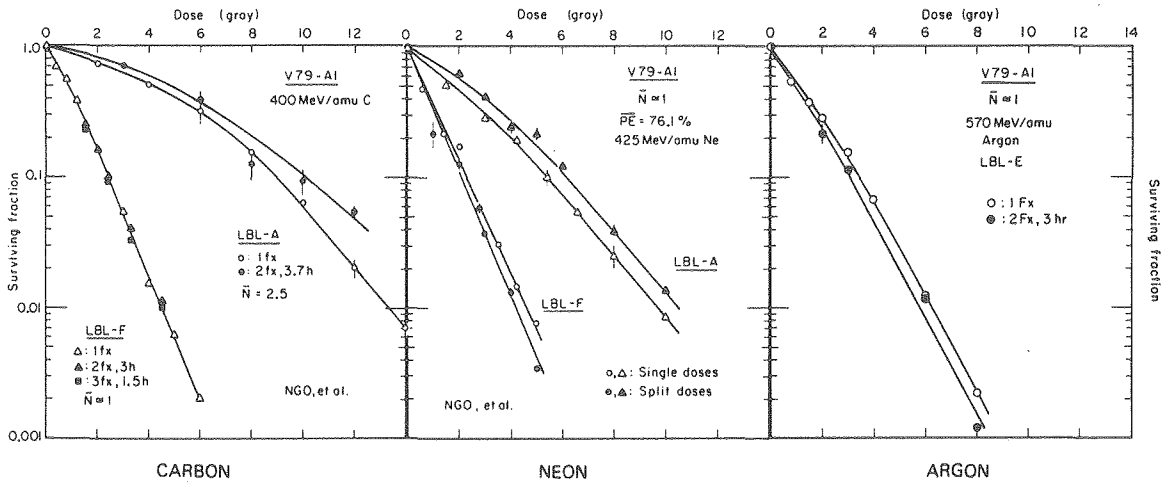

Figure 18 Survival data for asynchronous V-79 cells irradiated with single doses (open symbols) or fractionated doses (closed symbols) of carbon, neon, and argon ions. The letters A, E and F (which designate the irradiation positions in depth of water) are defined in terms of their residual range relative to the Bragg peak in Figure 3. (From: Ngo et al., 1980a). (XBL 7810-3668A)

demonstrated at the plateau positions of these beams, but not at the peak. Although these results were obtained with unmodified beams, this study suggests that there could possibly be a potential gain factor for heavy-ion radiotherapy utilizing certain dose-fractionation protocols, at least for the carbon and neon beams.

3. Potentiation Effects

A more interesting, yet unexpected finding, is shown by the split-dose data for the neon and argon (570 MeV/u) peaks, where split-dose exposures were slightly more effective in cell killing than the single-dose ones. This phenomenon, called potentiation, had previously been seen in in vivo systems with neutrons (Ainsworth et al., 1974, 1976; Grahn et al., 1979) with respect to life shortening and mutagenesis, but was a unique finding in the radiobiology of synchronized cells in vitro as demonstrated below. It was known, however, that a first dose of radiation to asynchronous cells could lead to an accumulation of cells in a sensitive phase, resulting in an apparent increase in cell killing from a second dose, compared to the normal sparing effect of dose fractionation (Elkind and Whitmore, 1967).

In order to clarify the complication of synchrony effects, Ngo et al. (1980a, 1980b, 1982), have designed experiments using Bragg peak neon ions and V-79 cells. In the first type of experiment, synchronous cells were incubated at room temperature between fractionated exposures. At room temperature V-79 cells are halted or slowed from progression (however, mitotic cells can still progress toward division even at 4°C). In the left panel of Figure 19 are data from an experiment in which cells were synchronized by the mitotic selection method. The cells were incubated at 37°C until 5.5 hours after mitotic selection (mid S), and then were irradiated with single- and split-dose

schemes. The temperature during the 3-hour fractionated interval was 22°C, and the cultures were maintained in a 5 percent CO_2 incubator to maintain pH control.

If we assume that the cells in mid-S phase are not being delayed by the first fractionated exposure and that these cells could still progess at a reduced rate due to lower temperature, the average cell age would be at most in late S phase at the time the second dose was given. Previous studies indicate that V-79 cells in late S phase are more resistant to neon ions than those at mid-S phase (Blakely et al., 1980c). This suggests that even in the absence of repair, the survival response would be slightly more resistant after the split-dose than after the single-dose schemes. Nevertheless, the data clearly show the opposite, indicating that although cell progression between exposures was slowed or absent there was a net potentiation effect from fractionated irradiation.

Additional evidence in support of this interpretation is shown in a second type of experiment in the right panel of Figure 19. Here, asynchronous cells were irradiated either with a single dose or two split doses, the latter separated in time ranging from one to seven hours. Between exposures, one set of samples was kept at room temperature, and the other at 37°C. Partial cell synchronization after irradiation, which may happen if the cells are incubated at 37°C after a first dose, would probably not occur if the cells are incubated at room temperature or at least would do so at an insignificant rate. The data indicate that a net potentiation was observed under either incubation temperature. The fact that even at room temperature there was still a net potentiation due to the split exposures indicates that the observed potentiation cannot be attributed entirely to the effect due to any radiation-induced

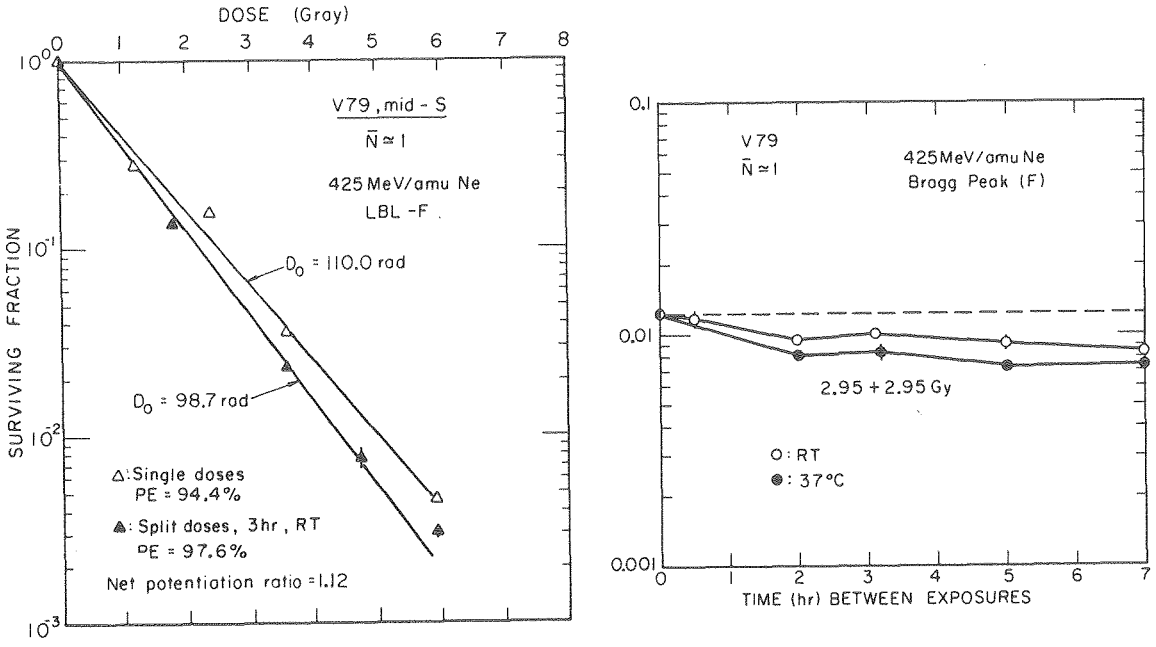

Figure 19 Dose-fractionation effects on V-79 cells irradiated in Bragg peak neon ions.
Left-panel: Survival data for single- and split-doses to synchronized V79 cells in mid-S stage. The fractionation interval for the split dose experiment was three hours at room temperature (~22°C).

Right panel: Survival data of asynchronous V79 cells irradiated with two doses as a function of fractionation time separated by various incubation times at either room temperature (RT) or 37°C. (From: Ngo et al., 1980.) (XBL 806-3389A)

cell-phase synchrony, and thus suggests that a mechanism in addition to cell synchrony must be involved. Such a mechanism is unknown at the present time.

Despite the present incomplete knowledge with regard to its mechanism, the split-dose potentiation demonstrated by Ngo et al. (1981) suggests that attempts to predict results of fractionated exposures on the basis of acute single-dose response should be made with caution. The failure of this approach has been evidenced by the inconsistent conclusion reached earlier by Todd (1968) and by Skarsgard et al. (1967) and has been noted by Ngo et al. (1979) with regard to repair of sublethal neutron damage. In vivo potentiation effects with fractionated heavy ion doses have been noted by Goldstein et al. (1981b) and Burns and Albert (1980).

4. Combined High- and Low-LET Radiations

Low- and high-LET radiations are used in combination (1) to provide an alternate technique for investigating mechanisms of radiation effects, (2) to explore the potential therapeutic advantages of combined photons and high-LET particles in radiotherapy, and (3) to study cell killing and the mutagenic and carcinogenic consequences resulting from exposure to mixed-radiation fields (e.g., γ-rays and high-z particles, or γ-rays and neutrons).

Several laboratories have recently investigated cell killing effects due to combined low- and high-LET radiations, extending the earlier work by Barendsen et al. (1960) and Todd (1973). All reports using fast neutrons and x- rays or γ-rays demonstrate that cells exposed to the two radiation types spaced only a few minutes apart, exhibit a greater cell death than that expected on the basis of the independent action of each radiation alone. Furthermore, with one exception (Durand and Olive, 1976), the majority of the reports showed that the interaction between neutron-induced damage and x-ray

induced damage diminishes with the time that separates the two irradiations (Masuda, 1970; Railton et al., 1975; Ngo et al., 1977a; and Hornsey et al., 1977). Attempts to understand the mechanisms underlying the interactive effect observed with fast neutrons and x or γ rays is hampered by the relatively broad spectrum in LET generally associated with the neutron beams. Katz and Sharma (1974) suggested that the damage responsible for interaction was due to the "γ-kill" component associated with fast neutrons. Presumably the "γ-kill" component is low LET in nature. However, this hypothesis was not supported by the work of Ngo et al. (1977a) who used a fission neutron source in which γ ray contamination was reduced to approximately 3 percent of the total dose.

One important question in radiobiology is whether high-LET radiation and low-LET radiation act independently in inhibiting cell proliferation. Barendsen et al. (1960) and Todd (1973) concluded earlier that the two types of radiation kill cells by independent actions. This problem is also pertinent to the basic question as to whether or not high-LET particles cause only irreversible lethal lesions in cells. Ngo et al. (1981) have addressed these questions using x rays and heavy charged particles of which the LET spectrum is more well defined than a cyclotron-produced fast neutron beam. Moreover, particles of a variety of specific mean LET values could be examined with regard to their interaction with low-LET radiation.

A Chinese hamster lung fibroblast V-79 cell line was used in their study. They found that charged particles such as neon ions with a mean LET of 183 keV/μm and x rays each produce damage that interacts with the other (see left panels of Figure 20), despite the fact that the neon-alone survival curve was exponential in appearance. This finding led them to suggest that low- and high-LET radiations act by a synergistic mode, rather than by independent

Figure 20 Combined high- and low-LET radiation effects on asynchronous V79 cell survival.

Upper left panel: Survival data of V79 cells irradiated first with a priming dose of neon ions as indicated, and subsequently with graded doses of X rays. Cells were incubated at ice temperatures shortly before neon-ion irradiation and between neon-ion and X irradiation. The survival curves are the best fits to the data points obtained by the procedure described in the text. The curve with no data points is the X ray survival curve. $\overline{N}$ denotes averaged cell multiplicity.

Upper right panel: Survival data of V79 cells irradiated with neon ions alone or with graded doses of X rays at varius time intervals after single doses of neon ions. The times indicated represent the incubation intervals at 37°C between the neon-ion and X ray exposures. For the 0 hr interval, the cultures were handled by the same procedures described for the upper left panel.

Lower left panel: Survival data of V79 cells plotted as a function of the neon-ion dose. Data for the two lower survival curves were obtained when cells were first irradiated with a primary X-ray dose shortly before graded doses of neon ions. Cultures were maintained at ice temperatures shortly before X irradiation and between X and neon-ion irradiation. Each survival curve represents the best fit of the data to an exponential dose-survival relationship. The dotted curves are reproductions of the neon-ion-only curve normalized with respect to the surviving fraction due to 500 or 800 rad of X rays. The dotted curves are given to indicate what would be expected if the doses of X rays and neon ions killed cells independently. Other details are similar to the figures in the upper panels.

Lower right panel: Survival data of V79 cells irradiated with neon ions, with or without a preceding dose (800 rad) of X rays. The times indicated are the incubation intervals at 37°C between the X ray and argon ion exposures. For 0 hr. the cultures were handled by the same procedures described for the other panels. Each survival curve and its associated D_0 value represent the best fit of the data to an exponential dose-survival function. The dashed curve is a translation of the neon-only survival curve normalized with respect to the surviving fraction due to 800 rad X rays. Thus, this curve shows what might be expected when there is no longer an interaction between the two radiation treatments. Errors bars represent the standard error of the mean. (XBL 791-3017B)

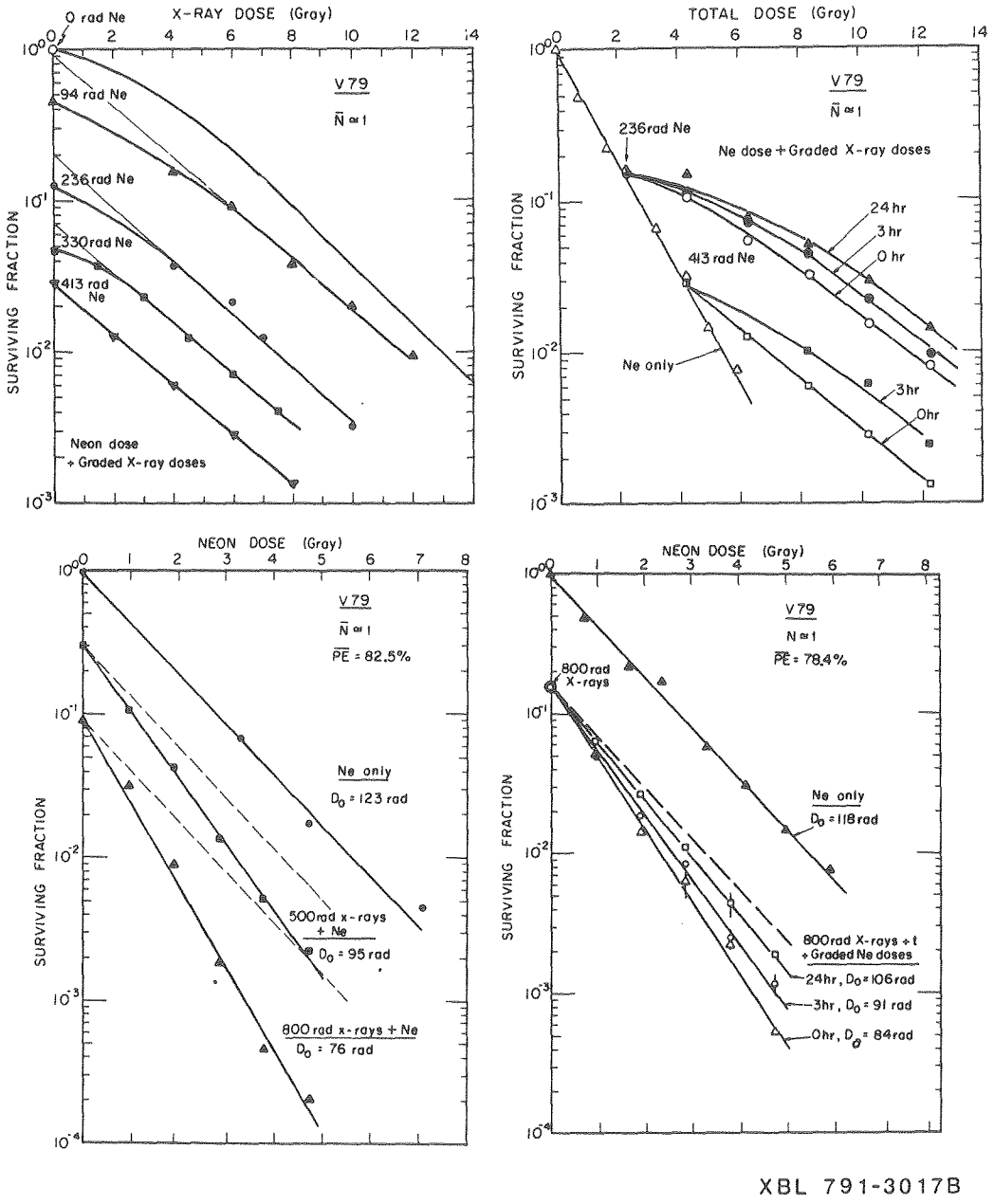
0 rad Ne
X-RAY DOSE (Gray)
V79
N̄ ≈ 1
94 rad Ne
236 rad Ne
330 rad Ne
413 rad Ne
Neon dose
+ Graded X-ray doses
SURVIVING FRACTION
TOTAL DOSE (Gray)
236 rad Ne
Ne dose + Graded X-ray doses
24 hr
3 hr
0 hr
413 rad Ne
Ne only
3hr
Ohr
NEON DOSE (Gray)
PE = 82.5%
Ne only
D0 = 123 rad
500 rad x-rays
+ Ne
D0 = 95 rad
800 rad x-rays + Ne
D0 = 76 rad
PE = 78.4%
800 rad
X-rays
D0 = 118 rad
800 rad X-rays + t
+ Graded Ne doses
24hr, D0 = 106 rad
3hr, D0 = 91 rad
Ohr, D0 = 84 rad
XBL 791-3017B

Figure 20

actions. They further demonstrated that the damage induced by the high-LET particle beam involved in the interactive process can be repaired by cells (see right panels of Figure 20). Further experiments by Ngo et al. (1980b) using x rays and charged particles with LET values ranging from 16 keV/μm up to 1800 keV/μm suggest that the conclusions reached from the neon experiment were generally applicable to all high-LET radiation qualities.

The repair of high-LET induced damage demonstrated by the combined high- and low-LET radiation technique, together with the potentiation of cell killing observed with fractionated high-LET particles alone, can be reconciled. There appear to be at least two entirely opposite processes in operation after dose-fractionation of high-LET radiation, one of which is repair and the other is potentiation or sensitization. With cell survival as an end point, one can only measure the net effect resulting from these two distinct processes.

The mechanism underlying the synergistic effect between high- and low-LET radiation was also studied by Ngo et al. (1980b) with partially synchronized cell populations. Their data indicate that cells in late S phase exhibit a greater synergistic effect than those in G_1, G_1/S, or G_2. These findings suggest that the interaction appears to be related to the inhibition of the radiation damage repair capacity of cells. More work is required before this conclusion can be substantiated.

Basic radiobiological research designed to explore the usefulness of mixed LET beams is still limited, despite the fact that this clinical approach has been underway at a few neutron centers for several years. The differential interactive cell killing effect throughout the cell-cycle stages, if generally proven, would be a built-in therapeutic advantage for fast neutrons, high energy heavy ions, and pions because these particle beams consist of mixed

radiation qualitites. This advantage would be anticipated only if tumor cells were rapidly proliferating, with the probability that these cells would be in S phase (where the potentiation of high- and low-LET radiation killing is greatest), and if the cells of the surrounding normal tissues were in G_0 or G_1 stage (where presumably the potentiation would be minimal).

The potential use of simultaneous exposures of a cancer patient to a high-LET source and to photons is limited by the dose size and by how rapidly a radiotherapist can deliver a tumor dose with high-LET particles and photons. If a dose of high-LET radiation were given first, the subsequent low-LET radiation dose ideally should follow immediately or within a few minutes in order to achieve a maximum synergistic effect. This means that a photon source has to be in the vicinity of a high-LET beam. At the present time, the only neutron center that provides this capabilty is the Cleveland Clinic neutron facility. The existing heavy ion facility at Berkeley and the few pion centers around the world can also provide this option by using the Bragg plateau region as a low-LET source.

Radiation-induced synchronization by high-LET modalities is another potential advantage afforded by combined radiation therapy. The reason for this stems from the observation that high-LET particles (including neutrons, particles, and heavy ions) are more effective in accumulating proliferating cells in G_2 stage, which are known to be more sensitive to x rays than an asynchronous cell population (Schneider and Whitmore, 1963; Ngo et al., 1977b; Lücke-Hühle et al., 1979; Blakely et al., 1980c; and Raju et al., 1980a). The problem is, however, to determine when the maximum number of G_2 cells occur in any given tumor following a high-LET radiation dosage. For Chinese hamster V-79 cells in vitro, this time is about 7 to 9 hours as reported by Lücke-Hühle

et al. (1979) and by Ngo in Blakely et al. (1980c). Clearly, much work in this area is needed.

5. Repair of Potentially Lethal Damage

a. Delayed Plating

The presence of potentially lethal damage (PLD) caused by ionizing radiation is usually implied by the change in survival when the cultivation conditions are altered after irradiation (Phillips and Tolmach, 1966; Little, 1971). Information regarding heavy-ion induced PLD is limited in the literature. Lyman and Haynes (1967), using a delayed plating technique, reported that diploid yeast cells, S. cerevisiae, repair PLD following x rays, ^{4}He, ^{12}C, or ^{20}Ne irradiation in a manner that is independent of LET. The radiation qualities of these particles were described as 0.2 keV/μm for 50 kVp x-rays, 9.9 MeV/u (18 keV/μm) for ^{4}He, 9.1 MeV/u (176.5 keV/μm) for ^{12}C, and 8.2 MeV/u (492 keV/μm) for ^{20}Ne. The charged particles were produced at the Berkeley HILAC.

Experiments designed to study PLD following heavy-ion irradiation in mammalian cells were not available until recently. Two assay methods were adopted to investigate this problem. Yang in Ngo et al. (1980a) studied repair of PLD in delayed plating experiments in mouse 10T-1/2 cells which were irradiated in a confluent or plateau phase. Figure 21 shows the change in survival with postirradiation time in a confluent state after 225 kVp x rays and 570 MeV/u argon ions. The increase in survival with time for each radiation indicates that these cells repair PLD, despite the difference in radiation quality between x rays and the ^{40}A particles. Yang then compared the amount of PLD repair at 24 hours postirradiation for x rays, ^{12}C, ^{20}Ne, and ^{40}A ions. These experiments usually involved measurement of whole dose-survival curves, and a typical set of data is demonstrated in Figure 21.

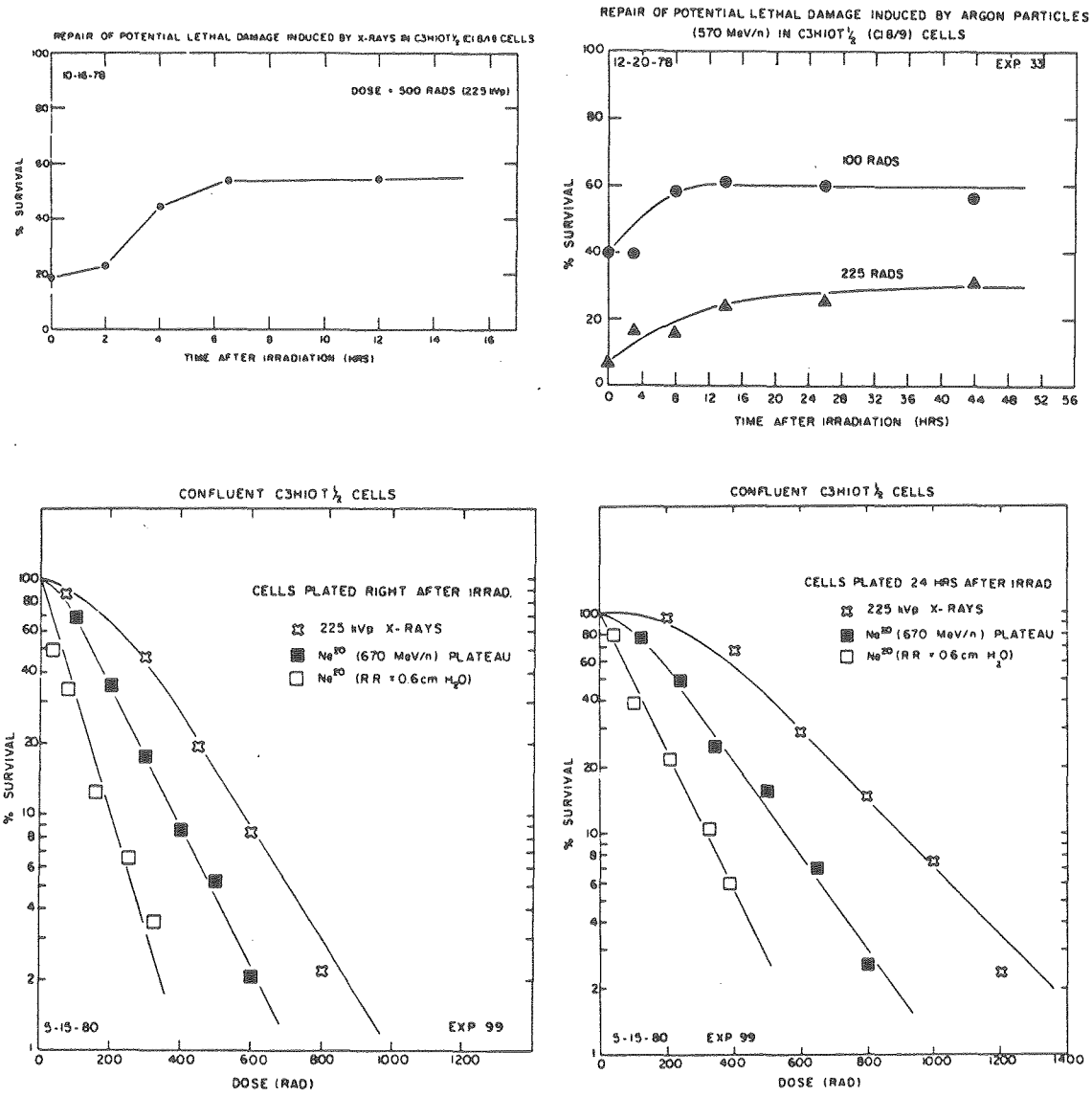

Figure 21 Repair kinetics of potentially lethal damage measured by delayed plating techniques in confluent C3H10T1/2 cells.

Upper left panel: PLD repair after x-ray irradiation.

Upper right panel: PLD repair after plateau 570 MeV/u argon ion irradiation.

Lower left panel: Whole survival curves demonstrating cell killing measured when confluent C3H10T1/2 cells are plated immediately after irradiation.

Lower right panel: Whole survival curves demonstrating repair of PLD when C3H10T1/2 cells are plated 24 hrs. after irradiation. (From: Ngo et al., 1980a). (XBL 807-10656B)

A summary of the results from this investigation is given in Table III. It is evident from the repair factors shown in Table III that the amount of PLD repair in the 10T1/2 cells is quantitatively the same for x rays as for each of the heavy-ion beams with LET values ranging from 10 keV/μm to 105 keV/μm. Note that these particle beams are considered high-energy beams, but that appreciable nuclear fragments are by-products from the primary particles. However, no repair of PLD was measurable when the cells were irradiated with an argon beam having a lower initial energy (8.3 MeV/u) and therefore no fragmentation events, but a higher LET (1800 keV/μm).

b. Delayed Plating of Tumors In Situ

Repair of potentially lethal damage has been evaluated in vitro following in situ heavy ion irradiation of three different tumor systems. Wheeler et al. (1980) found that the extent of recovery from PLD in 9L rat gliosarcoma cells irradiated intracerebrally with carbon ions (mid 4-cm Bragg peak of a 400 MeV/u beam) and held in situ for up to 24 hr was virtually identical to that observed after irradiation with X rays. Guichard et al. (1982) measured the response of human Na11 melanomas growing in nude mice exposed to neon ions (mid 10-cm Bragg peak of a 557 MeV/u beam) and found the repair of PLD after 6 hr and 24 hr in situ was comparable to that observed after gamma irradiation. They also found that the administration of misonidazole could completely inhibit the PLD repair following either gamma or extended peak neon ion irradiation (see Section IVF). Sakamoto et al. (1983) have measured PLD repair of murine epithelioma cells and found that after 6 hr in situ the repair ratio of 3.2 obtained for 8.0 Gy neon ions (distal 10-cm Bragg peak of a 557 MeV/u beam) was significantly lower than the repair ratio of 11.2 observed for an X ray dose of 10 Gy. The results of all three tumor studies indicate that there is

Table III. Repair Factors for Potentially Lethal Damage Caused by Ionizing Radiations of Various Qualities in Confluent Mouse 10T1/2 Cells in Culture

Radiation	Energy (MeV/u)	Residual Range (cm in water)	LET_∞ keV/μm	Immediate Plating LD_{50}* (rad)	Immediate Plating LD_{10}† (rad)	24-Hour Delayed Plating LD_{50}* (rad)	24-Hour Delayed Plating LD_{10}† (rad)	Repair Factor‡ LD_{50}*	Repair Factor‡ LD_{10}†
X rays	225 kVp	--	--	300	600	500	900	1.66	1.53
Carbon	470	31.9	10	300	600	420	840	1.40	1.40
Carbon	70	1.3	35	210	420	330	620	1.57	1.47
Neon	670	32.0	24	150	380	220	560	1.46	1.47
Neon	60	0.6	105	60	210	100	320	1.66	1.52
Argon	570	13.4	85	80	250	120	360	1.50	1.44
Argon	8.3	0.015	1,500	330	1,100	330	1,100	1.00	1.00

* LD_{50} = dose required to yield 50% survival.

† LD_{10} = dose required to yield 10% survival.

‡ Repair Factor = $\frac{\text{Dose that yields a given surviving fraction by a delayed plating}}{\text{Dose that yields the same surviving fraction by immediate plating}}$

a difference between the LET dependence of heavy ion effects on the repair of PLD of tumor cells in situ and on the repair of SLD observed with cells in vitro using extended Bragg peaks (Goldstein et al., 1981b). It appears that repair of PLD damage may be diminished only at high LET values as shown by the work of Sakamoto et al. (1983) who irradiated in the distal peak of the extended Bragg curve and therefore, of the three tumor PLD studies, they were using Bragg peak ions of the highest LET. However, differences in the biological systems cannot be ignored as an explanation for the different degrees of repair. It is of interest to further explore the possible differences in various cellular targets for PLD and SLD using particle beams.

c. Anisotonicity

Another assay, which was used to investigate the repair of PLD induced by heavy ions, involves the treatment of cultured cells with anisotonic solutions. This method allows an examination of PLD repair in cells that are in a state of active growth, in contrast to the plateau-growth cells used for the previous assay. Treatments with hyper- or hypotonic solution at a sublethal dose enhance cellular radiosensitivity to x rays or to fast neutrons (Ngo et al., 1977b). This effect due to anisotonic treatments has been interpreted to be a result of inhibition of the repair of radiation-induced PLD. In fact, the elegant work of Utsumi and Elkind (1979) led them to conclude that the enhanced radioresponse caused by anisotonic solutions was mainly a reduction in the repair of PLD, and had little or no effect on the repair of sublethal radiation damage.

Using anisotonic solutions, Ngo et al. (1980a, 1980c) have conducted experiments on Chinese hamster V-79 cells to investigate the following questions associated with several heavy-ion beams : (1) Does the radiosensitization effect have a sequence dependence for treatment with the anisotonic

salt solution and the radiation? (2) How does the sensitization effect vary with radiation quality? (3) Can the fraction of cell killing described by a single-hit mechanism still be modified by treatment with anisotonicity? (4) Does the repair rate of the PLD in question vary with the density of ionization?

For this study, carbon and neon particle beams at the Bevalac were chosen with mean LET values of 16, 38, 85, and 183 keV/μm. The anisotonic and isotonic solutions were prepared in phosphate buffered solution (PBS) with concentrations of NaCl at 0.04 M (hypotonic), 0.5 M (hypertonic), and 0.14 M (isotonic). The pH of all the salt solutions was adjusted to 7.3-7.4, a normal pH for the cultured cells. The exposure time of cultures to each salt solution was 20 min. at 37°C. The NaCl concentrations for the hypo- and hypertonicitiy were selected because each treatment alone was nonlethal, and the radiosensitization effects for cells treated postirradiation with either concentration of salt were approximately the same.

The survival responses of V-79 cells exposed to each radiation and then treated with the 0.14 M NaCl/PBS solution are shown in Figure 22A. Control treatment of the cells with an isotonic salt solution did not significantly alter the radiation response. Figures 22B to 22E demonstrate the effects of 0.5 M NaCl/PBS, given prior to and continuously until the end of irradiation, or given immediately after radiation. The data clearly show that the post-irradiation treatment was more effective than treatment given before and during irradiation. These results imply that anisotonicity can effectively inhibit the repair process of some radiation-induced lesions after they are formed. Furthermore, the dependence of the sensitization effect on the treatment sequence suggests that fast radiation chemistry is not necessarily required in the inhibition of this repair mechanism.

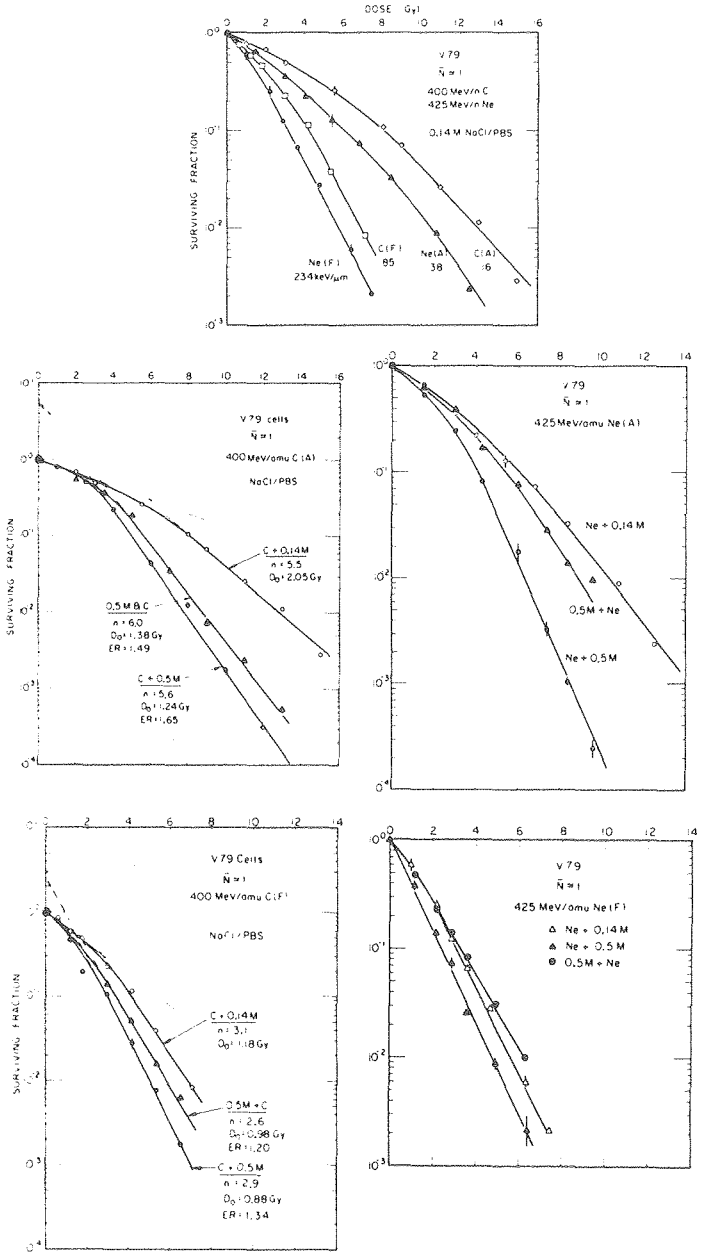

Figure 22 (A) Survival data of V79 cells irradiated with various heavy-ion beams of four different LET_∞ values. The cells were treated with isotonic salt/PBS solution for 20 minutes at 37°C postirradiation. (B) through (E): The hypertonic solution (0.5 M NaCl/PBS) was given before and during irradiation, or immediately after irradiation. For each radiation, data obtained from postirradiation treatment with isotonic salt solution served as controls. (From: Ngo et al., 1980). (XBL 806-3387A)

In order to quantitatively evaluate the salt effects on the single-hit (low dose region) and the multihit (high dose region) inactivations associated with the various radiation qualities, Ngo et al. (1980a) further defined the enhancement ratios:

$$(\alpha)_{\text{anisotonicity}}/(\alpha)_{\text{isotonicity}} \tag{13}$$

and

$$(D_0)_{\text{isotonicity}}/(D_0)_{\text{anisotonicity}} \tag{14}$$

where the parameters α and D_0 were the initial and the final slopes respectively, determined from the measured survival curve.

Analysis of the change of the enhancement ratios described by Eqs. (13) and (14) as a function of LET for postirradiation treatment of hypertonic or hypotonic solution has demonstrated that the effects of hypertonicity and hypotonicity on the single-hit inactivation appear to be different although the relatively large errors inherent in the analysis make it difficult to separate the effects at higher LET. It can nevertheless be concluded that the single-hit inactivation (or the initial slope) can be made more sensitive by treatment with the hypertonic solution. On the other hand, analysis of the effects of the hyper- and hypotonicity on D_0 show that the effects of the two treatments are indistinguishable, and that this enhancement ratio decreases progressively with increasing LET. Thus, these data indicate that the hyper- and hypotonic salt treatments inhibit the repair of PLD, the magnitude of which is less for higher LET radiations.

Ngo et al. (1980a) further compared the repair rate of the PLD that becomes lethal by hypertonic salt treatments with several radiation qualities: 225 kVp

x rays and carbon ions at LET values of 16 and 85 keV/μm, respectively. Figure 23 shows that the sensitization effect diminished as the time between the treatments with radiation and the 0.5 M NaCl/PBS was prolonged. It can be assumed that the kinetics of the loss of sensitization represents the repair rate associated with the radiation damage. As shown in Figure 23, the half time of the initial repair was approximately 15 minutes and was essentially independent of the quality of the radiation that induced the lesions. These repair kinetics are faster than the overall repair times for sublethal damage; the latter is known to take several hours to complete. Consequently, one may infer that the lesions expressible by salt treatments are different from sublethal damage, or at most they are only a fraction of the sublethal damage.

E. Cell Age Response and Progression Effects

Variations in the radiosensitivity of cultured mammalian cells at different phases of the division cycle have been known since the early 1960s (Tersima and Tolmach, 1961, 1963; Sinclair and Morton, 1963, 1965, 1966). It was not, however, until the late 1960s and early 1970s that the high LET radiations were found to diminish the amplitude of the variation between the most sensitive and the most resistant phases. This effect has been observed with fast neutrons (Sinclair, 1970; Hall, 1969; Masuda, 1971; Hall et al., 1975; Sapozink and Djordjevic, 1974; Gragg et al., 1978), with alpha particles from an isotonic source (Hall et al., 1972; Raju et al., 1975), with pions (Raju et al., 1978d,e), with helium ions (Bird et al., 1980) and with heavy-ion particle beams (Skarsgard 1967; Elkind, 1970; Bird, 1972; Bird and Burki, 1971, 1975; Bird et al., 1980; Hall et al., 1977; Raju et al., 1980b).

Although it is generally agreed that the variation in radiosensitivity to high-LET radiation is reduced compared to that observed for x rays, there are

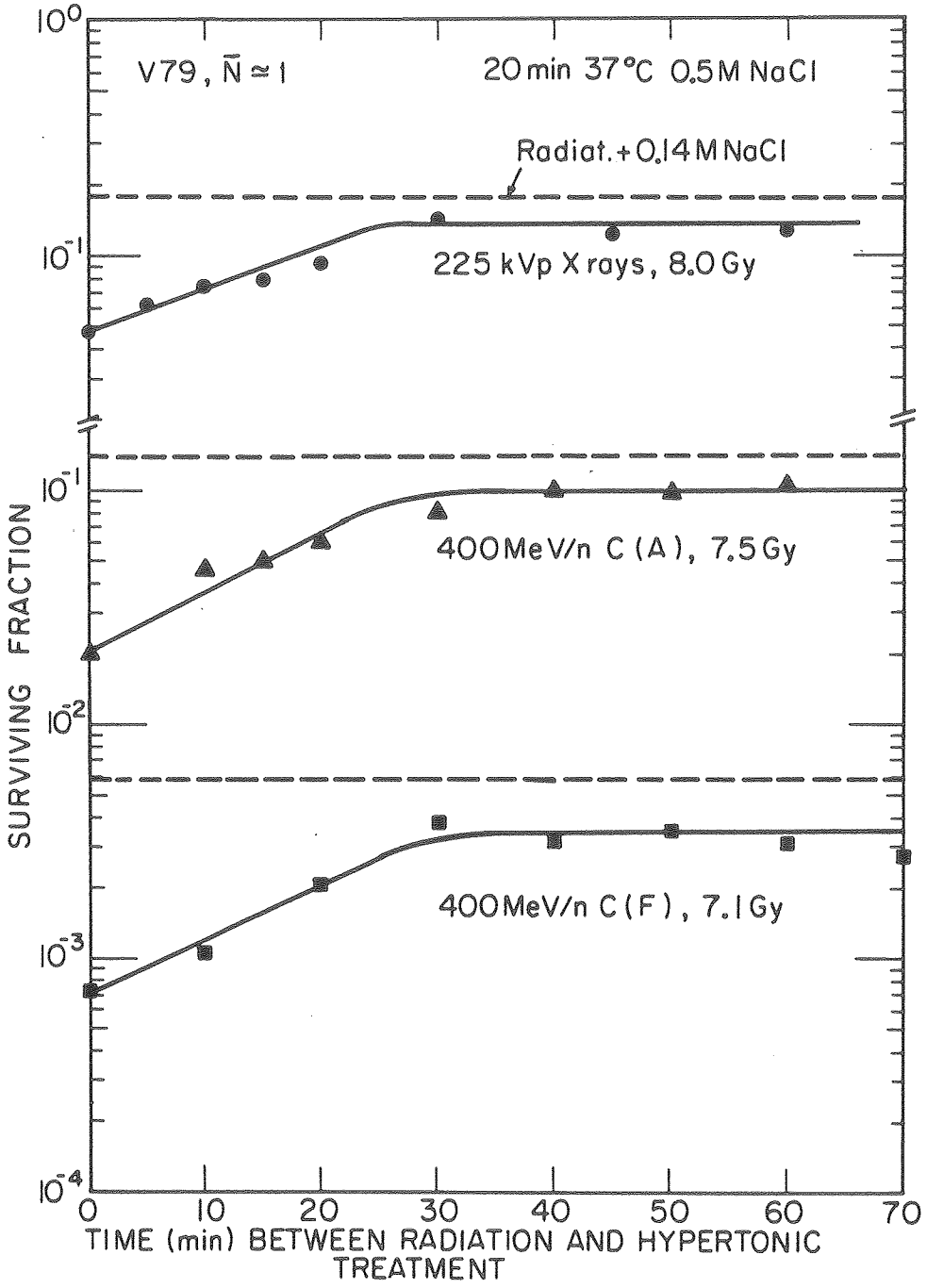

Figure 23 PLD repair kinetics for actively growing V79 cells. The PLD can be made lethal by hypertonic salt treatments. Comparisons are made between X-rays, carbon plateau (A), and carbon peak region (F) at doses as indicated. (From: Ngo et al., 1980a.) (XBL 805-3346)

not sufficient data in the literature to make quantitative comparisons as to the dose, LET and cell-line dependence of the reduction. Complicating these studies is evidence that differences in age response can occur when comparisons are made between cells that have been synchronized by various methods (Raju et al., 1975). More systematic studies are needed to establish the LET dependence of the cell age reduction phenomenon.

The cellular age response to low-LET radiations can be generalized into two forms: one for cells with a short G_1 phase, and one for cells with a long G_1 phase (Sinclair, 1972). Both forms show a similar response at cell cycle ages beyond the sensitive G_1/S interface, through a maximally resistant late S phase, and finally a sensitive G_2 and M population. However, in those cells with a long G_1 phase, there is an additional radioresistance early in G_1 that declines at the G_1/S transition to a value about equal to that for mitotic cells.

Bird and Burki (1975) suggested that the reduction of cell cycle variation in survival for Chinese hamster cells is a gradually decreasing function of LET. They calculated the percent variation in the radioresponse through the cell cycle as the ratio of the maximum and minimum surviving fraction for a single dose. To compare radiations, they selected the dose for each radiation that resulted in the same minimum surviving fraction. Their analysis included their own work as well as that of several investigators. The age variation in radioresponse was greatest for x rays and decreased with increasing LET. At LET values greater than 200 keV/μm, the age response was invariant. This does not agree with the earlier results of Skarsgard et al. (1966) who used low energy oxygen ions, or recent work by Bird et al. (1980) with protons, deuterons, and helium-3 ions, both of which demonstrated an age response

variation at LET values near 200 keV/μm. The explanation for this discrepancy is unknown; however, the cell synchronization techniques were not uniform.

Most reports that demonstrate a reduced age variation with high-LET radiation indicate that the variation seen is qualitatively similar to x rays. However, there is conflicting evidence for this point. Skarsgard et al. (1966) found that hamster cells in late S phase were most resistant to boron (126 keV/μm) and carbon ions (190 keV/μm), but that cells in G_2 were most resistant to oxygen (350 keV/μm) and neon ions (560 keV/μm). Raju et al. (1975) using alpha particles (LET = 125 keV/μm), have found that cells are most sensitive to particle irradiation in S phase, whereas the peak of radioresistance appears to be in G_2 or early G_1. These qualitative changes in radiosensitivity of various stages of the cell cycle in these two reports of particle irradiations, compared to similar x ray data, have not been explained.

Bevalac beams have been used to examine quantitative and qualitative reductions in the age response. Chapman (1980) studied inactivation of mitotic G_1-phase and stationary phase Chinese hamster cells as a function of LET for x rays, helium, carbon, neon, and argon beams. Figure 24 is the best fitted α parameter for these cell phases plotted versus median LET from linear quadratic analyses of the survival data. The values of α are most different for the three cell ages at low LET, and are most similar at high LET (~100 keV/μm).

The age response of synchronized Chinese hamster V-79 lung and Chinese hamster ovary cells have both been studied in more detail at various ages through the cell cycle using high energy Bevalac argon ion beams. Hall et al. (1977), using hydroxyurea-induced synchrony, observed a reduction of the seventeen-fold age-variation x-ray response to a factor of two with pristine 429 MeV/u Bragg peak argon ion irradiation. Qualitatively they found the

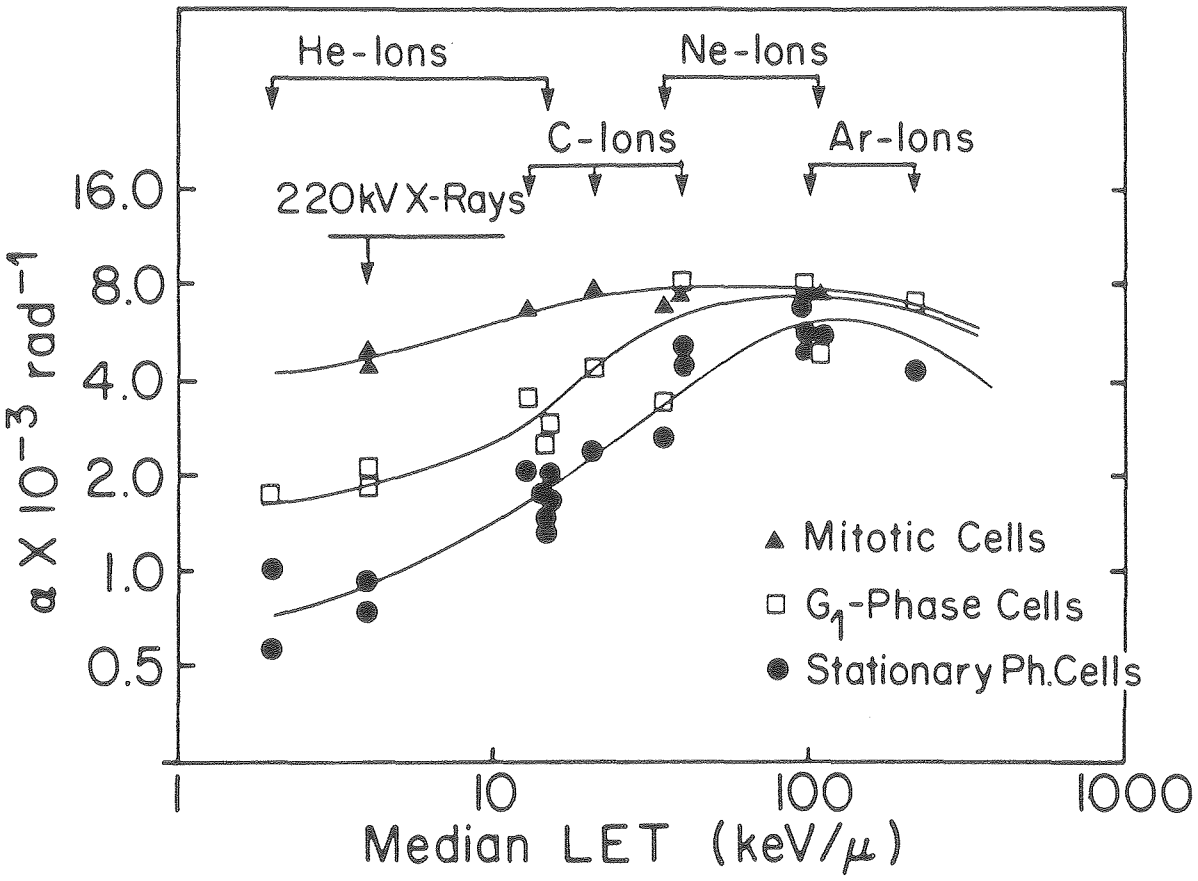

Figure 24 Single-hit inactivation coefficients for homogeneous populations of mitotic, G_1-phase, and stationary phase Chinese hamster cells irradiated with 220 kVp x-rays and various charged-particle beams as a function of median LET in units of keV/μm. (From: Chapman, 1981.) (XBL 819-4965)

pattern of the age response to 8 Gy of x rays and 4.11 gray of argon ions to be similar (see left panel, Figure 25). Raju et al. (1980b) using a dual synchronization method of mitotic selection followed by treatment with hydroxyurea, obtained a twenty-five fold extreme age variation to 9 Gy of x rays, and an insignificant age response with cells from the same population exposed to 4 Gy of distal extended 4-cm Bragg peak argon 550 MeV/u ions (right panel, Figure 25).

Ngo in Blakely et al. (1980c) measured cell age responses of synchronized Chinese hamster V-79 cells to 225 kVp x rays or 425 MeV/u Bragg peak neon ions (234 keV/μm). These data which are presented in the upper panels of Figure 26, were taken from a single experiment in which the cell growth after mitotic selection was controlled identically for both x and neon irradiations. The results in the left upper panel of Figure 26 show that at doses of x rays and neon ions that yield approximately identical killing of G_1 cells, the amplitude of the survival variation throughout the cell cycle for x rays is approximately 1.5 times greater than for neon.

The cell-cycle variation amplitude (the difference in survival between the most radioresistant and the most radiosensitive phases of the cell cycle) increases with increasing dose of both x rays and neon ions. This point is clearly demonstrated in the upper right hand panel of Figure 26 where cells from the same mitotic population were used to obtain whole survival curves at G_1/S and late S phase after irradiation with either neon ions or x rays. Per unit of absorbed dose, the difference in survival response between the two ages is approximately the same for both radiations; however, at doses of each radiation that give the same level of cell killing, the difference in survival

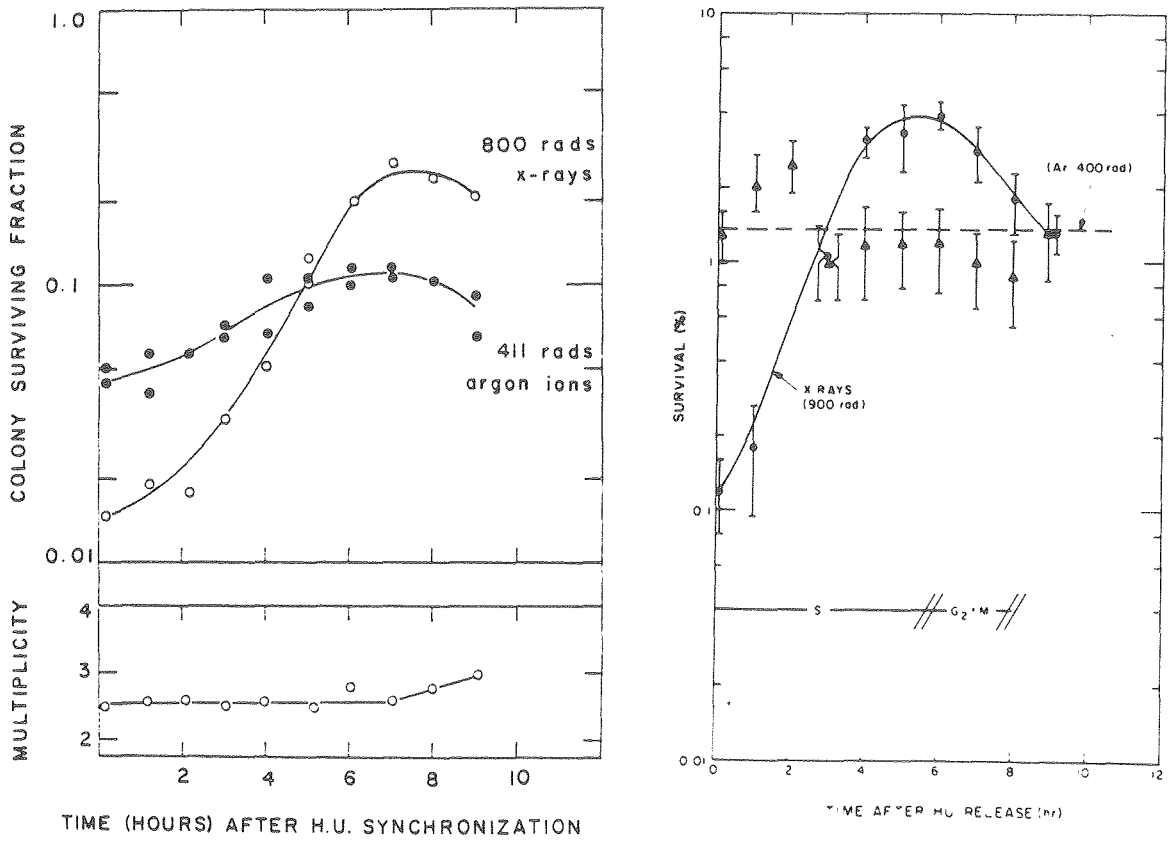

Figure 25 Left panel, top: Response of synchronized Chinese hamster V79 cells to a dose of either 8 Gray of x-rays or 4.11 Gray of unmodified Bragg peak argon ions with an initial energy of 429 MeV/u. The cells were irradiated at various times after synchronization with hydroxyurea.

Left panel, bottom: The multiplicity, or average number of cells per colony forming unit, as a function of time after synchronization. (From: Hall et al., 1977.)

Right panel: Synchronized Chinese hamster ovary cell survival after exposure to 9 Gray of x-rays or 4 Gray of 4-cm extended peak argon ions are plotted as a function of time after release from hydroxyurea. The argon data points were measured with a beam having an initial energy of 550 MeV/u. Each point represents the average survival of three exposures. The error bars show one standard deviation. The dashed line represents the average survival level of all argon-ion data points. The solid line shows the trend of variation for x rays. (From: Raju et al., 1980b). (XBL 819-4962)

response between the two ages is much reduced for neon compared to x rays. This is consistent with the concept that the cell-age response variation at comparable cell survival levels decreases with increasing LET because S phase cells generally have a greater RBE relative to x rays than do G_1/S phase cells, especially at low dose.

Ngo in Blakely et al. (1980c) has also measured the V-79 cell age response at lower and higher LET values than the Bragg peak neon data. Bragg plateau 570 MeV/u Bevalac argon ions at 117 keV/μm gave age variation reductions similar to the neon data. Bragg peak, low-energy (8.5 MeV/u) argon ions accelerated at the super HILAC (1800 keV/μm) yielded exponential survival curves, but were clearly in the "overkill" region of killing effectiveness. The amplitude of the SuperHILAC argon response was virtually flat.

The age response of synchronized human kidney cells to Bragg peak argon ions is presented in the lower panels of Figure 26 (Blakely et al., 1980c). The argon survival curves are exponential at 245 keV/μm and show a major reduction in differences between cells of different ages compared to those seen at low-LET (data not shown). The amplitude of the argon age response shows some structure, but is quite flat in contrast to published studies of x ray age response with T-1 cells (Vos et al., 1966). S-phase cells are the most radioresistant, and the G_1/S boundary appears to be the most radiosensitive phase.

In addition to studies of cell age radiosensitivity using the clonogenic capacity of the irradiated cell as an end point, division delay and/or G_2 block induced by high-LET radiations have also been studied with neutrons (Schneider and Whitmore, 1963; Ngo et al., 1977b), with pions (Schlag et al.,

Figure 26 Upper left panel: Radiation response of synchronized Chinese hamster V79 cells to 225 kVp x rays and Bragg peak 425 MeV/u neon ions. Age response for 5.5 and 8.5 Gray of x rays, and 3.3 and 4.7 Gray of Bragg peak neon ions.

Upper right panel: Survival dose-response of synchronized G_1/S (2.5 h) and late S (7 h) phase Chinese hamster V79 cells to x rays and Bragg peak neon ions (same cell population as cells in upper left panel).

Lower left panel: Radiation response of synchronized human kidney T-1 cells to Bragg peak 570 MeV/u argon ions. Age response for 1.87 and 4.62 Gray of Bragg peak argon ions.

Lower right panel: Survival dose response of synchronized (G_1, G_1/S, S, G_2) human kidney cells to Bragg peak argon ions determined in the same cell population as shown in lower left figure. (From: Blakely et al., 1980c). (XBL 794-9460A)

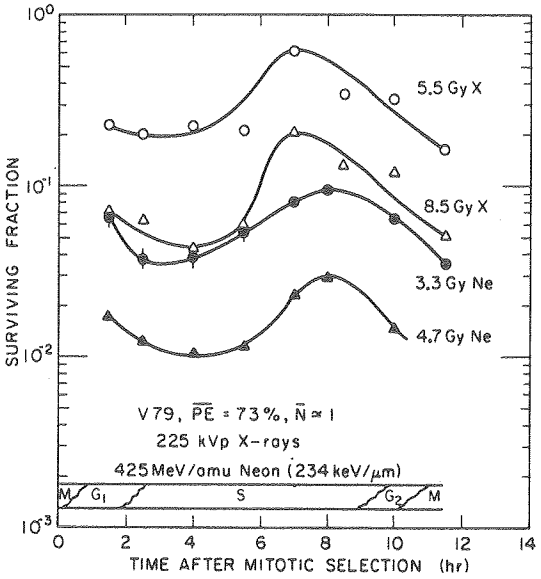
SURVIVING FRACTION
5.5 Gy X
8.5 Gy X
3.3 Gy Ne
4.7 Gy Ne
V79, PE = 73%, N̄ ≃ 1
225 kVp X-rays
425 MeV/amu Neon (234 keV/μm)
M G1 S G2 M
TIME AFTER MITOTIC SELECTION (hr)

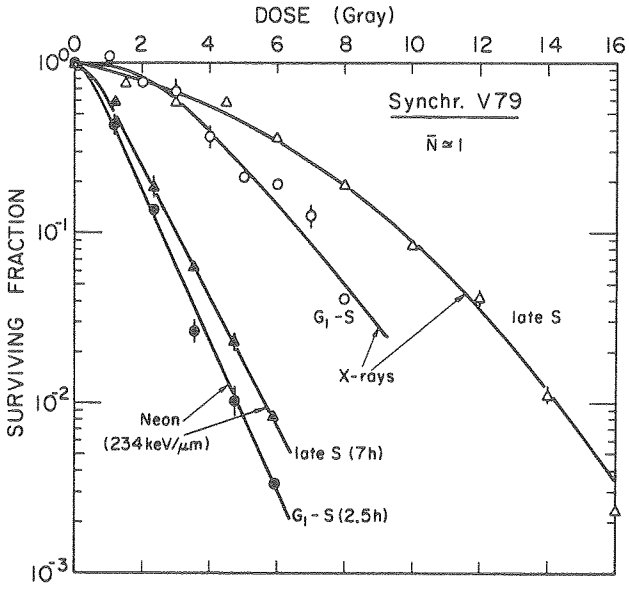
DOSE (Gray)
SURVIVING FRACTION
Synchr. V79
N̄ ≃ 1
G1 - S
late S
X-rays
Neon
(234 keV/μm)
late S (7h)
G1 - S (2.5h)

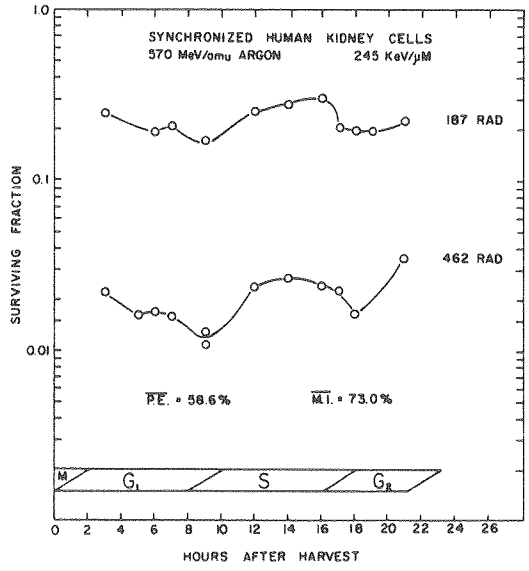
SYNCHRONIZED HUMAN KIDNEY CELLS
570 MeV/amu ARGON 245 KeV/μM
187 RAD
462 RAD
PE. = 58.6%
MI. = 73.0%
SURVIVING FRACTION
M G1 S G2
HOURS AFTER HARVEST

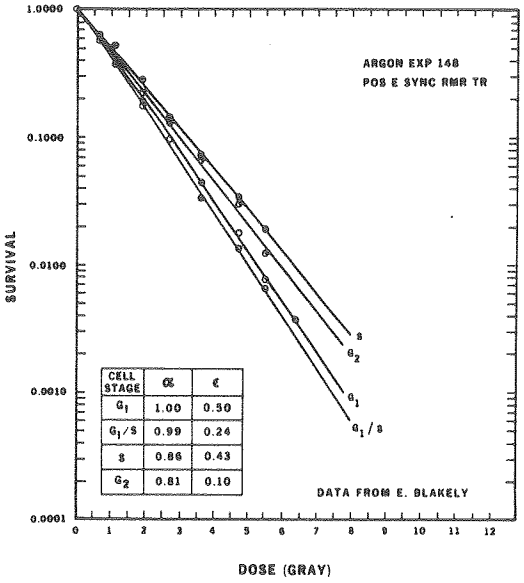
ARGON EXP 148
POS E SYNC RMR TR
SURVIVAL
CELL STAGE | α | ε
G1 | 1.00 | 0.50
G1/S | 0.99 | 0.24
S | 0.86 | 0.43
G2 | 0.81 | 0.10
DATA FROM E. BLAKELY
DOSE (GRAY)

1978), with alpha particles (Raju et al., 1980a), and with heavy-ion beams (Skarsgard, 1964, 1967; Lücke-Hühle et al., 1979; Collyn-d'Hooghe et al., 1981).

Lücke-Hühle et al. (1979) quantitatively measured cell cycle progression effects induced by high-energy monoenergetic heavy ions at the Bevalac using Chinese hamster V-79 monolayers in track segment experiments. They observed a profound G_2 block that had a LET dependence similar to the cell killing end point, but with a greater biological effectiveness (Figure 27). An example of the profound G_2 block measured after 4.0 gray of carbon peak ions is given in the upper panels of Figure 27. In contrast to gamma and x rays, they found heavy ions did not affect cell traversal through the G_1 and S phase.

Schlag and Lücke-Hühle (1981) have extended their analysis of high LET effects on cell progression to include a recent study of the influence of ionization density on DNA synthesis. Both ^{241}Am α-particles and ^{60}Co-γ-rays caused a depressed rate of DNA synthesis in V-79 cells; however, the α-particle lesion did not prolong the duration of S phase as was observed during the first four hours after gamma rays. Thus, α-particles were similar to peak pions (Schlag et al., 1978) and high-LET neon ions (Lücke-Hühle et al., 1979) in this respect.

Contrary results were obtained by Raju et al. (1980a) who found that exposure to ^{238}Pu α-particles did result in a longer retention of Chinese hamster V-79 cells in late S phase than that observed for cells exposed to x rays. For a given survival dose, the S phase specific retention caused the mitotic accumulation to occur later in α-irradiated cells than in cells exposed

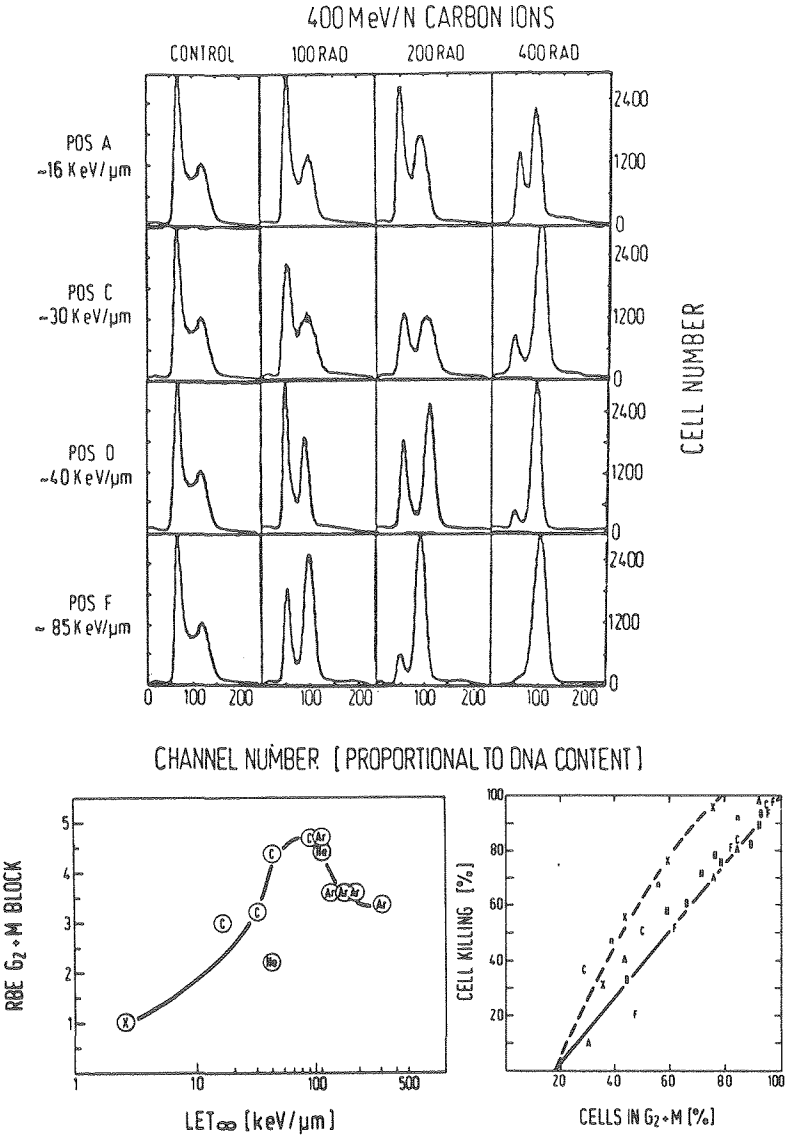

Figure 27 Upper panel: DNA histogram from CH-V79 cells after 1, 2 and 4 Gray of 400 MeV/u carbon ions at different positions of beam range.

Lower left panel: RBE values for G_2 + M block in CH-V79 cells plotted against ionization density expressed as LET_∞ for ^{12}C, ^{20}Ne, and ^{40}Ar.

Lower right panel: Relationship between the block in G_2 + M and CH-V79 cell killing for x rays (X), carbon ions at positions A, C, D, F and neon ions at position A(n) and D(N). (From: Lücke-Hühle et al., 1979). (XBL 819-4967B)

to x rays. Autoradiographic evidence of Schlag and Lücke-Hühle (1981) indicates that 8-10 hours after irradiation with α-particles, a fraction of cells which presumably were exposed during G_1 or early S phase do become delayed in S phase. They concluded that such a late and dose-dependent delay is in agreement with the observations of Raju et al. (1980a) at higher doses and is not seen after ^{60}Co-irradiation.

Pulse labeled mitoses (PLM) experiments have been done with Bevalac carbon and neon beams using the V-79 hamster cells (Blakely et al., 1980c). The lower left panel of Figure 28 summarizes the specific G_2 + M delay examined as a function of dose for both x rays and heavy ion experiments. The data are preliminary, but indicate a linear dose response. The slope of the x-ray curve is about 0.2 min/rad. The slope of the dotted line drawn through the single carbon plateau point is very similar (close to 0.2) which would be expected since carbon plateau ions have a low LET value of 11 keV/μm. Despite the almost identical survival curves obtained with the neon and carbon peak ions, the slopes of the lines for the mitotic delay end point are slightly different for the two ions (0.8 min/rad for neon and 0.6 min/rd for carbon). With this type of plot it is possible to calculate an RBE value for the G_2 + mitotic delay induced by the particle beams by taking the ratio of doses of x ray and of the particle beam that yield the same level of effect. This has been done at several levels of G_2 + M delay and the results are plotted in the upper panel of Figure 28.

Figure 28 shows RBE as a function of heavy-ion dose for the two end points (G_2 + mitotic delay and cell killing). The top two lines on the figure indicate that the RBE for the delay end point is independent of heavy ion dose in the dose region studied. This reflects the linear relationship between the

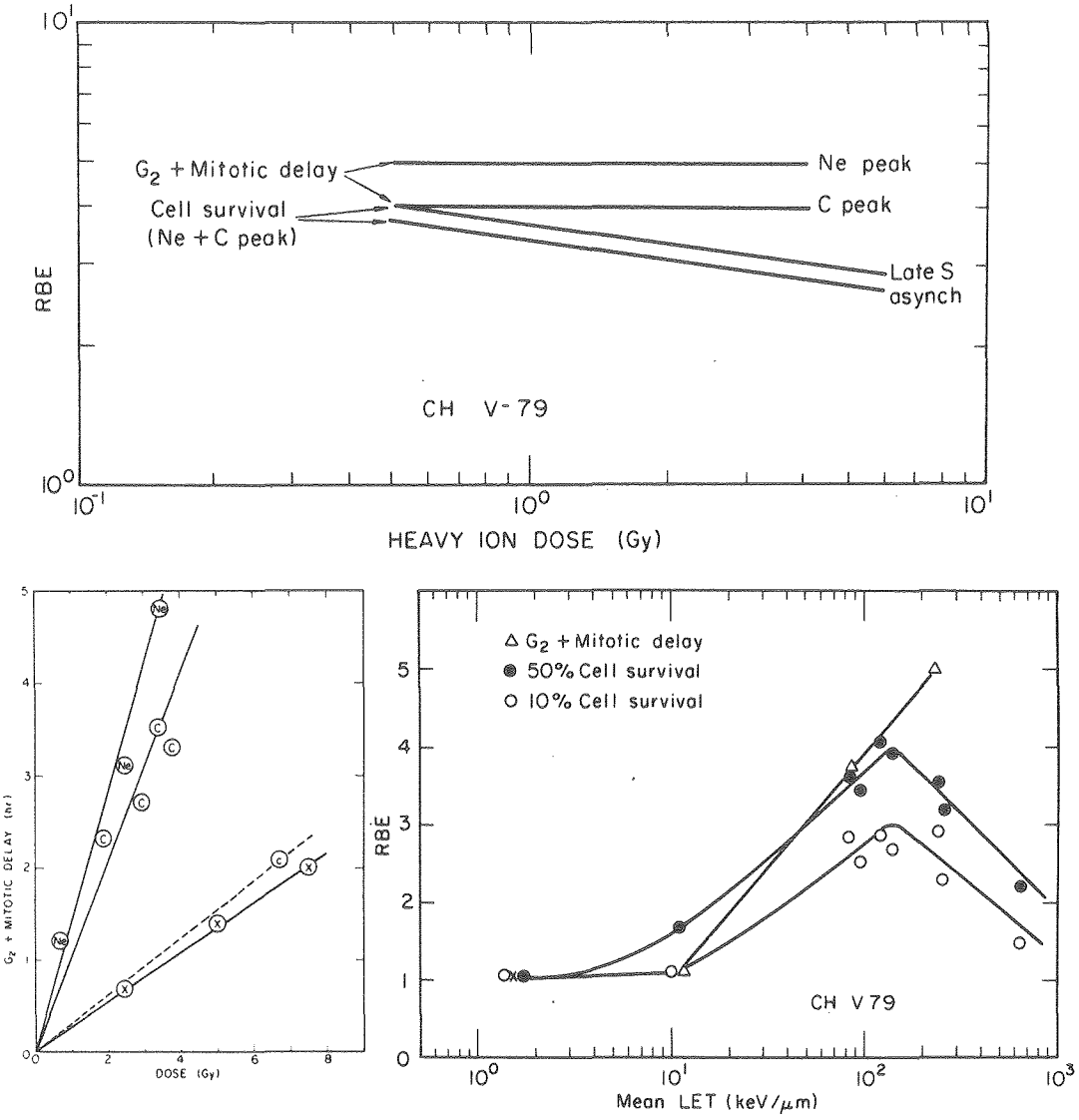

Figure 28 Upper panel: RBE for two end points (CH-V79 cell survival and G_2 + M delay) versus heavy ion dose. Survival data show the response of asynchronous and late S phase cells to Bragg peak 403 MeV/u carbon ions and 429 MeV/u neon ions.

Lower left panel: Duration of G_2 + mitotic delay in CH-V79 cells as a function of dose of 225 kVp X rays (X); Bragg plateau 400 MeV/u carbon ions (C); Bragg peak 403 MeV/u carbon ions (C); or Bragg peak 429 MeV/u neon ions (Ne).

Lower right panel: RBE for two end points (CH-V79 cell survival at 50 percent and 10 percent, G_2 + M delay) versus mean track average LET_∞ (keV/μm). Data are taken from carbon, 425-429 MeV/u neon, and 570 MeV/u argon ions beams. (From: Blakely et al., 1980c). (XBL 805-3368A)

x ray and heavy-ion dose response of the G_2 + M delay. The effect is the same at all delay levels studied, with the RBE for the neon peak observed as greater than that for the carbon peak. In contrast, the lowest lines on the figure demonstrate that the RBE for cell killing has a dose dependence, with a higher RBE at low-dose for asynchronous cells irradiated with the neon or carbon peak ions. Cell killing for synchronized late S phase V-79 cells was measured in separate experiments (Ngo, in Blakely et al., 1980c). The S phase RBE data are more representative of the population followed in the PLM experiments. The S phase cells are more x-ray radioresistant, and the RBE for the synchronized population is greater than that seen for the asynchronous population. The RBE for G_2 + mitotic delay is greater than the RBE for cell killing, especially at high doses and even at doses that give equivalent cell killing.

The lower right panel of Figure 28 is a plot of RBE at 50 percent and 10 percent survival as a function of mean average LET. The data are based on carbon, neon, and argon ion experiments. A single curve has been drawn through all the points, although there is evidence (Blakely et al., 1979) to indicate it is more appropriate to draw a line through the data from each ion at LET values above 100 keV/μm. To simplify the discussion, this has not been done. Carbon and neon at 85 and 234 keV/μm, respectively, yield the same RBE for cell killing because these data appear to lie on equal sides of a peak in the RBE curve. The open triangles show the LET dependence of RBE for the G_2 + M delay. A straight line has been drawn through the delay data points, but results at more LET values need to be examined. The maximum RBE of the G_2 + M delay may have been missed by not examining an LET of 100 keV/μm, or perhaps it may peak at a greater LET than the cell killing end point.

Skarsgard (1967) using Chinese hamster cells ($CH2B_2$) and low-energy heavy-ion beams of helium, lithium, oxygen, boron, and carbon has shown that the RBE values for mitotic delay, chromatid exchanges, and cellular survival all reach maxima at LET values of approximately 150 to 200 keV/μm, and then fall off for higher values of LET. Skarsgard used higher doses for his RBE determination for mitotic delay than did Blakely et al., 1980c; however, their RBE values for G_2 + M delay are similar to his, with both sets of data reaching a maximum of about 4.0 to 5.0.

In contrast to Skarsgard's results, however, Blakely et al. (1980c) did not see an exponential dose dependence for mitotic delay. They saw a linear dose response, similar to that seen by Lücke-Hühle et al. (1979). The latter authors used the flow cytometry (FCM) method to analyze the number of cells arrested in G_2 + M, and observed similar (i.e., 4.4 to 4.7) RBE values for carbon 400 MeV/u and neon 425 MeV/u Bragg peak Bevalac beams when the RBE was calculated as a ratio of the slopes of the plots of maximum number of accumulated G_2 + M cells vs. dose. They obtained even higher values (i.e., 8.3 for carbon peak) when they calculated the RBE by comparing doses yielding 50 percent of the maximum number of cells in G_2 + M at 8 hours after irradiation. These differences may be a result of the fact that the FCM technique scores all cells in the G_2 + M block no matter at which stage the irradiation or block occurred, whereas the PLM technique only scores the G_2 + M block incurred by cells in S phase at the time of irradiation. Using PLM techniques, Geard (1980) studied cell cycle progression of Chinese hamster V-79 cells irradiated with helium ions of various energies and found that radiation-induced delays of cellular progression through the cell cycle are optimally affected by particles depositing about 100 keV/μm.

The PLM curves of Blakely et al. (1980c) for x ray or heavy-ion irradiated V-79 cells indicate that within the resolution of the curve fits made by eye, there is no obvious increase in the duration of the S phase subsequent to irradiation. This observation appears to support the heavy-ion results of Lücke-Hühle et al. (1979) and the pion results of Schlag et al. (1978), however, PLM curves are not the most sensitive way to estimate S phase delay.

The PLM studies of Geard (1980) show only a slight, and probably not a significant, increase in the duration of S phase after irradiation with helium ions, even at LET values between 63 and 138 keV/μm. In contrast, Raju et al. (1980a) using FCM techniques, concluded that there was a significant prolongation of the S phase of V-79 cells irradiated with alpha particles compared to comparable cell killing doses of x rays. Work is needed to resolve these differences, and to elucidate the mechanism of the G_2 block and division delay for low and high LET radiations.

F. Radiosensitizers and Radioprotectors

Oxygen is a potent radiosensitizer, but as described in Section IVB, modification by oxygen of the radiation response of mammalian cells diminishes as LET is increased, and disappears within the limits of the experimental error at around 250 keV/um. This has been demonstrated with charged particle beams of both low initial energy (Todd, 1967; Barendsen et al., 1966) and of high initial energy (Blakely et al., 1979). The explanation for the diminishing OER with increasing LET is thought to be most likely due to the dense production of free radicals at high LET. This results in increased radical-radical interactions and a diminished importance of DNA free-radical interactions with reactive chemical species like O_2 in the environment of the cell (Alper and Howard-Flanders, 1956; Brustad, 1962). This explanation is being evaluated in

view of recent studies with glutathione deficient human fibroblasts which have a very reduced OER with x rays (Endgren et al., 1980; Midander, 1982), presumably due to the inability of the endogenous sulfhydryl compounds under hypoxia to restore the low LET radiation-induced lesions in DNA. One may expect that these cells would also be unable to restore high-LET radiation-induced lesions.

Other radiosensitizers have been used to examine mechanistic questions regarding modification of high LET damage. Tym and Todd (1964), for example, found that the sensitization to the lethal effects of ionizing radiation by halogenated pyrimidines incorporated into DNA that they observed with low LET x rays and also at 25 keV/μm with helium ions was eliminated at LET values greater than 220 keV/μm with carbon ions. At LET values that yielded survival curves with a shoulder, it was possible to increase the radiosensitivity with these agents. However, where high LET radiation yielded an exponential survival curve, these agents were ineffective.

The broadening of the LET distribution in the extended Bragg peak of a heavy ion beam with the use of a spiral ridge filter for therapeutic treatment increases the amount of low-LET modifiable damage (see Section III B). Although the OER is greatly diminished at high LET in the Bragg peak of pristine Bevalac beams, as described above in Section IV C, the use of the spiral ridge filters increases the OER across extended Bragg peak regions. It therefore became of clinical interest to examine the extent of additional radiosensitization of hypoxic cells which would be achievable with the combined use of hypoxic sensitizers and heavy ion beams with extended peaks.

Drugs which have been studied include metronidazole (Chapman et al., 1977, 1978), misonidazole (Chapman et al., 1977, 1978; Tenforde et al., 1981b;

Guichard et al., 1982), RO-07-0741 (Chapman et al., 1978) and desmethylmisonidazole (Tenforde et al., 1982b).

Table IV summarizes the in vitro mammalian cell work of Chapman et al. (1978) with 5 mM concentrations of three different radiosensitizers and four charged particle beams. The results show that hypoxic cell sensitizers can further reduce the low OERs obtained with high LET radiations. This point has also been demonstrated for other high LET radiation modalities including neutrons (Hall et al., 1975; Denekamp et al., 1977), alpha particles (Raju et al., 1977), and pions (Raju et al., 1978f).

Rat rhabdomyosarcoma tumor growth delay studies with hypoxic cell sensitizers in vivo have confirmed the in vitro sensitizer work by demonstrating that administration of misonidazole in combination with either single or fractionated doses of carbon-ion or neon-ion radiation in the narrow 4-cm extended Bragg peak can result in enhancement ratios of 1.1 - 1.3 (Tenforde et al., 1981b). In addition, single doses of misonidazole have been demonstrated to completely inhibit PLD repair by human melanoma tumors transplanted into nude mice after Bragg peak neon ion irradiations (Guichard et al., 1982).

The degree of sensitization of hypoxic cell sensitizers is of course dependent on the drug concentration in the tumor. Recent tumor growth delay work using neon ions has shown that desmethylmisonidazole, which is less cytotoxic and therefore can be administerd at a greater concentration intraperitoneally, can exert a significantly greater (1.4 - 1.5) radiosensitizing effect than is feasible with misonidazole (Tenforde et al., 1982b). The results of all the clinically relevant hypoxic cell sensitizer studies indicate the potential improvement in therapeutic gain that can be

Table IV. Oxygen Enhancement Ratios* for Chinese Hamster Cells Irradiated with 250 kVp X rays and Various Heavy Charged-Particle Beams in the Presence of Various Hypoxic Cell Sensitizers†

	No Drug	5mM Metronidazole	5mM Misonidazole	5mM Ro-07-0741
250 kVp X rays	2.8	1.60	1.27	1.17
Helium ions (8-cm spread peak	2.40	1.62	1.30	1.13
Carbon ions (plateau)	2.55	1.78	1.46	1.23
Carbon ions (4-cm spread peak)	1.65	1.40	1.23	1.15
Neon ions (4-cm spread peak)	1.57	---	1.10	---
Argon ions (4-cm spread peak)	1.43	---	1.28	---

* At 10% survival level.

† From Chapman et al., 1978.

achieved in enhancing tumor response with combined treatment of sensitizers and high-LET radiation from charged-particle beams.

In addition to the sensitizer studies that are of clinical interest, there have been some more fundamental chemical studies with charged particle beams directed toward the mechanism of high-LET damage on cellular systems. Using particle beams of H^{2+}, Li^{3+}, C^{6+}, Ne^{10+}, and Ar^{18+} of initial energies from 8.5 to 570 MeV/u, Roots et al. (1980b, 1981) found that the contribution to cell killing by hydroxyl radicals was highly dependent on particle velocity and atomic number, but that the results did not correlate well with LET_∞ for the high energy particles. Although, in general, the fraction of the total radiation damage caused by hydroxyl radicals decreased with increasing LET as has also been shown by others (Brustad, 1962; Manney et al., 1963; Takeshita and Sawada, 1974; Singh et al., 1976; Chapman et al., 1979). In the case of the low energy particle beams where fragmentation is minimal, the decrease in the extent of hydroxyl-radical induced cell lethality with respect to LET, corresponded to the decrease in $G_{(OH)}$ values from Vereschinskii and Pikaev (1964) as a function of LET. The data also indicated that hydroxyl radical-mediated damage could not be completely eliminated even at high-LET values where radical-radical recombination was high.

Studies of the cellular inactivation by charged particle beams and the radioprotection afforded by dimethyl sulfoxide (DMSO) have also been examined (Chapman et al., 1979). Interest in these studies stems from the fact that the extent and concentration range for DMSO protection of single and double event mechanisms of x ray inactivation (using the linear-quadratic model) have been shown to be qualitatively and quantitatively different from each other (Reuvers et al., 1973). Since the radioprotection by DMSO has been attributed

to its ability to scavenge hydroxyl radicals generated by radiation in the vicinity of cellular targets, Chapman et al. (1979) have attempted to titrate the relative hydroxyl radical concentration produced at 10^{-9} sec in various charged particle tracks. Use of the Bevalac beams for this purpose is somewhat complicated by the presence of a wide distribution of ionization densities which result from the primary and secondary particles, as well as low LET delta-rays. However, Figure 29 presents a summary of their work with synchronized G_1 phase Chinese hamster cells comparing the ability of DMSO to protect against the single- and double-event mechanisms of cell inactivation by x rays and various particle beams. The data show that the proportion of single-event lesions protected by various concentrations of DMSO are similar for these radiations except for argon ions. DMSO appears to be less effective in protecting against the double-event mechanism of carbon and neon ions, and is much less effective in protecting against both the single- and double-event lesions induced by argon ions. The reduction in the effectiveness of DMSO to protect against cell killing as the LET increases is because the fraction of the hydroxyl mediated damage decreases with LET as discussed above for the track segment studies with ethylene glycol as a radioprotector, using both low and high energy charged particles (Roots et al., 1981).

Sulfhydryl compounds, which protect both by free radical scavenging and by chemical restoration of target (DNA) free radicals, have been employed in some high LET studies (Barendsen and Walter, 1964; Bird, 1980; Antoku, 1975). In similarity to the effects of hydroxyl-radical scavengers, the extent of protection by sulfhydryl agent was found to diminish as the LET increased, presumably due to the lower hydroxyl yields at high LET as well as due to an ineffectiveness of sulfhydryl compounds to restore some types of

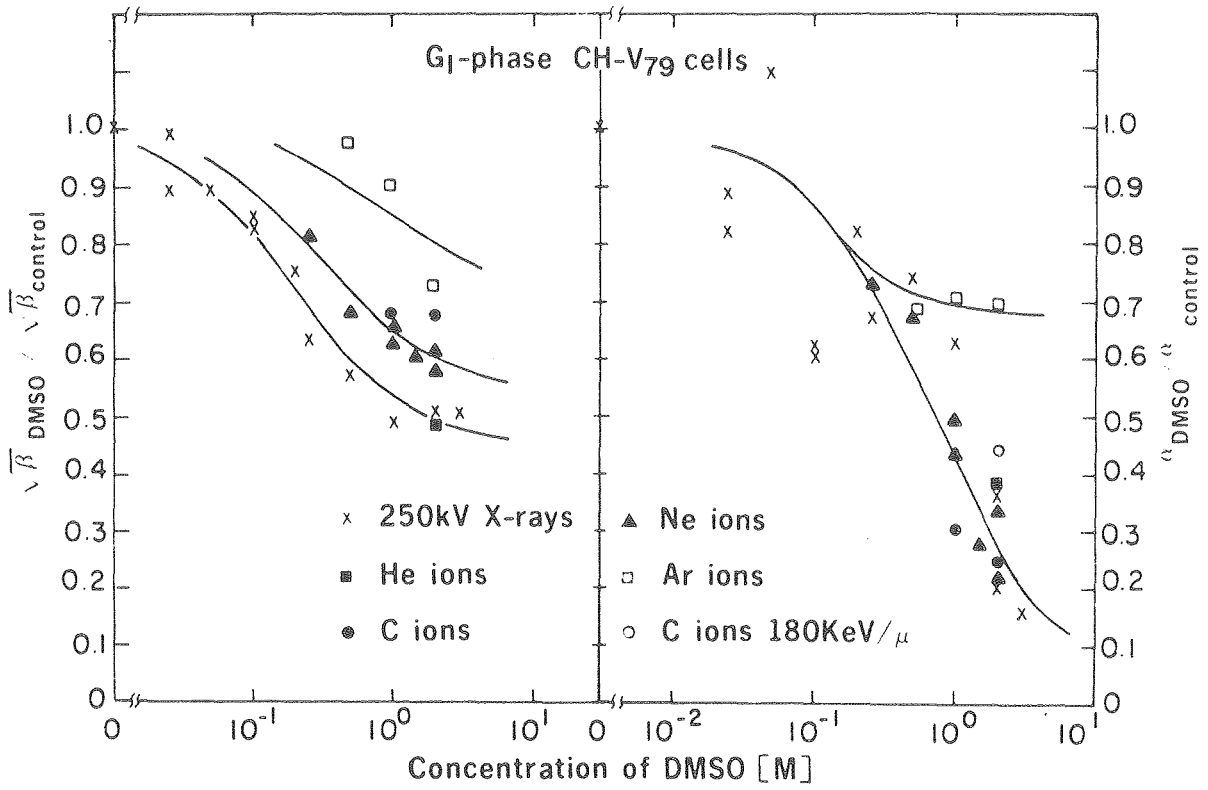

Figure 29 A comparison of the level of DMSO protection against the single- and double-event mechanisms of CH-V79 cell inactivation by the various radiations studied. The lines drawn represent best-fits to a simple competition-kinetic model. (From: Chapman et al., 1979.) (XBL 8110-7162)

high-LET-induced lesions. Recent experiments with synchronized Chinese hamster cells by Bird (1980) have demonstrated that a high concentration (75 mM) of cysteamine can protect against damage from helium ions with LET values of 90 or 170 keV/μm. The extent of protection for cells both at the G_1/S boundary and in late S phase decreased with increased LET but, although more than a factor of two reduced compared to x rays, the dose-modifying factor was still approximately 1.5 at 170 keV/μm. This shows that high LET damage can still be modified by maximal removal of hydroxyl radicals and by maximal chemical restoration of the lesions.

The effects of caffeine on DNA synthesis, cell progression and cell survival after exposure to low LET radiation have been examined in detail (Tolmach et al., 1977; Walters et al., 1974; Nilsson and Lehmann, 1975, and Busse et al., 1977). Caffeine has also been used to test the hypothesis that post-irradiation treatment with the drug can enhance the single-hit component of cell inactivation of ionizing radiations of both low and high LET (Schroy and Todd, 1979a, 1979b; Schroy et al., 1980a, 1980b). Conclusions from work with X and γ rays and both fast neutrons and high-energy carbon ions indicate that caffeine, when present at 2 mM for 60 hr or more after irradiation, can modify the expression of potentially lethal single-hit radiation damage.

Only one study has been completed to study the effects of hyperthermia (41° - 44°C) on high LET radiation damage from Bevalac beams. Gerner and Leith (1977) have measured cellular survival parameters after exposure to pristine Bragg peak carbon ions (34.1 keV/u) combined with exposures to thermal doses administered immediately before irradiation. Gerner et al. (1976) had previously found that hyperthermia interacted in a similar manner with sublethal x-ray and helium-ion radiation damage, but that elevated temperatures

did not potentiate lethal helium-ion damage to the same extent as lethal x ray damage. The results with the carbon ions showed that hyperthermia and a relatively high-LET radiation interacted mainly additively, and not in the greater than additive, or synergistic manner that hyperthermia interacts with low-LET radiation. It appears from their work that only a small high-LET component may be required in combination with hyperthermia to eradicate the shoulder region of the single-dose survival curve measured with carbon ions. Further work is needed to clearly define the ability of combined treatments with hyperthermia and mixed high- and low-LET radiations to limit cellular repair and/or expressions of damage.

In summary, the modification of cellular damage from mixed-LET radiation fields by hypoxic cell radiosensitizers has been demonstrated to show promise in improving the therapeutic advantages of heavy ions by further diminishing the resistance of hypoxic cells, and by eliminating the repair of potentially lethal damage. Fundamental cellular studies with unmodified and extended Bragg peaks have been done to examine modification of heavy-ion damage by chemicals and by hyperthermia. Radiosensitization and radioprotection have been demonstrated, even at very high LET values above 100 keV/μm. The extent of lethality modifiable by the available concentrations of hydroxyl-radical scavengers diminishes as the ionization density increases. In aerobic systems the extent of hydroxyl radical induced cell inactivation is about 60 percent of the total radiation damage at low LET, but only about 25 percent at high LET. In nitrogen saturated cells this percentage is 20 to 25 percent for low LET radiation and probably is not changed much with high LET radiation. There is some evidence with caffeine and perhaps hyperthermia indicating that modification of repair processes can change the expression of high-LET damage.

Additional work is needed in the Bragg peak of particle beams of low initial energy, or in the plateau of high energy Bevalac beams, both of which have more well-defined particle track structure. These studies are important for a complete quantitative analysis of the radiation chemistry of particle tracks for the purpose of resolving specific effects of the core and penumbra and for quantitative correlation with cellular targets. The recent development of a theoretical model that can accommodate experimental data of this type (Tobias et al., 1980), and also recent discussions of the biochemical consequences of the spatial distribution of ionizing radiation-produced free radicals (Barendsen, 1979; Goodhead et al., 1980; Chapman and Gillespie, 1981; Ward, 1981; Virsik and Harder, 1981), indicate that there are several testable hypotheses that can be examined with heavy-ion beams.

G. Spheroid Studies

Multicellular spheroids of certain cell lines are known to have an increased radioresistance to low-LET radiation compared to survival of cells in monolayer (Durand and Sutherland, 1975; Dertinger and Lücke-Hühle, 1975). The presence of hypoxic cells within the architecture of the spheroid does not always completely account for the enhanced survival of the cell irradiated while growing in tight three-dimensional contact (Dertinger et al., 1982).

There are two cell systems that have been used to examine the effects of Bevalac charged particle beams on cell killing in multicellular spheroid cultures as shown in Figure 30. Lücke-Hühle et al. (1980) using Chinese hamster V-79 spheroids and Rodriguez and Alpen (1980, 1981) using rat 9-L gliosarcoma spheroids both demonstrated that the increased resistance of spheroid cultures due to hypoxia and/or intercellular effects is reduced in the Bragg peak of high LET beams of carbon, neon, and argon ion beams compared

Figure 30 Upper panel: Survival of V79 spheroid cells after exposure to heavy ion beams at a plateau (▲) and mid 4-cm extended Bragg peak position (●), respectively. Each point represents the mean ±SE. Argon data are from one experiment only. For comparison survival after x-ray (○) is included. (From: Lücke-Hühle et al., 1980.)

Lower left panel: Survival curves for 9 L-21 rat brain gliosarcoma cells irradiated with x rays as spheroids (○) and as cell suspensions (●). The curve for spheroid cells represents the pooled results for small (100 μm) and large (300 μm) diameter spheroids. Standard deviations are indicated by bars. (From: Rodriguez and Alpen, 1981.)

Lower right panel: Survival curves for cells irradiated as spheroids (○) and cell suspensions (●,△) in the plateau, proximal, mid, and distal portion of the 4-cm spread Bragg peak positions P, Q, R, and S) of a 570 MeV/u argon ion beam. (From: Rodriguez and Alpen, 1980.) (XBL 797-3640A)

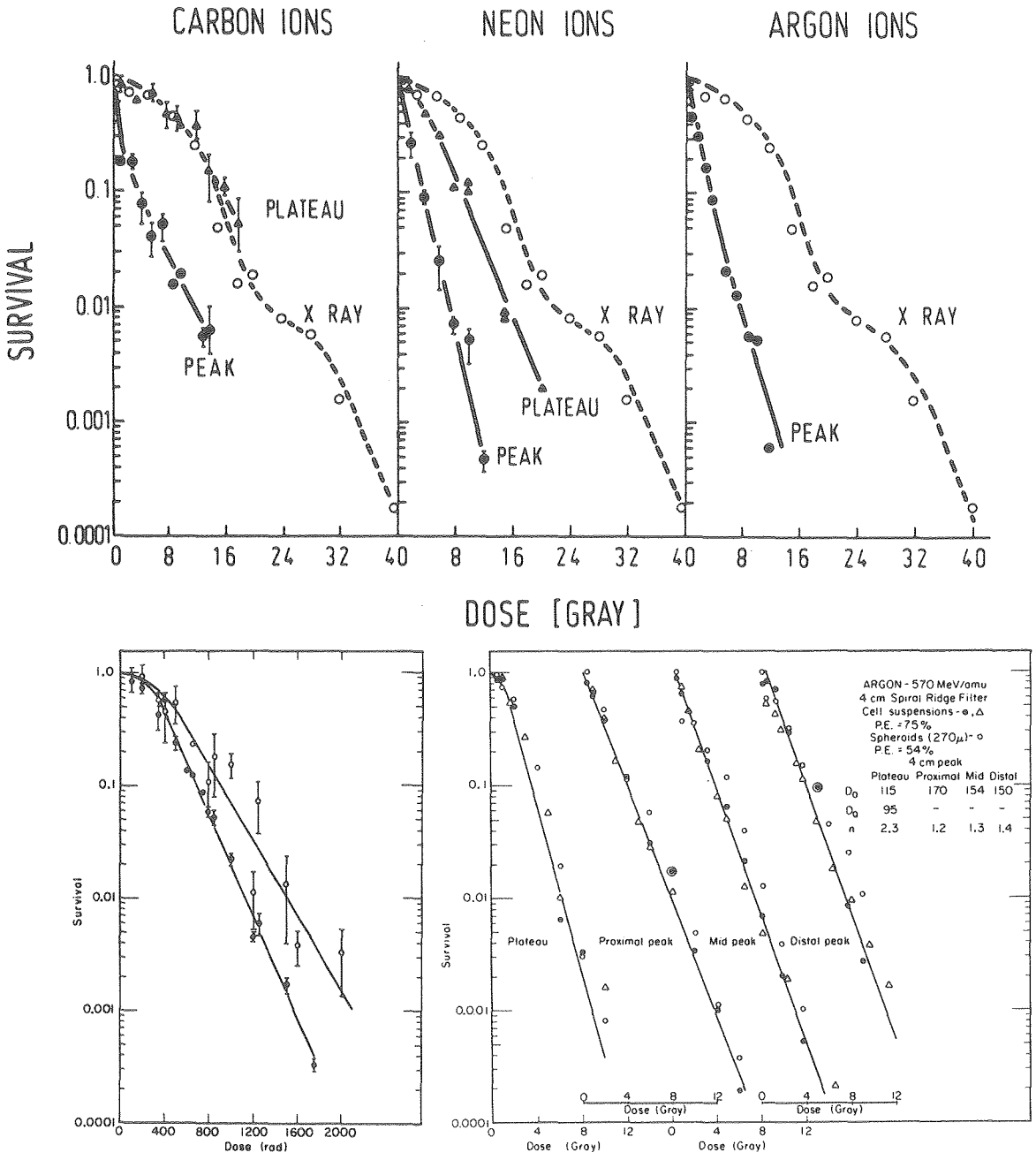
CARBON IONS
NEON IONS
ARGON IONS
SURVIVAL
1.0
0.1
0.01
0.001
0.0001
PLATEAU
X RAY
PEAK
0 8 16 24 32 40
DOSE [GRAY]
Survival
0.0001
0 400 800 1200 1600 2000
Dose (rad)
ARGON - 570 MeV/amu
4 cm Spiral Ridge Filter
Cell suspensions - ●, △
P.E. = 75%
Spheroids (270μ) - ○
P.E. = 54%
4 cm peak
Plateau Proximal Mid Distal
D0 115 170 154 150
D0 95 - - -
n 2.3 1.2 1.3 1.4
Plateau
Proximal peak
Mid peak
Distal peak
0 4 8 12
Dose (Gray)

Figure 30

Table V. Summary of RBE Values for Monolayers and Spheroids Irradiated with Heavy Ions Relative to 225 kVp X rays.

	RBE for V-79* Survival of 10 %	RBE for 9-L† Survival of 10 %
X ray, 225 kVp		
monolayer	1.0	1.0
spheroids	1.0	1.0
Carbon, 400 MeV/u		
Plateau		
monolayer	1.0	1.0
spheroids	1.0	0.97
Mid 4-cm Bragg peak		
monolayer	1.8	—
spheroids	4.2	1.9
Neon, 425 MeV/u		
Plateau		
monolayer	1.4	1.1
spheroids	1.5	1.2
Mid 4-cm Bragg peak		
monolayer	2.4	—
spheroids	4.1	2.5
Argon, 570 MeV/u		
Mid-4 cm Bragg peak		
monolayer	2.1	2.1
spheroids	4.1	2.2

* Data are from Lücke-Hühle et al., 1980.

† Data are from Rodriguez and Alpen, 1980, 1981.

to single cell survival measured after exposure to low LET radiations (x rays) or measurements of survival in the plateau of the Bragg ionization curves. As shown in Table V, the RBE values for cell killing in the V-79 spheroid system irradiated with the 4 cm extended Bragg peak were significantly greater than the RBE values for cell killing in the 9-L spheroid system. This is thought to be due to the fact that the large diameter (390 μm) V-79 spheroid has an hypoxic cell fraction (Lücke-Hühle et al., 1980), whereas the 9-L spheroid of similar diameter (302 μm) is reported to be devoid of an hypoxic fraction. Both systems demonstrated that heavy ions reduced the radioresistance due to intercellular factors within the spheroid.

V. APPLICATIONS TO CANCER RESEARCH

Heavy ions were initially proposed for clinical radiotherapy based on two key requirements for effective treatment: (1) to deliver high killing dose to a localized tumor target while sparing normal tissue lying in the treatment volume, and (2) to reduce the radioresistance of hypoxic cells (i.e. to obtain an optimally low OER).

With the accumulation of additional information on the effects of charged particles, other potential therapeutic advantages became apparent including a reduction in the efficiency of certain radiation damage repair processes, a reduction in the differences in radiosensitivity that are dependent on the cell division cycle and increased delays in cell progression. The observation of potentiation of cell killing with fractionated heavy ions doses, and with combined treatments of high and low LET radiation needs further examination but may also be of importance to therapy planning. It also appears that certain types of noncycling tumor cells are more sensitive to heavy ions than to low LET radiation. Tumor cells that are aneuploid and have larger amounts of DNA than normal may also be more sensitive to heavy ions than normal tissue cells. In addition there are "interactions" between the cells in contact in spheroids and probably in organized tissues that are associated with an increased resistance to low LET radiation. These interactions are significantly altered by heavy ions. Charged particle beams with high LET values between 100–250 keV/μm can significantly decrease the OER. Several of the additional effects described above also occur at high LET values in this range, however, more research is needed to correlate these complex processes.

The evaluation of therapeutic advantages of heavy ions we have just described led to a comparison of each of the beams with other available therapy modalities. Using the criterion of the oxygen gain factor and the ratio of the biologically effective doses for cellular survival endpoints in vitro, we have constructed a vector representation to compare the following radiations: low-LET sources (gamma and x rays), protons, helium, carbon, neon, silicon, and argon ion beams. These plots were made to describe the treatment of two targets: a 10 cm x 10 cm field, 4 cm deep at 12 cm average tissue depth (upper panel) and a 10 cm x 10 cm x 10 cm field at 19 cm average tissue depth (lower panel).

The most advantageous positions of the figure for therapy are located at the upper right quadrant. For the smaller, more shallow target volume (upper panel of Fig. 31), it appears that 308 MeV/u carbon is superior in the ratio of biologically effective dose, with 425 MeV/u neon, 530 MeV/u silicon and 570 MeV/u argon falling off to BED ratios that are similar to protons. On the other hand, argon (570 MeV/u), and silicon (530 MeV/u) have the best OGF advantages, with neon and carbon showing successively less OGF advantage. Helium and protons show an enhanced biologically effective dose ratio, but are most similar to the low-LET radiations with respect to OGF, which results in their intermediate placement in the vector plot.

For a larger, deeper tumor (lower panel of Fig. 31), the relative placement of each of the therapy modalities is altered, except for the location of the 187 MeV/u proton and 225 MeV/u helium data. At this range, the effects of 400 MeV/u carbon and 228 MeV/u helium beams are quite similar. The 557 MeV/u neon beam has a somewhat greater OGF advantage. The low-LET modalities have

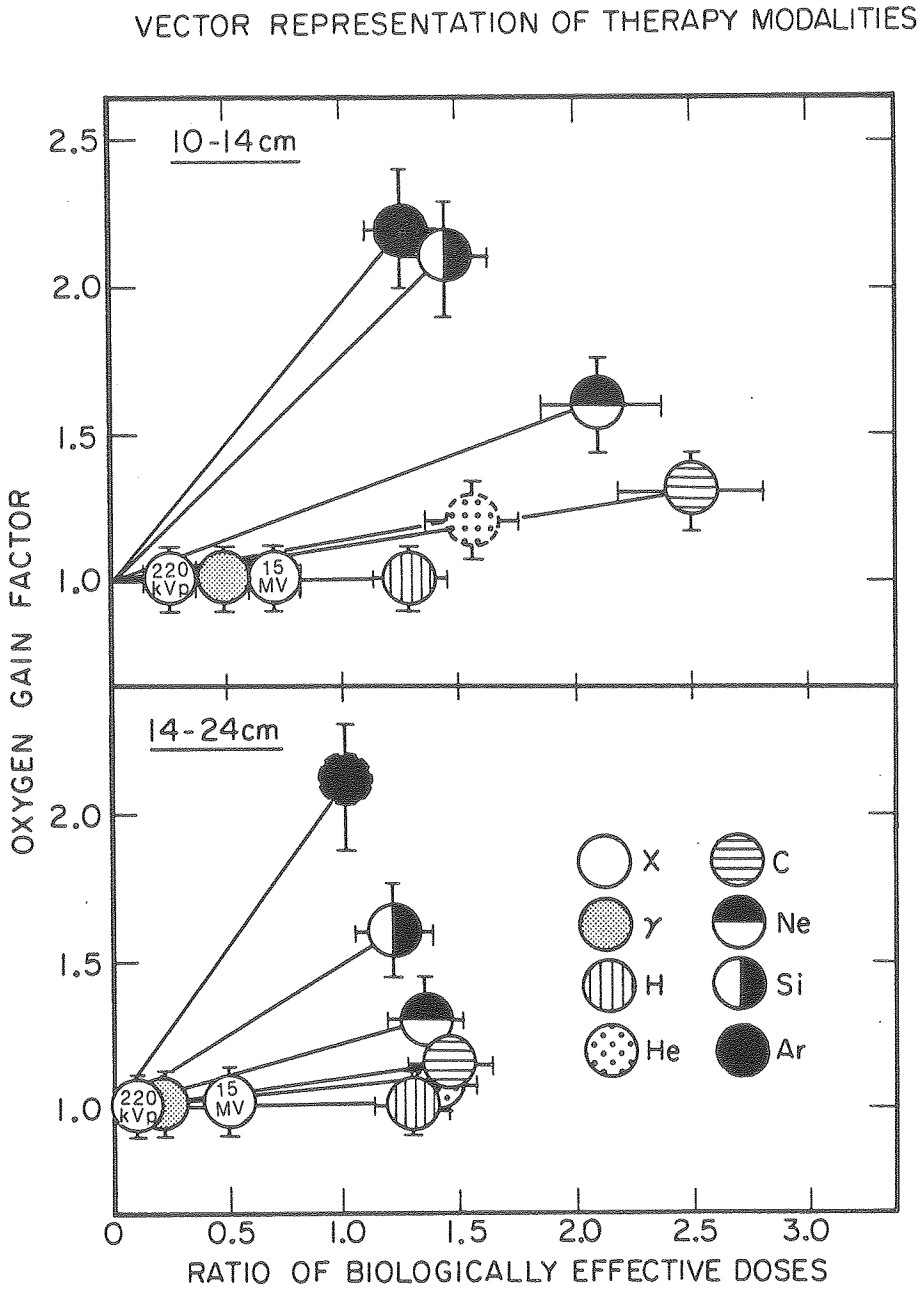

Figure 31 Vector representation of low-LET and high-LET particle therapy modalities for treatment of: a small, shallow field (upper panel) and a large, deep field (lower panel). Explanation of the labels for each axis of the plot (ordinate: oxygen gain factor; abscissa: ratio of biologically effective doses) can be found in the text. (XBL 8110-4238)

deteriorated considerably in their effective dose ratio. The argon data (estimated for a 700 MeV/u beam) and the 670 MeV/u silicon data clearly have an advantageous OGF value even at the greater depth.

Based on this comparison, the best biologically effective depth-dose ratio for situations corresponding to therapy needs can be obtained with accelerated carbon beams. All other heavy beams tested, as well as pions, are markedly better than the effective depth dose ratios achievable with neutrons, x or γ rays. A significant depression of the OER at the various depths required for therapy has been achieved with silicon and argon beams, while these beams still retained advantageous biologically effective depth dose ratios. The depression of the oxygen effect with silicon or argon ion beams is greater than that achievable with neutrons or pions, or with heavy ions of lower atomic number.

The assumptions regarding the importance of oxygenation in the radiocurability of human tumors has been under scrutiny (Withers and Suit, 1974). Recent experimental evidence based on measurements of the local variation in oxygen tension across the width of a spheroid has suggested that a low concentration of oxygen is only one of the factors causing degenerative changes in the center of spheroids. Gradients also exist in a spheroid for nutrients (e.g., glucose), pH and osmolarity, similar to what is expected within a tumor (Carlsson et al., 1979). The observation that heavy ions reduce the radioresistance due to hypoxia and to intercellular contact needs further research but holds additional promise for heavy-ion radiotherapy.

The accumulated cellular radiobiological data obtained with particle beams has demonstrated reasonable predictive value for the response of a limited number of human skin nodules irradiated with either carbon, neon, silicon, or

argon ion beams (J. R. Castro, private communication). Since the cellular experiments were single dose studies and the human skin exposures were done in a fractionated schedule, this similarity in biological effect may only be fortuitous. Differences between in vitro and in vivo results need to be examined in view of the finding in vivo that at the same LET there is not only a tissue specific dependence of heavy ion effects on particle atomic number, but that the peak efficiency for killing cells of certain tissues (e.g., testes) and cells within spheroids may occur at a somewhat lower LET (~100 keV/μm) than that found with cells in vitro (~100 - 200 keV/μm). For a review of the tissue results see Leith et al., 1983. The resolution of these disagreements are of obvious importance.

Whereas the cellular radiobiological results seem to pinpoint properties of particle beams that may be useful for therapy, as we proceed to clinical applications it is important to devise methods to test the efficacy of their use in man. Skin irradiations of patients with superficial nodules allow quantitation of the responses. Lung tumor nodules are also suitable for critical evaluation of depth effects of heavy ion beams. There is an obvious need for additional experimental methods to pinpoint the location of hypoxic tissues in the body and methods for determining cell proliferation in vivo in order to quantitatively assess radiotherapeutic procedures. An evaluation of methods for testing the effects of chemotherapeutic agents has recently been made (Fidler and White, 1982). Chapman et al. (1981) have also demonstrated in animal tumors that radioactively labelled hypoxic cell sensitizers may have diagnostic potential for assessing degrees of tumor hypoxia. Another approach to making in vivo evaluations by measuring the chemiluminescence of cells in vivo has been made by Boveris et al. (1980). Hyperthermia experiments and

work with hypoxic cell radiosensitizers indicate that studies with combined modalities continue to be of interest. Although further work is needed, the overall conclusion of cellular studies with heavy-ion charged particle beams substantiates the conceptual basis for physical and radiobiological advantages of accelerated heavy-ion beams for potential cancer therapeutic trials.

VI. SUMMARY

The effects of accelerated heavy charged particles on cellular systems in vitro are reviewed and physical characteristics and beam monitoring and dosimetry are briefly described. In summarizing this work the following general comments can be made:

1. A variety of cellular systems have been used to examine the biological effects of high energy (eg., 308-670 MeV/u) heavy-ion charged particle beams of carbon, neon, silicon, and argon. The beams were studied in several configurations (e.g., unmodified Bragg peaks, and 4-cm and 10-cm extended Bragg peaks) which represented LET distributions extending from 10 to more than 1000 keV/μm.

2. Cellular survival dose response measurements under aerobic and hypoxic conditions were the major biological end points studied with the particle beams. These measurements permitted estimates of OER and RBE values relative to x or gamma rays. In monoenergetic beams the RBE continuously increased as the residual range decreased until near the end of the range, where within the last centimeter, the maximum RBE was reached and then it declined. The OER declined along the range of penetration for each particle, and at the Bragg peak it was within a few percent near unity. The OER values were less than 2.0 for the last 6 cm of the argon ion beams range studied, and for the last 4 cm of the silicon beam of similar full depth of penetration.

Radiobiological studies are also reported for beams with extended Bragg peaks intended to model dose distributions to be used in therapy. In general, the results depend on the method of attenuating and spreading the beam, on the construction of spiral ridge filters, and on the depth of the extended Bragg peaks. The filters are designed in a first approximation to produce

isosurvival across the extended Bragg peak. Because higher RBE values occur near the distal end of the treatment volume, and the proximal peak and plateau have lesser RBE values, in that order, filters are constructed to produce maximal dose near the proximal end of the extended peak. When isosurvival is produced for aerobic cells, the survival is usually not uniform for hypoxic cells. The OGF is highest in the distal region of the extended peaks and lowest at the plateau. The weight of the evidence shows that carbon and neon beams had greater RBE values in the extended peaks than in the plateau and similar OGF advantage for beams of 24 cm full range. Argon beams had higher RBE values in the plateau and proximal peak than in the distal peak indicating that the LET values of particles in the mid and distal peaks were in the overkill region of biological effectiveness. Both silicon and argon beams had significantly greater OGF values than were measured for carbon and neon beams. Based on preliminary results, it appears that silicon beams at an intermediate atomic number between neon and argon have an LET spectrum that (like argon) is superior in reducing the oxygen effect (high OGF), but that they also have RBE characteristics more like neon. Silicon may therefore be potentially the most useful beam for clinical radiotherapy, especially where dual parallel-opposed fields can be used.

3. Split dose studies of cellular repair of heavy-ion damage indicate that repair of sublethal damage is greatly diminished in the Bragg peak of all heavy ion beams studied. However, SLD repair does occur in the entrance plateau of these beams, and therefore may enhance the therapeutic RBE advantage at depth. Similar repair studies in the plateau of the silicon and argon beam have not been completed. Two types of repair of potentially lethal damage have been evaluated: delayed plating of confluent cells and treatment of exponentially

growing cells with anisotonicity. The results indicate that heavy ion beams reduce liquid holding repair to a lesser extent than SLD repair, and that each treatment with hyper- or hypotonic medium demonstrates different repair kinetics and different LET-dependence than liquid holding repair. These factors contribute to the complexity involved in identifying the potentially lethal lesion.

4. Potentiation of cell killing has been shown to result from fractionation of heavy ion doses and from rapid sequential irradiation with heavy ions and low LET radiation. In experiments with synchronized cells, potentiation of cell killing by sequential exposure to low and high LET radiations has been shown to be greatest for cells irradiated in S phase. Furthermore, this work has substantiated the fact that an apparent single-hit inactivation process, as implied by an exponential dose-effect curve, cannot exclude the existence of repair processes.

5. Heavy ions generally reduce the differences observed in the low LET radiation response of cells at various stages of the cell division cycle. This is evidenced by a heavy-ion induced reduction in the shoulder of the survival curve of cells resistant to x rays, and is most marked with argon, the heaviest ion studied. Cell progression studies of heavy ion effects have demonstrated a marked G_2 block that has an LET dependence similar to cell killing but a greater biological effectiveness.

6. The modification of cellular damage from heavy-ion mixed-LET radiation fields by hypoxic cell radiosensitizers has been demonstrated, and may improve the therapeutic advantages of heavy ions by further diminishing the resistance of hypoxic cells and by eliminating the repair of potentially lethal damage. Fundamental cellular studies with unmodified and extended Bragg peaks have been

done to examine modification of heavy-ion damage by chemicals and by hyperthermia. Radiosensitization and radioprotection have been demonstrated, even at every high average LET values, above 100 keV/μm.

7. Bragg peak carbon, neon, and argon ion beams have been shown to reduce the radioresistance due to hypoxia and intercellular factors within multicellular spheroids.

VII. ACKNOWLEDGEMENTS

The authors wish to acknowledge the assistance of the Office of the Radiation Biophysics Group of Donner Laboratory for their assistance in the preparation of this manuscript. In particular we would like to express gratitude for the invaluable editorial work of M. C. Pirruccello, and for the patient typing of the numerous drafts by D. C. Morris and especially L. E. Hawkins. Helpful comments were provided by E. L. Alpen, E. J. Ainsworth, J. R. Castro, A. Chatterjee, H. Crawford, T. L. Criswell, J. L. Magee, J. T. Lyman, R. J. Roots, and T. C. H. Yang. We thank R. G. Stevens for drafting the figures.

These studies were supported by the Office of Health and Environmental Research Division of the Department of Energy under Contract No. W-7405-ENG-48 and No. DE-AC03-76SF00098, and by Research Grant CA-15184 awarded by the National Cancer Institute, DHEW.

VIII. REFERENCES

Ainsworth, E. J., Fry, R. J. M., Grahn, D., Williamson, F. S., Brannan, P. C. Stearner, S. P., Carrano, A. V., and Rust, J. H. (1974). In "Biological Effects of Neutron Irradiation," pp. 359-379. International Atomic Energy Agency, Vienna.

Ainsworth, E. J., Fry, R. J. M., Brennan, P. C., Stearner, S. P., Rust, J. H., and Williamson, F. S. (1976). In "Biological and Environmental Effects of Dose-Level Radiation," Vol. I. pp. 77-92. International Atomic Energy Agency, Vienna.

Ainsworth, E. J., Kelly, L. S., Mahlmann, L. J., Schooley, J. C., Thomas, R. H., Howard, J., and Alpen, E. L. (1983). Radiat Res., in press.

Alonso, J. R., Benton, E. V., Chu, W., Llacer, J., Richier, J., and Tobias, C. A. (1980). In "Biological and Medical Research with Accelerated Heavy Ions at the Bevalac 1977-1980" (M. C. Pirruccello and C. A. Tobias, eds.), pp. 21-34. Lawrence Berkeley Laboratory Report LBL-11220.

Alpen, E. L., and Powers-Risius, P. (1981). Radiat. Res. 88, 132-143.

Alpen, E. L., Powers-Risius, P., and McDonald, M. (1980). Radiat. Res. 83, 677-687.

Alper, T. (1956). Radiat. Res. 5, 573-586.

Alper, T. and Bryant, P. E. (1974). Int. J. Radiat. Biol. 26, 203-208.

Alper, T. and Howard-Flanders, P. (1956). Nature 178, 978-979.

Alper, T., Moore, J. L., and Smith, P. (1967). Radiat. Res. 32, 780-791.

Antoku, S. (1975). Int. J. Radiat. Biol. 27, 287-292.

Appleby, A. and Christman, E. A. (1974). Radiat. Res. 60, 34-41.

Archambeau, J. O., Bennett, G. W., Levine, G. S., Cowen, R., and Akanuma, A. (1974). Radiology 110, 445-457.

Barendsen, G. W. (1962). Nature (London) 193, 1153-1155.

Barendsen, G. W. (1968a). Curr. Top. Radiat. Res. Q. 4, 293-356.

Barendsen, G. W. (1968b). In "Proceedings of the First Symposium on Microdosimetry," Ispra, Italy (H. G. Ebert, ed.), pp. 249-263. Published by the Commission of the European Communities, Brussels.

Barendsen, G. W. (1979). Int. J. Radiat. Biol. 36, 49-63.

Barendsen, G. W., and Walter, H.M.D. (1964). Radiat. Res. 21, 314-329.

Barendsen, G. W., Beusker, T. L. J., Vergroesen, A. J., and Budke, L. (1960). Radiat. Res. 13, 841–849.

Barendsen, G. W., Walter, H. M. D., Fowler, J. F., and Bewley, D. K. (1963). Radiat. Res. 18, 106–119.

Barendsen, G. W., Koot, C. J., van Kersen, G. R., Bewley, D. K., Field, S. B., and Parnell, C. J. (1966). Int. J. Radiat. Biol. 10, 317–327.

Baum, J. W. (1970). In "Proceedings of the Second Symposium on Microdosimetry," Stresa (Italy), October 20–24, 1969 (H. G. Ebert, ed.), pp. 653–666. Published by the Commission of the European Communities, Brussels.

Baverstock, K. F., and Burns, W. G. (1976). Nature (London) 260, 316–318.

Baverstock, K. F., and Burns, W. G. (1981). Radiat. Res. 86, 20–33.

Benton, E. V., and Tochilin, E. (1966). Health Phys. 12, 49–52.

Benton, E. V., Henke, R. P., and Tobias, C. A. (1973). Science 182, 474–476.

Bethe, H. A. (1930). Ann. Physik 5, 325–400.

Bewley, D. K. (1968). Radiat. Res. 34, 446–458.

Bichsel, H. (1968). In "Radiation Dosimetry," (F. H. Attix and W. C. Roesch, eds.), Vol. I., pp. 157–228. Academic Press, New York.

Bird, R. P. (1972). Ph.D. Thesis, University of California, Berkeley.

Bird, R. P. (1980). Radiat. Res. 82, 290–296.

Bird, R. P., and Burki, J. (1971). In "Biophysical Aspects of Radiation Quality," pp. 241–250. International Atomic Energy Agency, Vienna, Austria.

Bird, R. P., and Burki, H. J. (1975). Int. J. Radiat. Biol. 17, 105–120.

Bird, R. P., Rohrig, N., Colvett, R. D., Geard, C. R., and Marino, S. A. (1980). Radiat. Res. 82, 277–289.

Birge, A. C., Anger, H. O., and Tobias, C. A. (1956). In "Radiation Dosimetry" (G. J. Hine and G. L. Brown, eds.), pp. 624–662. Academic Press, New York.

Blakely, E. A. (1983). In "Pion and Heavy Ion Radiotherapy: Preclinical and Clinical Studies" (L. D. Skarsgard, ed.), pp. 229–250. Elsevier Science Publishing Co., Amsterdam.

Blakely, E. A., Tobias, C. A., Ngo, F. Q. H., Yang, T. C. H., Smith, K. C., Chang, P. Y., and Yezzi, M. J. (1978). (Abstract) Int. J. Radit. Oncol. Biol. Phys. 4 (Suppl. 2), 93–94.

Blakely, E. A., Tobias, C. A., Yang, T. C. H., Smith, K. C., and Lyman, J. T. (1979). Radiat. Res. 80, 122-160.

Blakely, E. A., Tobias, C. A., Ngo, F. Q. H., and Curtis, S. B. (1980a). In "Biological and Medical Research with Accelerated Heavy Ions at the Bevalac" (M. C. Pirruccello and C. A. Tobias, eds.), pp. 73-86. Lawrence Berkeley Laboratory LBL-11220.

Blakely, E. A., Ngo, F. Q. H., Chang, P. Y., Lommel, L., and Tobias, C. A. (1980b). In "Biological and Medical Research with Accelerated Heavy Ions at the Bevalac" (M. C. Pirruccello and C. A. Tobias, eds.), pp. 119-124. Lawrence Berkeley Laboratory LBL-11220.

Blakely, E. A., Ngo, F. Q. H., Chang, P. Y., Lommel, L., Kraft-Weyrather, W. Kraft, G., and Tobias, C. A. (1980c). In "Biological and Medical Research with Accelerated Heavy Ions at the Bevalac" (M. C. Pirruccello and C. A. Tobias, eds.), pp. 125-135. Lawrence Berkeley Laboratory LBL-11220.

Boveris, A., Cadenas, E., Reiter, R., Filipkowski, M., Nakase, Y., and Chance, B. (1980). Proc. Natl. Acad. Sci. USA 77, 347-351.

Bradt, H. L., and Peters, B. (1950). Phys. Rev. 77, 35-70.

Brandt, W., and Ritchie, R. H. (1974). In "Physical Mechanisms in Radiation Biology" (R. D. Cooper and R. W. Wood, eds.), pp. 20-50. U.S. Atomic Energy Commission Conf-721001, Washington, D. C.

Brustad, T. (1962). Adv. Biol. Med. Phys. 8, 161-224.

Bryant, P. E., and Alper, T. (1976). In "Proceedings, Fifth Symposium on Microdosimetry, Verbania Pallanza, Italy, 1975" (J. Booz, H. G. Ebert, and B. R. Smith, eds.), Vol. 2, pp. 871-888. Commission of the European Communities, Luxembourg.

Burns, F. J., and Albert, R. E. (1980). In "Biological and Medical Research with Accelerated Heavy Ions at the Bevalac" (M. C. Pirruccello and C. A. Tobias, eds.), pp. 233-235. Lawrence Berkeley Laboratory, LBL-11220.

Burns, W. G., May, R., and Baverstock, K. F. (1981). Radiat. Res. 86, 1-19.

Busse, P. M., Bose, S. K, Jones, R. W., and Tolmach, L. J. (1977). Radiat. Res. 71, 666-677.

Carlssen, J., Stalnacke, C. G., Acker, H., Haji-Karin, M., Nilsson, S., and Larsson, B. (1979). Int. J. Radiat. Oncol. Biol. Med. 5, 2011-2020.

Castro, J. R. (1981). Seminars in Oncology 8, 103-109.

Castro, J. R., and Lawrence, J. H. (1978). In "Recent Advances in Nuclear Medicine" (J. H. Lawrence and T. F. Budinger, eds.), Vol. 5, pp. 119-137. Grune and Stratton, New York.

Castro, J. R., and Quivey, J. M. (1977). Int. J. Radiat. Oncol. Biol. Phys. 3, 127-131.

Castro, J. R., Quivey, J. M., Lyman, J. T., Chen, G. T. Y., Phillips, T. L., Tobias, C. A., and Alpen, E. L. (1980). Cancer 46, 633-641.

Castro, J. R., Saunders, W. M., Tobias, C. A., Chen, G.T.Y., Curtis, S. B., Lyman, J. T., Collier, J. M., Pitluck, S., Woodruff, K. A., Blakely, E. A., Tenforde, T. S., Char, D., Phillips, T. L., and Alpen, E. A. (1982). Int. J. Radiat. Biol. 8, 2191-2198.

Chadwick, K. H., and Leenhouts, H. P. (1975). Phys. Med. Biol. 18, 78-87.

Chadwick, K. H., and Leenhouts, H. P. (1978). Int. J. Radiat. Biol. 33, 517-529.

Chapman, J. D. (1980). In "Radiation Biology and Cancer Research" (R. E. Meyn and H. R. Withers, eds.), pp. 21-32. Raven Press, New York.

Chapman, J. D., and Gillespie, C. J. (1981). In "Advances in Radiation Biology" (J. Lett, ed.), Vol. 9. Academic Press, Inc., New York.

Chapman, J. D., Blakely, E. A., Smith, K C., and Urtasun, R. C. (1977). Int. J. Radiat. Oncol. Biol. Phys. 3, 97-102.

Chapman, J. D., Blakely, E. A., Smith, K. C., Urtasum, R. C., Lyman, J. T., and Tobias, C. A. (1978). Radiat. Res. 74, 101-111.

Chapman, J. D., Doern, S. C., Reuvers, A. P., Gillespie, C. J., Chatterjee, A., Blakely, E. A., Smith, K. C., and Tobias, C. A. (1979). Radiat. Environ. Biophys. 16, 29-41.

Chapman, J. D., Franko, A. J., and Sharpin, J. (1981). Br. J. Cancer 43, 546-550.

Chatterjee, A., and Magee, J. L. (1980a). J. Phys. Chem. 84, 3537-3543.

Chatterjee, A., and Magee, J. L. (1980b). In "Biological and Medical Research with Accelerated Heavy Ions at the Bevalac, 1977-1980" (M. C. Pirruccello and C. A. Tobias, eds.), pp. 53-61. Lawrence Berkeley Laboratory Report LBL-11220.

Chatterjee, A., and Schaefer, H. J. (1976). Radiat. Environ. Biophys. 13, 215-227.

Chatterjee, A., and Tobias, C. A. (1975). (Abstract). Radiat. Res. 62, 561.

Chatterjee, A., Maccabee, H. D., and Tobias, C. A. (1973). Radiat. Res. 54, 479-494.

Chatterjee, A., Tobias, C. A., and Lyman, J. T. (1976). In "Spallation Nuclear Reactions and Their Applications" (B.S.P. Shen and K. Merker, eds.), pp. 169-191. D. Reidel Publ. Co., Dordrecht, Holland.

Chen, G. T. Y., and Pitluck, S. (1983). In "Pion and Heavy Ion Radiotherapy: Preclinical and Clinical Studies" (L.D. Skarsgard, ed.), pp. 149-158. Elsevier Science Publishing Co, Amsterdam.

Chen, G. T. Y., Castro, J. R., and Quivey, J. M. (1981). Ann. Rev. Biophys. Biol. 10, 499-529.

Christman, E. A., Appleby, A., and Jayko, M. (1981). Radiat. Res. 85, 443-457.

Cohen, L., and Awschalom M. (1982). Ann. Rev. Biophys. Bioeng. 11, 359-390.

Collyn-d'Hooghe, M., Hemon, D., Gilet, R., Curtis, S. B., Valleron, A. J. and Malaise, E. P. (1981). Int. J. Radiat. Biol. 39, 297-306.

Cox, R., and Masson, W. K. (1980). Int. J. Radiat. Biol. 38, 575-576.

Cox, R., Thacker, J., Goodhead, D. T., and Munson, R. J. (1977). Nature (London) 267, 425-427.

Curtis, S. B. (1970). In "Charged Particle Tracks in Solids and Liquids" (G. E. Adams, D. K. Bewley, and J. W. Boag, eds.), pp. 140-142. Institute of Physics and the Physical Society, London, England.

Curtis, S. B. (1977). Int. J. Radiat. Oncol. Biol. Phys. 3, 87-92.

Curtis, S. B. (1979). In "Proceedings, Sixth International Congress of Radiation Research" (S. Okada, M. Imamura, T. Terashima, and H. Yamaguchi, eds.), pp. 780-787. Japanese Assocation for Radiation Research, Tokyo, Japan.

Curtis, S. B., Tenforde, T. S., Parks, D., Schilling, W. A., and Lyman, J. T. (1978). Radiat. Res. 74, 274-288.

Curtis, S. B., Schilling, W. A., Tenforde, T. S., Crabtree, K. A., Tenforde, S. D., Howard, J., and Lyman, J. T. (1982). Radiat. Res. 90, 292-309.

Denekamp, J., Morris, C., and Field, S. B. (1977). Radiat. Res. 70, 425-432.

Dertinger, H., and Lucke-Huhle, C. (1975). Int. J. Radiat. Biol. 28, 255.

Dertinger, H., Lucke-Huhle, C., Schlag, H., and Weibezahn, K. F. (1976). Int. J. Radiat. Biol. 29, 271-277.

Dertinger, H., Hing, G., and Jakobs, K. H. (1982). Biophys. Struct. Mech. 9, 89-93.

Durand, R. E., and Olive, P. L. (1976). Int. J. Radiat. Biol. 30, 589-592.

Durand, R. E., and Sutherland, R. M. (1972). Exp. Cell Res. 71, 75-80.

Edgren, M., Larsson, A., Nilsson, K., Revesz, L., and Scott, O. C. A. (1980). Int. J. Radiat. Biol. 37, 299-306.

Elkind, M. M. (1970). In "Current Topics in Radiation Research" (M. Ebert and A. Howard, eds.), Vol. VII, pp. 1-44. Elsevier/North-Holland, New York/Amsterdam.

Elkind, M. M., and Sutton, H. (1960). Radiat. Res. 13, 556-593.

Elkind, M. M., and Whitmore, G. F. (1967). "The Radiobiology of Cultured Mammalian Cells." Gordon and Breach, New York.

Fano, U. (1952). In "Symposium on Radiobiology. The Basic Aspects of Radiation Effects on Living Systems" (J. J. Nickson, ed.). J. Wiley and Sons, Inc., New York.

Fertil, B., and Malaise, E. P. (1981). Int. J. Radiat. Biol. Phys. 7, 621-629.

Fertil, B., Deschavanne, P. J., Lachet, B., and Malaise, E. P. (1980). Radiat. Res. 82, 297-309.

Fidler, I. J., and White, R. J.., eds. (1982). "Design of Models for Testing Cancer Therapeutic Agents." Van Nostrand-Reinhold Co., New York.

Fowler, J. F. (1981). In "Nuclear Particles in Cancer Treatment." Adam Hilger Ltd. Techno-House, Radcliffe Way, Bristol, England.

Fu, K. K., and Phillips, T. L. (1976). Radiology 120, 439-441.

Geard, C. R. (1980). Radiat. Res. 83, 696-709.

Gerner, E. W., and Leith, J. T. (1977). Int. J. Radiat. Biol. 31, 283-288.

Gerner, E., Leith, J., and Boone, M. (1976). Radiology 119, 715-720.

Ghiorso, A., Grunder, H. A., Hartsough, W., Lambertson, G., Lofgren, E., Lou, K., Main, R., Mobley, R., Morgada, R., Salsig, W., and Selph, F. (1973). (Abstract). IEEE Trans. Nucl. Sci. NS-20 111.

Goldstein, L. S., Phillips, T. L., and Ross, G. Y. (1981a). Radiat. Res. 86, 542-558.

Goldstein, L. S., Phillips, T. L., Fu, K. K., Ross, G. Y., and Kane, L. J. (1981b). Radiat. Res. 86, 529-541.

Goodhead, D. T. (1977). Int. J. Radiat. Biol. 32, 43-70.

Goodhead, D. T., Munson, R. J., Thacker, J., and Cox, R. (1980). Int. J. Radiat. Biol. 37, 135-167.

Goodman, L. J., and Colvett, R. D. (1977). Radiat. Res. 70, 455-468.

Graffman, S. and Larsson, B. (1975). In "Proceedings of an International Workshop on Particle Radiation Therapy," pp. 505-527. American College of Radiology, Philadelphia, PA.

Gragg, R. L., Humphrey, R. M., Thames, Jr., H. D., and Meyn, R. E. (1978). Radiat. Res. 76, 283-291.

Grahn, D., Friptak, B. H., Lee, C. H., Russell, J. J., and Lindenbaum, A. (1979). In "Proceedings, International Symposium on Biological Implications of Radionuclides Released from Nuclear Industries," Vol. I, pp. 163-184. International Atomic Energy Agency, Vienna, Austria.

Gray, L. H., Conger, A. D., Ebert, M., Hornsey, S., and Scott, O. C. A. (1953). Br. J. Radiol. 26, 638-648.

Green, A. E. S., and Burki, J. (1972). Radiat. Res. 60, 536-540.

Grunder, H. A., Hartsough, W. D., and Lofgren, E. J. (1971). Science 174, 1128-1129.

Guichard, M., Tenforde, T., Curtis, S., and Malaise, E. P. (1982). Radiobiology 142, 219-223.

Hahn, D. F, Bale, W. F., Lawrence, E. O., and Whipple, G. H. (1939). J. Exp. Med. 69, 739-753.

Hall, E. J. (1969). Br. J. Radiol. 42, 805-813.

Hall, E. J. (ed.) (1982). Int. J. Radiat. Oncol. Biol. Phys. Supplement 8, 2041-2044.

Hall, E. J., Gross, W., Dvorak, R. F., Kellerer, A. M., and Rossi, H. H. (1972). Radiat. Res. 52, 88-98.

Hall, E. J., Roizin-Towle, L., Theus, R. B., and August, L. S. (1975). Radiology 117, 173-178.

Hall, E. J., Bird, R. P., Rossi, H. H., Coffey, R., Varga, J., and Lam, Y. M. (1977). Radiat. Res. 70, 469-479.

Hamilton, J. G., and Soley, M. H. (1939). Am. J. Physiol. 127, 557-572.

Hamilton, J. G., and Stone, R. S. (1937a). Proc. Soc. Exp. Biol. Med. 35, 595-598.

Hamilton, J. G., and Stone, R. S. (1937b). Radiology 28, 178-188.

Haynes, R. H. (1966). Radiat. Res. Suppl. 6, 1-29.

Heckman, H. A., Perkins, B. L., Simon, W. G., Smith, F. M. and Barkas, W. H. (1960). Phys. Rev. 117, 544-556.

Heckman, H. H., Greiner, D. E., Lindstrom, P. J., and Shive, H. (1978). Phys. Rev. C17, 1735-1747.

Henshaw, P. S. (1940). J. Natl. Cancer Inst. 1, 277-290.

Holloway, M. G., and Livingston, S. M. (1938). Phys. Rev. 54, 18–37.

Holthusen, H. (1921). Pflueger Arch. 187, 1–24.

Hornsey, S., Androzzi, U., and Warren, P. R. (1977). Br. J. Radiol. 50, 513–517.

ICRU (International Commission on Radiological Protection and the International Commission on Radiation Units and Measurements) (1963). Report of the RBE Subcommittee to the International Commission on Radiological Protection and the International Commission on Radiation Units and Measurements. Health Phys. 9, 357–386.

ICRU (International Commission on Radiation Units and Measurements) (1979). "Quantitative Concepts in Dosimetry and Radiobiology," Report No. 30, pp. 49–52. ICRU, Washington, D. C.

Isaila, M. V., Schimmerling, W., Vosburgh, K. G., White, M. G., Fritz, R. C. and McNulty, P. J. (1972). Science 117, 424–425.

Jacobson, B. S. (1957). Radiat. Res. 7, 395–406.

Janni, J. F. (1966). In "USAF Technical Report No. AFWL-TR-65-150," Research and Technology Division, Air Force Weapons Laboratory, Air Force Systems Command, Kirkhead Air Force Base, New Mexico.

Jones, H. B., Chaikoff, I. L., and Lawrence, J. H. (1939). J. Biol. Chem. 128, 631–644.

Karlsson, B. G. (1964). Strahlentherapie 124, 481–492.

Katz, R. (1970). In "Proceedings of the Second Symposium on Microdosimetry" (H. G. Ebert, eds.), pp. 631–652. Published by the Commission of the European Communities, Brussels.

Katz, R., and Pinkerton, F. E. (1975). Nucl. Instr. Meth. 130, 105–119.

Katz, R., and Sharma, S. C. (1974). Int. J. Radiat. Biol. 26, 143–146.

Katz, R., Ackerson, B., Homayoonfar, M., and Sharma, S. C. (1971). Radiat. Res. 47, 402–425.

Kellerer, A. M., and Chmelevsky, D. (1975). Radiat. Res. 63, 226–234.

Kellerer, A. M., and Rossi, H. H. (1972). Curr. Top. Radiat. Res. Q. 8, 85–158.

Kellerer, A. M., and Rossi, H. H. (1978). Radiat. Res. 75, 471–488.

Keng, P. C., and Lett, J. T. (1981). Int. J. Radiat. Biol. 39, 655–664.

Kiefer, J. (1975). In "Radiation Research-Biomedical, Chemical and Physical Perspectives" (O. F. Nygaard, H. I. Adler, and W. K. Sinclair, eds.), pp. 1025–1037. Academic Press, New York.

Kliauga, P., and Rossi, H. H. (1975). In "Proceedings of the Fifth Symposium on Microdosimetry" (J. Booz, H. G. Ebert, B. G. R. Smith, eds.), pp. 127-138. Published by the Commission of the European Communities, Luxembourg.

Kliauga, P., Cobrett, R. D., Goodman, L. J., and Lam, Y. M. (1978). In "Proceedings of the Sixth Symposium on Microdosimetry," pp. 1173-1183. Published by the Commission of the European Communities, Luxembourg.

Lacassagne, A. (1942). C. R. Acad. Sci. (Paris) 215, 231-232.

Larsson, B. (1980). In "Advances in Radiation Protection and Dosimetry in Medicine" (T. H. Thomas and V. Perez-Mendez, eds.), pp. 367-394. Plenum Publishing Corporation, New York.

Lawrence, J. H., and Tobias, C. A. (1967). In "Modern Trends in Radiotherapy" (T. J. Delley and C. A. Wood, eds.), pp. 260-276. Butterworths, London.

Lawrence, J. H., Scott, K G., and Tuttle, L. N. (1939). In "New International Clinics," Vol. III, Series 2, pp. 33-58. J. B. Lippincott Co., Philadelphia.

Lawrence, J. H., Tobias, C. A., Linfoot, J. A., Born, J. L., and Chong, C. Y. (1976). J. Am. Med. Assn. 235, 2307-2310.

LBL (Lawrence Berkeley Laboratory) (1977). "Biological and Medical Research with Accelerated Heavy Ions at the Bevalac, 1974-1977." Lawrence Berkeley Laboratory Report LBL-5610.

Lea, D. E. (1955). In "Action of Radiation on Living Cells." Cambridge University Press, London/New York.

Leith, J. T., Arcellana, V., Lyman, J. T., and Wheeler, K. T. (1975). Int. J. Radiat. Biol. 28, 91-97.

Leith, J. T., Smith, P., Ross-Riveros, P., and Wheeler, K. T. (1977). Int. J. Radiat. Biol. 32, 401-407.

Leith, J. T., Ainsworth, E. J., and Alpen, E. A. (1982). Adv. Radiat. Biol. 10, in press.

Linfoot, J. A., ed. (1979). In "Recent Advances in Diagnosis and Treatment of Pituitary Tumors," Raven Press, New York.

Little, J. B. (1971). Int. J. Radiat. Biol. 20, 87-92.

Llacer, J., Chu, W., Tobias, C. A., Fabrikant, J. I., and Alonso, J. R. (1980). In "Biological and Medical Research with Accelerated Heavy Ions at the Bevalac, 1977-1980" (M. C. Pirruccello and C. A. Tobias, eds.), pp. 367-374. Lawrence Berkeley Laboratory Report LBL-11220.

Lucke-Huhle, C., Blakely, E. A., Chang, P. Y., and Tobias, C. A. (1979). Radiat. Res. 79, 97-112.

Lucke-Huhle, C., Blakely, E. A., Ngo, F. Q. H., Chang, P. Y., and Tobias, C. A. (1980). Int. J. Radiat. Biol. 37, 483-492.

Luxton, G., Fessenden, P., and Hoffman, W. (1979). Radiat. Res. 79, 256-272.

Lyman, J. (1983). In "Pion and Heavy Ion Radiotherapy: Preclinical and Clinical Studies" (L. D. Skarsgard, ed.), pp. 139-148. Elsevier Science Publishing Co, Amsterdam.

Lyman, J. T., and Haynes, R. H. (1967). Radiat. Res., Suppl. 7., 222-230.

Lyman, J. T., and Howard, J. (1977). Int. J. Radiat. Oncol. Biol. Phys. 3, 81-86.

Lyman, J. T., Howard, J., Kanstein, L., and Alonso, J. R. (1980). In "Biological and Medical Research with Accelerated Heavy Ions at the Bevalac, 1977-1980" (M. C. Pirruccello and C. A. Tobias, eds.), pp. 319-324. Lawrence Berkeley Laboratory Report LBL-11220.

Madhvanath, U., Raju, M. R., and Kelly, L. S. (1976). In "Radiation and the Lymphatic System" (J. E. Ballou, Chairman), pp. 125-139. ERDA Symposium Series 37, Energy Research and Development Administration, Washington, DC, 1976." (Available as CONF-740930 from the National Technical Information Service, Springfield, VA 22161.)

Magee, J. L. (1961). Ann. Rev. Phys. Chem 12, 389-410.

Magee, J. L., and Chatterjee, A. (1980). J. Phys. Chem. 84, 3529-3536.

Manney, T. R., Brustad, T., and Tobias, C. A. (1963). Radiat. Res. 18, 374-388.

Masuda, K. (1970). J. Radiat. Res. 11, 107-112.

Masuda, K. (1971). Int. J. Radiat. Biol. 20, 85-86.

McDonald, J. C., Laughlin, J. S., and Freeman, R. E. (1976). Med. Phys. 3, 80-85.

Midander, J. (1982). Int. J. Radiat. Biol. 42, 195-198.

Mozumder, A., and Magee, J. L. (1966). Radiat. Res. 28, 203-214.

Mozumder, A., Chatterjee, A., and Magee, J. L. (1968). Adv. Chem. Series 81, 27-47.

Neary, G. J. (1965). Int. J. Radiat. Biol. 9, 477-502.

Ngo, F. Q. H. (1983). In "Pion and Heavy Ion Radiotherapy: Preclinical and Clinical Studies" (L. D. Skarsgard, ed.), pp. 251-268. Elsevier Science Publishing Co, Amsterdam.

Ngo, F. Q. H., Han, A. and Elkind, M. M. (1977a). Int. J. Radiat. Biol. 32, 507-511.

Ngo, F. Q. H., Han, A., Utsumi, H., and Elkind, M. M. (1977b). Int. J. Radiat. Oncol. Biol. Phys. 3, 187-193.

Ngo, F. Q. H., Utsumi, H., Han, A., and Elkind, M. M. (1979). Int. J. Radiat. Biol. 36, 521-530.

Ngo, F. Q. H., Blakely, E. A., Yang, T. C. H., Yezzi, M. J., and Tobias, C. A. (1980a). In "Biological and Medical Research with Accelerated Heavy Ions at the Bevalac, 1977-1980" (M. C. Pirruccello and C. A. Tobias, eds.), pp. 89-102. Lawrence Berkeley Laboratory Report LBL-11220.

Ngo, F. Q. H., Blakely, E. A., and Tobias, C. A. (1980b). In "Biological and Medical Research with Accelerated Heavy Ions at the Bevalac, 1977-1980" (M. C. Pirruccello and C. A. Tobias, eds.), pp. 103-112. Lawrence Berkeley Laboratory Report LBL-11220.

Ngo, F. Q. H., Tobias, C. A., Blakely, E. A., Chang, P. Y., Oleszko, O., and Lommel, L. (1980c). (Abstract). Radiat. Res. 83, 402-403.

Ngo, F. Q. H., Blakely, E. A., and Tobias, C. A. (1981). Radiat. Res. 87, 59-78.

Nilsson, K., and Lehmann, A. R. (1975). Mutat. Res. 30, 255-266.

Northcliffe, L. C., and Schilling, R. F. (1970). Nucl. Data A7, 233-463.

Paretzke, H. F. (1980). In "Proceedings of the Sixth International Congress of Radiation Research" (S. Okada, M. Imamura, T. Terashima, and H. Yamaguchi, eds.). Japanese Association for Radiation Research, Tokyo, Japan.

Paretzke, H. and Burger, G. (1970). In "Proceedings of the Second Symposium on Microdosimetry" (H. G. Ebert, ed.), pp. 615-630. Commission of the European Communities, Brussels.

Paretzke, H. G., Leuthold, G., Burger, G., and Jacobi, W. (1973). In "Proceedings of the Fourth Symposium on Microdosimetry." Commission of the European Communities, Brussels.

Patrick, J W., Stephens, L. D., Thomas, R. H., and Kelly, L. S. (1976). Health Phys. 30. 295-296.

Phillips, R. A., and Tolmach, L. J. (1966). Radiat. Res. 29, 413-432.

Phillips, T. L., Fu, K. K., and Curtis, S. B. (1977). Int. J. Radiat. Oncol. Biol. Phys. 3, 109-113.

Pirruccello, M. C., and Tobias, C. A., eds (1980). "Biological and Medical Research with Accelerated Heavy Ions at the Bevalac, 1977-1980." Lawrence Berkeley Laboratory Report LBL-11220.

Platzman, R. L. (1952). In "Symposium on Radiobiology-The Basic Aspects of Radiation Effects on Living Systems, Oberlin College, June 14-18, 1950" (J. J. Nickson, ed.). J. Wiley and Sons, Inc., New York.

Pollard, E. C., Powell, W. F., and Reaume, S. H. (1952). Proc. Natl. Acad. Sci. U.S.A. 38, 173.

Powers, E. L. (1965). In "Cellular Radiation Biology," pp. 186-304. Williams and Wilkins Company, Baltimore, Maryland.

Powers, E. L., Lyman, J. T., and Tobias, C. A. (1968). Int. J. Radiat. Biol. 14, 313-330.

Puck, T. T., and Marcus, P. I. (1955). Proc. Natl. Acad. Sci. U.S.A. 41, 432-437.

Railton, R., Lawson, R. C., and Porter, D. (1975). Int. J. Radiat. Biol. 27, 75-82.

Raju, M. R. (1980). "Heavy Particle Radiotherapy." Academic Press, New York.

Raju, M. R., and Carpenter, S. G. (1978). Br. J. Radiol. 51, 720-727.

Raju, M., and Phillips, T. (1977). In "The Potential for Heavy Particle Radiation Therapy." Los Angeles Scientific Laboratory Report No. LA-6588-MS.

Raju, M. R., Lyman, J. T., Brustad, T., and Tobias, C. A. (1969). In "Radiation Dosimetry" (F. H. Attix and E. Tochilin, eds.), Vol. 3, pp. 151-193. Academic Press, New York.

Raju, M. R., Tobey, R. A., Jett, J. H., and Walters, J. A. (1975). Radiat. Res. 63, 422-433.

Raju, M. R., Blakely, E. A., Howard, J., Lyman, J. T., Kalofonos, D. P., Martins, B., and Yang, T. C. H. (1976). Radiat. Res. 65, 191-194.

Raju, M. R., Frank, J. P., Bain, E., Trujillo, T. T., and Tobey, R. A. (1977). Radiat. Res. 71, 614-621.

Raju, M. R., Amols, H. I., Dicello, J. F., Howard, J., Lyman, J. T., Koehler, A. M., Graves, R., and Smathers, J. B. (1978a). Br. J. Radiol. 51, 699-703.

Raju, M. R., Bain, E., Carpenter, S. G., Cox, R. A., and Robertson, J. B. (1978b). Br. J. Radiol. 51, 704-711.

Raju, M. R., Amols, H. I., Bain, E., Carpenter, S. G., Cox, R. A., and Robertson, J. B. (1978c). Br. J. Radiol. 51, 712-719.

Raju, M. R., Amols, H. I., Carpenter, S. G., Tobey, R. A., and Walters, A. (1978d). Radiat. Res. 76, 219-223.

Raju, M. R., Amols, H. I., Bain, E., Carpenter, S. G., Dicello, J. F., Frank, J. P., Tobey, R. A., and Walters, R. A. (1978e). Int. J. Radiat. Oncol. Biol. Phys. 3, 327-334.

Raju, M. R., Amols, H. I., and Carpenter, S. G. (1978f). Br. J. Cancer 37, Suppl. III, 189-193.

Raju, M. R., Johnson, T. S., Tokita, N., Carpenter, S., and Jett, J. H. (1980c). Radiat. Res. 84, 16-24.

Raju, M. R., Bain, E., Carpenter, S., Jett, J. H., Walters, R. A., Howard, J. and Powers-Risius, P. (1980b). Radiat. Res. 84, 152-157.

Raju, M. R., Bain, E., Carpenter, S. G., Howard, J., and Lyman, J. T. (1980a). Radiat. Res. 84, 158-163.

Reuvers, A. P., Greenstock, C. L., Borsa, J., and Chapman, J. D. (1973). Int. J. Radiat. Biol. 24, 533-536.

Richard-Serre, C. (1972). In "Report CERN 72-19, European Organization for Nuclear Research." Geneva, Switzerland.

Ritter, M. A., Cleaver, J. E., and Tobias, C. A. (1977). Nature (London) 266, 653-655.

Rodriguez, A. and Alpen, E. L. (1980). In "Biological and Medical Research with Accelerated Heavy Ions at the Bevalac, 1977-1980" (M. C. Pirruccello and C. A. Tobias, eds.), pp. 177-188. Lawrence Berkeley Laboratory Report LBL-11220.

Rodriguez, A., and Alpen, E. L. (1981). Radiat. Res. 85, 24-37.

Rofstad, E. K. and Brustad, T. (1981). Int. J. Radiat. Biol. 40, 677-680.

Roisman, R., Kalofonos, D., Martins, B., Lyman, J. T., and Tobias, C. A. (1974). (Abstract) Radiat. Res. 69, 60.

Roots, R., Yang, T. C., Craise, L., Blakely, E. A., and Tobias, C. A. (1979). Radiat. Res. 78, 38-49.

Roots, R., Yang, T. C., Craise, L., Blakely, E. A., and Tobias, C. A. (1980a). Int. J. Radiat. Biol. 38, 203-210.

Roots, R., Chatterjee, A., Blakely, E. A., and Tobias, C. A. (1980b). (Abstract) Radiat. Res. 83, 495.

Roots, R., Chatterjee, C., Blakely, E. A., and Tobias, C. A. (1981). In "Oxygen and Oxy-Radicals in Chemistry and Biology" (E. L. Powers, eds.). Academic Press, Inc., New York.

Roots, R., Chatterjee, A., Blakely, E., Chang, P., Smith, K., and Tobias, C. A. (1982). Radiat. Res. 92, 245-254.

Rossi, B. (1952). In "High Energy Particles," pp. 22-24. Prentis-Hall, Incorporated, New York.

Roth, R. A., and Katz, R. (1980). Radiat. Res. 83, 499–510.

Sakamoto, K., Okada, S., Lam, G. K. Y., and Howard, J. (1983). In "Proceedings of the US–Japan Cooperative Research Program on High LET Particle Irradiation and other Approaches to Increasing Effectiveness of Radiation Therapy for Cancer, October 2–5, 1982." Chiba and Kyoto, Japan.

Sapozink, M. D., and Djordjevic, B. (1974). Radiology 110, 691–698.

Sauer, M. C., Schmidt, K. H., Jonah, C. D., Naleway, C. A., and Hart, E. J. (1978). Radiat. Res. 75, 519–528.

Sayeg, J. A., Birge, A. C., Beam, C. A., and Tobias, C. A. (1959). Radiat. Res. 10, 449–461.

Schambra, P. E. and Hutchinson, F. (1963). Radiat. Res. 23, 514–526.

Schimmerling, W. (1980). In "Biological and Medical Research with Accelerated Heavy Ions at the Bevalac, 1977–1980" (M. C. Pirruccello and C. A. Tobias, eds.), pp. 35–41. Lawrence Berkeley Laboratory Report LBL–11220.

Schimmerling, W., Vosburgh, K. G., and Todd, P. (1973). Phys. Rev. B 7, 2895–2899.

Schimmerling, W., Vosburgh, K. G., Todd, P. W., and Appleby, A. (1976). Radiat. Res. 65, 389–413.

Schimmerling, W., Curtis, S. B., and Vosburgh, K. G. (1977). Radiat. Res. 72, 1–17.

Schimmerling, W. S., Kaplan, S., Subramanian, T. S., McDonald, W. J., Gabor, G., Sadoff, A., and Alpen, A. (1983). "Proceedings of the Eighth Symposium on Microdosimetry, Julich, Federal Republic of Germany, 27 September–1 October, 1982." In press.

Schlag, H. and Lucke-Huhle, C. (1981). Int. J. Radiat. Biol. 40, 75–85.

Schlag, H., Weibezahn, K. F., and Lucke-Huhle, C. (1978). Int. J. Radiat. Biol. 33, 1–10.

Schneider, D. O., and Whitmore, G. F. (1963). Radiat. Res. 18, 286–306.

Schroeder, L. S., ed. (1981). In "Proceedings of the 5th High Energy High-Ion Study, May 18–22, 1981." Available from National Technical Information Service, U.S. Dept. of Commerce, 5285 Port Royal Road, Springfield, VA 22161.

Schroy, C. B., and Todd, P. (1979a). Radiat. Res. 78, 312–316.

Schroy, C. B., and Todd, P. (1979b). Radiat. Res. 80, 224.

Schroy, C. B., Furcinitti, P. S., Todd, P., and Kukulinsky, N. E. (1980a). Radiat. Res. 84, 353–358.

Schroy, C. B., Furcinitti, P. S., and Todd, P. (1980b). Radiat. Res. 83, 404 (Abstract).

Schuler, R. H. (1967). J. Phys. Chem. 71, 3712.

Schuler, R. H., and Allen, O. A. (1957). J. Am. Chem. Soc. 79, 1575.

Shekhtman, V. L. (1960). Akad. Nauk, USSR, (A. M. Kuzin, ed.), p. 116.

Sinclair, W. K. (1966). In "Biophysical Aspects of Radiation Quality." Technical Report Series 58, pp. 21-43. International Atomic Energy Commission, Vienna, Austria.

Sinclair, W. K. (1970). In "Time and Dose Relationships in Radiation Biology as Applied to Radiotherapy" (V. P. Bond, H. D. Suit, and V. Marcial, eds.), pp. 97-116. Report BNL-50203 C-58.

Sinclair, W. K. (1972). Curr. Top. Radiat. Res. Q. 7, 264-285.

Sinclair, W. K., and Morton, R. A. (1963). Nature (London) 199, 1158-1160.

Sinclair, W. K., and Morton, R. A. (1965). Biophys. J. 5, 1-25.

Sinclair, W. K., and Morton, R. A. (1966). Radiat. Res. 29, 450-474.

Singh, D. R., Mahajan, J. M., and Krishnan, D. (1976). Int. J. Radiat. Biol. 30, 585-588.

Skarsgard, L. D. (1964). Radiat. Res. 22, 235 (Abstract).

Skarsgard, L. D. (1967). In "The Radiobiology of Cultured Mammalian Cells" (M. M. Elkind and G. F. Whitmore, eds.), pp. 420-421. Gordon and Breach, New York.

Skarsgard, L. D. (ed.) (1983). "Pion and Heavy Ion Radiotherapy: Preclinical and Clinical Studies." Elsevier Science Publishing Co., Amsterdam.

Skarsgard, L. D., Pujara, C. M., and Richardson, S. (1966). In "Proceedings of Third International Congress of Radiation Research" pp. 24. (Abstract).

Skarsgard, L. D., Kihlman, B. A., Parker, L., Pujara, C. M., and Richardson, S. (1967). Radiat. Res. Suppl. 7, 208-221.

Smith, A. R. (1982). In "Proceedings, Particle III CROS Workshop" (E. J. Hall, ed.). Int. J. Radiat. Biol. Phys., 8, 2061-2063.

Smith, K. C., Hahn, G. M., Hoppe, R. T., and Earle, J. D. (1980). Int. J. Radiat. Oncol. Biol. Phys. 6, 1573-1575.

Stephens, L. D., Thomas, R. H., and Kelly, L. S. (1976). Phys. Med. Biol. 21, 570-576.

Steward, P. G. (1968). Ph.D. Thesis, University of California, Berkeley.

Suit, H. D., and Goitein, M. (1980). In "Radiation Biology and Cancer Research" (R. Meyn and R. Withers, eds.), pp. 195-230. Raven Press, New York.

Takeshita, K. and Sawada, S. (1974). In "Biological Effects of Neutron Irradiation," pp. 245-254. International Atomic Energy Agency, Vienna, Austria.

Terasima, T., and Tolmach, L. J. (1961). Nature (London) 190, 1210-1211.

Terasima, T., and Tolmach, L. J. (1963). Biophys. J. 3, 11-32.

Tenforde, T. S., Curtis, S. B., Crabtree, K. E., Tenforde, S. D., Schilling, W. A., Howard, J., and Lyman, J. T. (1980). Radiat. Res. 83, 42-56.

Tenforde, T. S., Tenforde, S. D., Crabtree, K. E., Parks, D. L., Schilling, W. A., Parr, S. S., Flynn, M. J., Howard, J., Lyman, J. T., and Curtis, S. B. (1981a). Int. J. Radiat. Oncol. Biol. Phys. 7, 217-221.

Tenforde, T. S., Curtis, S. B., Tenforde, S. D., Parr, S. S., Crabtree, K. E., Flynn, M. J., Howard, J., and Lyman, J. T. (1981b). Int. J. Radiat. Biol. 40, 117-129.

Tenforde, T. S., Afzal, S. M. J., Parr, S. S., Howard, J., Lyman, J. T., and Curtis, S. B. (1982a). Radiat. Res. 92, 208-216.

Tenforde, T. S., Curtis, S. B., Parr, S. S., Afzal, S. M. J., Howard, J., and Lyman, J. T. (1982b). Int. J. Radiat. Biol. 41, 677-684.

Thomas, R. H. (1982). Radiat. Res. 90, 437-440.

Thomas, R. H., Lyman, J. T., and DeCastro, T. M. (1980). Radiat. Res. 82, 1-12.

Tobias, C. A. (1971). In "Initial Radiobiological Experiments with Accelerated Nitrogen Ions at the Bevatron." Lawrence Berkeley Laboratory Report LBL-529.

Tobias, C. A. (1973). Radiology 108, 145-158.

Tobias, C. A., and Todd, P. W. (1967). In "Radiobiology and Radiotherapy," Monograph No. 24, pp. 1-21. National Cancer Institute, Washington, D.C.

Tobias, C. A., and Todd, P. W., eds. (1974). "Space Radiation Biology and Related Topics," pp. 142-187. Academic Press, New York.

Tobias, C. A., Anger, H. O., and Lawrence, J. H. (1952). Am. J. Roentgenol. Rad. Therm. Nucl. Med. 67, 1-27.

Tobias, C. A., Lyman, J. T., and Lawrence, J. H. (1971a). In "Progress in Atomic Medicine: Recent Advances in Nuclear Medicine" (J. H. Lawrence, ed.), Vol. 3, pp. 167-218. Grune and Stratton, New York.

Tobias, C. A., Chatterjee, A., and Smith, A. R. (1971b). Phys. Lett. 37A, 119-120.

Tobias, C. A., Blakely, E. A., Yang, T. C. H., and Chatterjee, A. (1977). (Abstract). Radiat. Res. 70, 694.

Tobias, C. A., Alpen, E. A., Blakely, E A., Castro, J. R., Chatterjee, A., Chen, G. T. Y., Curtis, S. B., Howard, J., Lyman, J. T., and Ngo, F. Q. H. (1979). In "Treatment of Radioresistant Cancers" (M. Abe, K. Sakamoto, and J. L. Phillips, eds.). Elsevier (North Holland Biomedical Press), Amsterdam.

Tobias, C. A., Blakely, E. A., Ngo, F. Q. H., and Yang, T. C. H. (1980). In "Radiation Biology and Cancer Research" (R. E. Meyn and H. R. Withers, eds.), pp. 195-230. Raven Press, New York.

Tobias, C. A., Blakely, E. A., Alpen, E. L., Castro, J. R., Ainsworth, E. J., Curtis, S. B., Ngo, F. Q. H., Rodriguez, A., Roots, R. J., Tenforde, T., and Yang, T. C. H. (1982). In "Proceedings of Particle III CROS Workshop" (E. J. Hall, ed.). Int. J. Radiat. Biol. Phys., in press.

Tochilin, E., Goldstein, N., and Lyman, J. T. (1968). In "Proceedings of the Second International Conference on Luminescence Dosimetry." Gatlinberg, Tennessee. Conference USAEC No. CONF680920. (Available from the National Technical Information Service, Springfield, Virginia).

Todd, P. W. (1964). Ph.D. Thesis, University of California, Berkeley.

Todd, P. W. (1967). Radiat. Res. Suppl. 7, 196-207.

Todd, P. W. (1968). Radiat. Res. 34, 378-389.

Todd, P. W. (1973). In "Proceedings, Conference on Particle Accelerators in Radiation Therapy" Report LA-5180-C, Los Alamos Scientific Laboratory, 1975, pp. 113-119. (Available from the National Technical Information Service, Springfield, VA 22161).

Todd, P. W., Schroy, C. B., Vosburgh, K. G., and Schimmerling, W. (1971). Science 174, 1127-1128.

Tolmach, L. J., Jones, R. W., and Busse, P. M. (1977). Radiat. Res. 71, 653-665.

Turner, J. E., and Hollister, H. (1965). (Abstract). Nature (London) 207, 36-37.

Turner, J. E., Magee, J. L., Hamm, R. N., Chatterjee, A., Wright, H. A., and Ritchie, R. H. (1981). In "Proceedings, VIII Symposium on Microdosimetry" pp. 507-517. Commission of the European Communities, Brussels.

Tym, R., and Todd, P. (1964). Int. J. Radiat. Biol. 8, 589-604.

Uehling, E. A. (1954). Ann. Rev. Nucl. Sci. 4, 315-350.

Utsumi, H., and Elkind, M. M. (1979). Radiat. Res. 77, 346-360.

Varma, M. N., and Baum. J. W. (1980). Radiat. Res. 81, 355-363.

Verhey, L. J., and Munzenrider, J. E. (1982). Ann. Rev. Biophys. Biol. 11, 331-357.

Vereschinskii, I. V., and Pikaev, A. K. (1964). In "Introduction to Radiation Chemistry." Israel Program for Scientific Translations.

Virski, R. P., and Harder, D. (1981). Radiat. Res. 85, 13-23.

Vos, O., Schenk, H.A.E.M., and Bottsma, D. (1966). Int. J. Radiat. Biol. 11, 495-503.

Walters, R. A., Gurley, L. R., and Tobey, R. A. (1974). Biophys. J. 14, 99-118.

Ward, J. F. (1981). Radiat. Res. 86, 185-195.

Weichselbaum, R. R., Nore, J., and Little, J. B. (1980). In "Radiation Biology in Cancer Research" (R. E. Meyn and H. R. Withers, eds.), pp. 345-351. Raven Press, New York.

Wheeler, K. T., Deen, D. F., Leith, J. T., and Norton, K. L. (1979). Radiobiology 133, 757-760.

Wheeler, K. T., Norton, K. L., Deen, D. F., and Leith, J. T. (1980). Int. J. Radiat. Biol. 37, 225-229.

White, M. G., Isaila, M., Predec, K., and Allen, H. C. (1971). Science 174, 1121-1123.

Wideroe, R. (1966). Acta. Biol. 4, 257-278.

Wilson, R. R. (1946). Radiology 47, 487-491.

Wingate, C. L. and Baum, J. W. (1969). (Abstract). In "Second International Conference on Medical Physics." Boston, MA.

Withers, H. R., and Suit, H. (1974). In "The Biological and Clinical Basis of Radiosensitivity" (M. Friedman, ed.), pp. 548-562. C. C. Thomas, Springfield, IL.

Yamawaki, Y., Yatagai, F., Kaneko, Sakamato, K., Oakda, S., and Matsuyama, A. (1976). IPCE Cyclotron Progress Report 10, 36-37.

Yang, T. C. H., and Tobias, C. A. (1980). Adv. Biol. Med. Phys. 17, 417-461.

Yang, T. C. H., Blakely, E., Chatterjee, A., Welch, G., and Tobias, C. A. (1977). Life Sci. Space Res. 25, 169-174.

Yang, T. C. H., Tobias, C. A., Blakely, E. A., Craise, L. M., Madfes, I. S., Perez, C., and Howard, J. (1980). Radiat. Res. 81, 208-223.

Zaider, M., Dicello, J F., Brenner, D. J., Takai, M., Raju, M. R., and Howard, J. (1981). Radiat. Res. 87, 511-520.

Zirkle, R. E. (1935). Am. J. Cancer 23, 558-567.

Zirkle, R. E. (1936). In "Biological Effects of Radiation" (B. M. Duggar, ed.), Vol. I, pp. 559-572. McGraw-Hill, New York.

Zirkle, R. E., and Tobias, C. A. (1953). Arch. Biochem. Biophys. 47, 282-306.